

## 5. CHEMISTRY OF ORGANIC MATERIALS

### 5.1. Lectures

#### L01 EFFECT OF WETTING/DRYING ON THE CONFORMATIONAL ARRANGEMENT OF A HETEROGENEOUS ORGANIC MIXTURE AS ASSESSED BY SOLID STATE $^{13}\text{C}$ NMR SPECTROSCOPY

PELLEGRINO CONTE<sup>a</sup>, ANNE E. BERNS<sup>b</sup>, HERBERT PHILIPP<sup>b</sup>, PETER BURAUER<sup>b</sup>, HANS-DIETER NARRES<sup>b</sup> and HARRY VEREECKEN<sup>b</sup>

<sup>a</sup>*Dipartimento di Ingegneria e Tecnologie Agro-Forestali (DITAF), Università degli Studi di Palermo, v.le delle Scienze 13, 90128 Palermo, Italy,*

<sup>b</sup>*Forschungszentrum Jülich GmbH, Institute of Chemistry and Dynamics of the Geosphere, Institute 4: Agrosphere, 52425 Jülich, Germany, pellegrino.conte@unipa.it*

#### Introduction

Cross-polarization magic angle spinning  $^{13}\text{C}$ -NMR (CPMAS  $^{13}\text{C}$ -NMR) spectroscopy is used to investigate nature of carbon skeletons in organic substances which are insoluble or poorly soluble in common NMR deuterated solvents. The technique is applied to achieve information either on the quality of complex mixtures or on the solid state structure and conformation of pure materials. One of the advantages of the technique is the possibility to analyze the structures of amorphous compounds which are not analysable by common

cristallographic methods (i.e. X ray diffraction)<sup>1</sup>. Moreover, direct quantification of molecular composition of complex organic matrices (which are not easily chromatografable such as humic substances<sup>2</sup>) is also possible.

The limiting factor in CPMAS  $^{13}\text{C}$ -NMR analyses is the low spectral sensitivity that is achieved when strength of the C-H dipolar interactions is weakened by rapid molecular motions and absence of protons in the neighbourhood of carbon atoms<sup>1</sup>. Moreover, presence of paramagnetic species decreases proton relaxation times, thereby allowing protons to be relaxed before full H  $\rightarrow$  C cross polarization is achieved<sup>3</sup>. When cross polarization rates are equal to or larger than proton relaxation velocities, CPMAS  $^{13}\text{C}$ -NMR spectra are not representative of the chemical composition of complex organic mixtures<sup>3</sup>. Sensitivity enhancement can be obtained by applying properly all the procedures for sample preparation as reported in Smernik<sup>4</sup>, Blann et al.<sup>5</sup> and Schilling and Cooper<sup>6</sup>.

The aim of the present paper was to understand the effect of wetting/drying treatments on the physical parameters achievable by CPMAS  $^{13}\text{C}$  NMR spectroscopy on organic mixtures. In order to reach our goal a mixture of three different standards was prepared and analyzed by CPMAS  $^{13}\text{C}$  NMR spectroscopy before and after water treatment and freeze-drying.

#### Experimental

##### Chemicals

Carboxymethylcellulose sodium salt (CMC), ferulic acid (FERAC) and sodium dodecylsulfate (SDS) were purchased from Sigma-Aldrich<sup>®</sup> (Steinheim, Germany) and used without further purification. They were mixed in an agate mortar with a weight ratio of 1:1:1 (corresponding to a molar ratio of 1:52:77 for CMC, SDS and FERAC, respectively). The solid mixture was divided into two portions. The first one (Mix 1) was left unchanged, whereas the second portion (Mix 2) was suspended in distilled water, stirred for one hour and then freeze-dried. Both portions were finally analyzed by CPMAS  $^{13}\text{C}$ -NMR spectroscopy by using the conditions reported below.

##### Solid State NMR Spectroscopy

A 7.05 T NMR spectrometer Unity INOVA<sup>™</sup> (Varian Inc., Palo Alto, CA, USA), equipped with a wide bore probe operating at a  $^{13}\text{C}$  frequency of 75.4 MHz, was used to acquire the CPMAS  $^{13}\text{C}$ -NMR spectra of Mix 1 and Mix 2. The samples were packed in 6 mm zirconium rotors with Teflon<sup>®</sup> bottom and top spacers and Vespel<sup>®</sup> drive tips. Temperature was kept constant at  $25.0 \pm 0.1$  °C. Magic angle spinning was carried out at  $5,000 \pm 1$  Hz. Acquisition time of 30 ms,  $^1\text{H}$   $90^\circ$  pulse of 4  $\mu\text{s}$  with a power level of 49 dB at the maximum decoupler power modulation, 1k data points and a recycle delay of 10 s were applied. A ramped cross-polarisation sequence with an ascending H-ramp of 15-kHz ramp width was applied. 256 transients were used to acquire all the spectra.

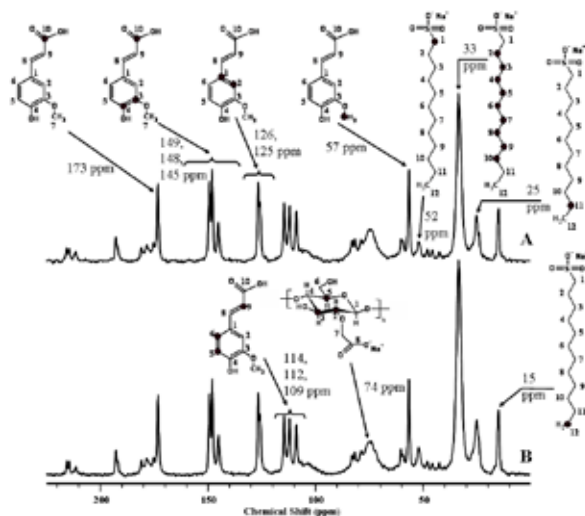


Fig. 1. CPMAS  $^{13}\text{C}$ -NMR spectra and signal attribution (black circles in the structures) of the three molecules used in our study. A – mixture before dissolution and freeze drying, B – mixture after the treatment. The non-assigned peaks are spinning side bands

Arrayed (or pseudo-2D) experiments were performed to precisely measure cross polarization time ( $T_{CH}$ ), and  $^1\text{H}$  spin-lattice relaxation times in the rotating frame ( $T_{1\rho}(\text{H})$ ).  $T_{CH}$  was measured by variable contact time experiments (VCT) carried out by arraying 30 different contact times from 0.1 to 7.0 ms. Variable spin lock experiments were conducted according to Tekely et al.<sup>7</sup> to measure  $T_{1\rho}(\text{H})$  values. An array of 35 spin lock times ranging from 0 to 50 ms was used.  $T_{1\rho}(\text{H})$  values obtained from VCT experiments were not considered due to the overestimation of this parameter by VCT experiments as compared to delayed spin lock measurements.

### Spectra Elaboration

VNMRJ software (Version 1.1 RevisionD, Varian Inc., Palo Alto, CA, USA) was used to acquire all the free induction decays (FID). Spectra elaboration was conducted by Mestre-C software (Version 4.9.9.9, Mestrelab Research, Santiago de Compostela, Spain). All the FIDs were transformed by applying, first, a 4k zero filling, and, then, an exponential filter function with a line broadening of 18 Hz. Fully automatic baseline correction using Bernstein algorithm was applied for baseline corrections. The intensities of all the peaks were measured and imported in OriginPro 7.5 SR6 (Version 7.5885, OriginLab Corporation, Northampton, MA, USA) to fit equation (1) for  $T_{CH}$  measurement, and equation (2) to obtain  $T_{1\rho}(\text{H})$  values.

$$I(t) = I_0 \alpha^{-1} \left[ 1 - \exp\left(-\alpha \frac{t_{CP}}{T_{CH}}\right) \right] \times \exp\left(-\frac{t_{CP}}{T_{1\rho}(\text{H})}\right) \quad (1)$$

$$I(t) = I_0 \exp\left(-\frac{t_m}{T_{1\rho}(\text{H})}\right) \quad (2)$$

In equations (1) and (2),  $I(t)$  is the signal area at the assigned  $t_{CP}$ , and  $t_m$  value,  $I_0$  is the total nuclear magnetization of  $^{13}\text{C}$  in thermal equilibrium,  $\alpha = 1 - T_{CH}/T_{1\rho}(\text{H})$ ,  $t_{CP}$  is the contact time, and  $t_m$  is the spin-locking time.

### Results and Discussion

Fig. 1. shows the spectra of Mix 1 (Fig. 1.A) and Mix 2 (Fig. 1.B). Structures of each standard and signal attribution are also reported. Namely, peaks at 173, 149, 148, 145, 126, 125, 114, 112, 109 and 57 ppm are assigned to FERAC and those at 52, 33, 22 and 15 ppm are due to the resonance of the SDS chain. The only visible signal of CMC is the signal at 74 ppm, as it appears in a spectral range free of other signals. The signal of carbon 4 at about 82 ppm is hidden beneath the spinning side bands of FERAC appearing in this region. The resonance of carbon 1 at 104 ppm only appears as a shoulder of the FERAC signal at 109 ppm. The signals of carbons 6 and 7 (60 and 62 ppm) as well as the signal of carbon 8 (177 ppm) are also hidden under prominent spinning side bands in these regions. The reason why CMC signals are almost negligible in the spectra of Fig. 1. can be related to the

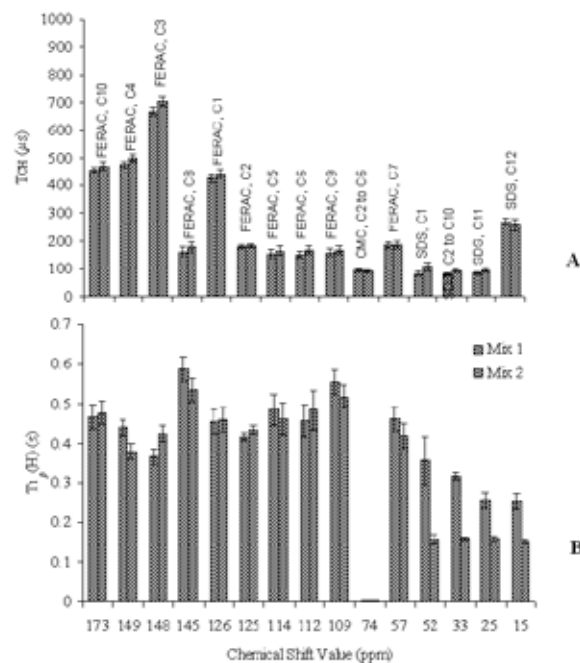


Fig. 2.  $T_{CH}$  (A) and  $T_{1\rho}(\text{H})$  (B) values as obtained from VCT and VSL experiments. See text for the meaning of acronyms

amount of CMC which is 52 and 77 times lower than that of SDS and FERAC, respectively (see Experimental section).

CPMAS  $^{13}\text{C}$  NMR experiments on Mix 1 and Mix 2 were done in VCT and VSL mode (see Experimental for details) in order to obtain information on  $T_{CH}$  and  $T_{1\rho}(\text{H})$  values.

$T_{CH}$  measures the cross polarization (CP) efficiency which depends on the strength of the C-H dipolar interactions<sup>1</sup>. The shorter the proton-to-carbon distances and the slower the local molecular motions, the stronger is the strength of the C-H dipolar interactions, thereby leading to faster CP rates<sup>1</sup> (shorter  $T_{CH}$  values).

$T_{1\rho}(\text{H})$  is associated to local molecular motions in the kilohertz (kHz) scale<sup>1</sup>. In particular, the faster the molecular motions in the lattice, the shorter is the  $T_{1\rho}(\text{H})$  value (fast proton relaxation processes). Conversely, when the molecular motions slow down, relaxation processes are slower and longitudinal relaxation times increase<sup>1</sup>. However, attention must be paid when dealing with the interpretation of the molecular motions in lattices by using  $T_{1\rho}(\text{H})$  values. In fact, proton relaxation times in the rotating frame are also affected by nuclear dipolar interactions. In the case of organic materials, where protons are very abundant, the H-H dipolar interactions are very strong and they predominantly control the rate of the magnetization transfer among protons in the lattice<sup>1</sup>. For this reason, if relaxation mechanisms related to dipolar interactions cannot be ruled out, short  $T_{1\rho}(\text{H})$  values cannot be associated solely to fast molecular motions in proton-rich organic compounds<sup>1</sup>.

The analysis of the  $T_{CH}$  values of the different carbon nuclei in FERAC (Fig. 2.A) revealed that they varied in the

order C3>C1, C4, C10>C2, C5, C6, C7, C8, C9. The cross polarization rate of the proton rich methyl group indicated as C7 (Fig. 1.) was similar to the CP rates of the monoprotinated FERAC carbons 2, 6, 7, 8 and 9. This was expected. In fact, CH<sub>3</sub> systems are terminal groups subjected to fast rotational motions. Fast motions weaken H-C dipolar interactions, thereby lowering CP efficiency of the highly protonated methyl groups compared to that of the less protonated methylene systems. A confirmation of a less efficient CP of non protonated C1, C4 and C10 carbons in FERAC as compared to the protonated C nuclei is also reported in Fig. 2.A. However, it must be noted that, among the cross polarization time values of the quaternary carbons (i.e. C1, C3, C4, C10), position 3 (Fig. 1.) showed the largest  $T_{CH}$  value. This was attributed to the combined effect of the non-protonation and the large rotational movements of the methoxy group directly bound to C3, which caused poor CP efficiency. Finally, the comparison of the  $T_{CH}$  values of the FERAC carbons in Mix 1 and Mix 2 (Fig. 2.A) shows that the CP mechanisms in the ferulic acid are not affected by the physical treatments to which the mixture was subjected in our study.

Fig. 2.B reports the  $T_{1\rho}(H)$  values measured for the signals of FERAC, either before or after water dissolution and freeze drying. All the  $T_{1\rho}(H)$  values are similar to each other and they did not change passing from Mix 1 to Mix 2. Since FERAC carbons are subjected to different molecular motions, as reported above, we may conclude that the proton longitudinal relaxation mechanisms in FERAC are affected more by H-H dipolar interactions than by fast local movements and chemical-physical treatments.

The  $T_{CH}$  values of CMC either in Mix 1 or Mix 2 are similar (Fig. 2A). Such similitude reveals that, as for FERAC, the water dissolution and the freeze drying processes did not affect the CP mechanisms in carboxymethylcellulose. Moreover, the polymeric nature of CMC should be responsible for slow molecular motions that, in turn, should provide longer  $T_{1\rho}(H)$  values as compared to FERAC and SDS. Conversely, Fig. 2.B shows the shortest  $T_{1\rho}(H)$  values for CMC in both Mix 1 and Mix 2. Also in CMC, as for FERAC, then, predominant relaxation mechanisms are mediated by homonuclear H-H dipolar interactions, rather than molecular motions.

Fig. 2.A shows also similarities in the  $T_{CH}$  values of the methylene carbons 1 to 11 of SDS, while the methyl C in the

same material (C12) was cross polarized less efficiently due to fast rotational motions as already previously outlined.

After the treatments, the  $T_{1\rho}(H)$  values of SDS were halved. Since the H-H dipolar interactions are the main responsible for the longitudinal proton relaxation mechanisms in organic materials, we may argue that the more efficient proton relaxation of SDS in Mix 2 can only be achieved by a strengthening of the homonuclear H-H dipolar interactions. This can be due to a closer proximity of the SDS alkyl chains that before freeze drying are arranged to form micelles.

## Conclusions

This work revealed that water treatment and freeze drying processes do not affect the cross polarization dynamics in a mixture of three molecules having known structure and conformation in the solid state. Conversely, proton relaxation, which is affected mainly by the strong H-H dipolar interactions, was fastened only in SDS which was able to form micelles in water solution before freeze drying. Although after the drying procedure micelles cannot be present anymore, the closer proximity of the protons in the alkyl chains as consequence of SDS behaviour in water, strengthened the homonuclear proton dipolar interactions, thereby favouring shorter  $T_{1\rho}(H)$  values.

## REFERENCES

1. Duer M. J.: *Solid-state NMR spectroscopy: principles and applications*. Blackwell Science, Oxford 2002.
2. Conte P., Piccolo A.: *Chemosphere* 38, 517 (1999).
3. Wilson M. A.: *NMR techniques and applications in geochemistry and soil chemistry*. Pergamon Press, London 1987.
4. Smernik R. J.: *Eur. J. Soil Sci.* 57, 665 (2006).
5. Blann W. G., Fyfe C. A., Lyster J. R., Yannoni C. S.: *J. Am. Chem. Soc.* 103, 4030 (1981).
6. Schilling M., Cooper, W. T.: *Anal. Chim. Acta* 508, 177 (2004).
7. Tekely P., Gérardy V., Palmas P., Canet D., Retournard A.: *Solid State Nucl. Magn. Res.* 4, 361 (1995).

## L02 AMINOACID PROFILES MONITORING FOR DIAGNOSIS

MONICA CULEA, ANDREEA IORDACHE and CORNELIA MESAROS

*Babes-Bolyai University, Str. Kogalniceanu, nr.1, 3400 Cluj-Napoca, Romania, mculea@phys.ubbcluj.ro*

### Introduction

Gas chromatography coupled with mass spectrometry (GC-MS) is largely used for the quantitative analyses of the organic compounds from biological fluids<sup>1,4</sup>. Metabolic fingerprinting, metabolite profiling or metabolite target analysis are strategies used in the metabolomics analysis for rapid diagnosis. Biological fluids are ideal candidates for diseases diagnosis because they can easily and inexpensively be isolated from the body.

The study deals with possible diagnosis of neonatal diseases caused by inborn error of metabolism using gas chromatography – mass spectrometry (GC-MS). Phenylketonuria (PKU) is a metabolic disease usually caused by phenylalanine hydroxylase deficiency, which leads to an increase of phenylalanine and a decrease of tyrosine content in plasma. Enzyme deficiency results in high levels of blood phenylalanine and an accumulation of phenylketones in the urine. Partial deficiency of the enzyme results in hyperphenylalaninemia. Maple syrup urine disease (MSUD) is a metabolism disorder caused by a gene defect, in which the body cannot break down some branched-chain amino acids<sup>3</sup>. In MSUD, the enzymes necessary to break down leucine, isoleucine, and valine are either absent, inactive, or only partially active. As a result of the enzyme deficiency, the branched-chain amino acids and ketoacids become elevated in the blood, resulting in an altered mental state and progressive neurodegeneration. PKU is general screened by a bacterial inhibition assay (BIA) of elevated blood phenylalanine levels on newborn filter paper samples of blood specimens. There are many chromatographic methods for screening PKU and also mass spectrometry as electrospray mass spectrometry, ESI-MS-MS<sup>5</sup>.

The main goal of the present work was to perform a rapid and precise analysis of volatile derivatives of amino acids from dry plasma and blood spots for diagnosis of two inborn errors diseases: PKU and MSUD. This minimum invasive method is based on profiling and quantitative determination of some amino acids in blood samples of 20  $\mu\text{l}$  by using filter paper blood specimens and the GC-MS technique. The method is useful for the diagnosis of the PKU disease, by determination of phenylalanine (Phe) and tyrosine (Tyr) content in blood or for the diagnosis of the MSUD disease, by estimation of valine (Val), leucine (Leu) and proline (Pro) content.

### Experimental

#### Chemicals and Samples

Acetyl chloride and ion exchange resin Dowex 50W-X8 50–100 mesh were purchased from Fluka, while acetone and trifluoroacetic anhydride were obtained from Merck (Darmstadt, Germany). Amino acids standards were purchased from Sigma. [<sup>15</sup>N]-isoleucine (99%) was produced by chemical synthesis. All the other chemicals were from Comchim (Bucharest). The blood and urine samples were obtained from patients and volunteers from the Pediatric Clinic III Cluj-Napoca. Written informed consents were obtained from each subject's parent prior to this study.

#### Extraction Procedure and Derivatization of Amino Acids

The blood was placed in a screw cap vial with 200  $\mu\text{l}$  methanol/HCl 0.1% and extraction was performed either 1 h at 4 °C or by sonication for 1 min. 100  $\mu\text{l}$  of the extract were placed in a vial and after the addition of the internal standard and removing of the reagent using a nitrogen stream, the amino acid extract was derivatized. Amino acids of the blood samples or standard samples were derivatized as trifluoroacetyl butyl ester derivatives. Derivatization was performed in screw-cap tubes, in two steps. Dry samples were esterified with 100  $\mu\text{l}$  butanol: acetyl chloride, 4:1 (v/v) for 30 min at 100 °C. The excess reagent was removed with a stream of nitrogen. The amino group was acetylated with 100  $\mu\text{l}$  trifluoroacetic anhydride (TFAA) at 100 °C for 30 min. After cooling, the excess reagent was removed under nitrogen at ice temperature and ethyl acetate was added<sup>1</sup>.

#### Instrumentation

A Trace DSQ ThermoFinnigan quadrupole mass spectrometer in the EI mode coupled with a Trace GC was used. The capillary column Rtx-5MS had 30 m in length, 0.25 mm as diameter and a film thickness of 0.25  $\mu\text{m}$ . The experiments were performed by using a temperature program from 50 °C (1 min), then 20 °C  $\text{min}^{-1}$  to 260 °C, 100 °C  $\text{min}^{-1}$  to 300 °C, in the selected ion monitoring mode (SIM). Helium (5.5) carrier gas had a flow rate of 1  $\text{ml min}^{-1}$ . The qualitative analysis was carried out in the 50–500 a.m.u. mass range. The following conditions were ensured: transfer line temperature 250 °C, injector temperature 200 °C, ion source temperature 250 °C, splitter 10:1, electron energy 70 eV and emission current 100  $\mu\text{A}$ .

In the SIM mode, the following ions were used (Fig. 1.):  $m/z$  168 for valine,  $m/z$  182 for leucine,  $m/z$  166 for proline,  $m/z$  91 and 148 for phenylalanine (Figs. 2., 3.),  $m/z$  203, 260, 316 (Fig. 3.) for tyrosine. 25  $\mu\text{g ml}^{-1}$  of the <sup>15</sup>N-isoleucine (<sup>15</sup>N-Ile,  $m/z$  183) internal standard was added at each sample. For Val, Leu and Pro amino acids, the important ions selected in the SIM experiment from the trifluoroacetyl butyl esters derivatives mass spectra correspond to the loss of butyl ester from the molecular ion  $[\text{M} - \text{COOC}_4\text{H}_9]^+$ .

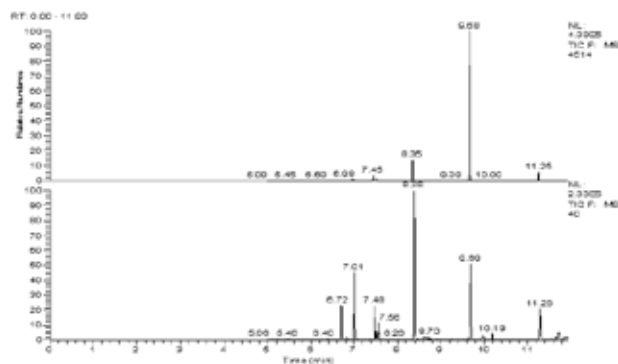


Fig. 1. SIM-GC-MS comparison of screening of the five amino acids in a PKU blood sample (top) and a standard mixture (bottom) of the amino acids (7.01 min: Val, 7.48 min: Leu, 7.56 min:  $^{15}\text{N}$ -Ile (IS); 8.38 min: Pro; 9.69 min: Phe and 11.28 min: Tyr

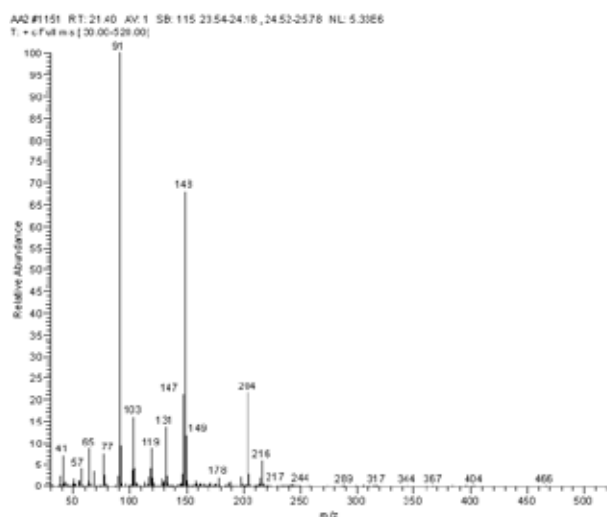


Fig. 2. The mass spectra of trifluoroacetyl butyl ester derivatives of Phe

Linearity of the method was calculated by representing the ratio of the selected ion peak area for each amino acid and the internal standard versus the amino acid standard concentrations (in  $\mu\text{g ml}^{-1}$ ). The regression curves were obtained by injecting standard solutions containing amino acids in concentration of 1, 5, 10, 20, 30 and 40  $\mu\text{g ml}^{-1}$  with 25  $\mu\text{g ml}^{-1}$  of  $^{15}\text{N}$ -Ile added to each standard solution per ml of blood sample. The regression curves obtained were: Val:  $y = 0.0912x + 0.0555$ , regression coefficient  $r = 0.999$ ; Leu:  $y = 0.0515x - 0.0097$ ,  $r = 0.998$ ; Pro:  $y = 0.1835x - 0.1382$ ,  $r = 0.998$ ; Phe:  $y = 0.1119x - 0.0665$ ,  $r = 0.988$ ; Tyr:  $y = 0.08x - 0.1938$ ,  $r = 0.984$ . The precision and the accuracy were studied by extracting four times the standard solutions of 1, 30 and 40  $\mu\text{g ml}^{-1}$ . The R.S.D. values obtained ranged between 9–12.9 % for 30  $\mu\text{g ml}^{-1}$  and 6.7–18.6 % for 40  $\mu\text{g ml}^{-1}$  (Table I). For 1  $\mu\text{g ml}^{-1}$ , the precision was between 45–50 %. Accuracy values were between 4–30% for 30  $\mu\text{g ml}^{-1}$  and lower than 5.5 for 40  $\mu\text{g ml}^{-1}$  ( $n = 4$ ). The limit of detection (L.O.D.) was lower than 0.1  $\mu\text{g ml}^{-1}$ .

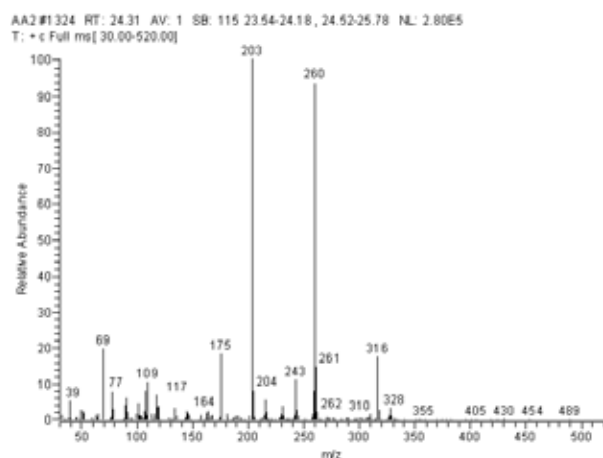


Fig. 3. The mass spectrum of Tyr trifluoroacetyl butyl ester derivative

Table I

Precision study for the same patient (6 spots,  $n = 6$ )

Amino acid	$[\mu\text{g ml}^{-1}]$	SD	RSD [%]
Val	4.05	0.28	6.97
Leu	3.39	0.17	5.00
Pro	3.40	0.27	6.57
Phe	1.32	0.14	10.41
Tyr	2.19	0.11	5.06

Table II

The amino acids quantitation in control blood samples, spot samples (mean values,  $n = 53$ )

Amino acid	$[\mu\text{g ml}^{-1}]$	$[\mu\text{M}]$
Val	11.66	99.62
Leu	13.19	100.71
Pro	17.82	155.00
Phe	17.15	103.95
Tyr	26.67	147.33
Phe/Tyr	0.64	0.71

Table III

Amino acids values  $[\mu\text{g ml}^{-1}]$  in PKU blood samples, spot samples

Val	22.27	21.73	21.47	23.22	22.16	21.51
Leu	22.96	24.56	16.97	25.84	33.16	19.92
Pro	37.76	23.67	19.85	25.64	65.66	31.42
Phe	93.18	134.13	89.75	142.7	131.3	119.3
Tyr	50.02	38.99	19.4	35.91	57.2	33.53
Phe/Tyr	1.86	3.44	4.63	3.97	2.30	3.56

In our study, 13 cases of PKU children were found, Phe/Tyr value being significantly higher than control.

Table IV  
Amino acids values [ $\mu\text{g ml}^{-1}$ ] in a PKU child blood samples; spots were taken at different intervals of the day; hour: 7, 9, 14 and 19

Val	8.9	10.86	10	8.95
Leu	23.16	41.3	35.59	36.57
Pro	16.34	40.09	43.52	43.68
Phe	262.33	608.71	548.85	491.65
Tyr	15.84	42.63	50.07	67.59
Phe/Tyr	16.56	14.28	10.96	7.27

## Results

Quantitative analysis of five amino acids, valine, leucine, proline, phenylalanine and tyrosine, in blood samples, by using blood spots<sup>1</sup> or 0.5 ml blood<sup>3,9</sup> gave similar results, the coefficient of regression obtained by comparing the amino acid values in the two extraction methods gave  $r = 0.91$  ( $n = 4$ ). Fig. 1. shows the chromatogram of separation of the five amino acids by using the minim invasive method, from 20  $\mu\text{l}$  blood.

The intraindividual amino acid values variation is shown in Table I. Table II shows the comparison of the results obtained for the amino acids average value in control blood samples ( $n = 53$ ). Good amino acid precision in the same child was obtained, R.S.D. lower than 10.4 %. The results obtained by using only 20  $\mu\text{l}$  of blood spots showed that the PKU diagnosis could be tested by calculating the Phe/Tyr ratio. Diagnosis of the MSUD disease should be obtained by calculating the ratio between aliphatic and aromatic amino acids in the blood samples<sup>1</sup>. The results for some PKU patients are presented in Tables III and IV. The high benefits of the early diagnosis and treatment are strong arguments for the neonatal screening of metabolic disorder. The classical bacterial inhibition assay (BIA) used for the diagnosis of PKU is a semi-quantitative method giving false positive results. More precise methods, such is the MS/MS technique, were developed, but they have the disadvantage of high price and less affordable equipment. By comparison, the proposed

GC/MS method is simple, inexpensive, easily operated and high-speed technique.<sup>5–8</sup> The internal standard used increased the precision of the method. The use of mass spectrometer as a detector for GC is important not only for its high sensitivity but also for selectivity and the identity of the analytes<sup>9</sup>.

## Conclusions

Measurements performed on amino acids from dried blood spots showed that GC-MS is a suitable method for PKU diagnosis in neonatal blood samples, from Phe/Tyr ratio and MSUD from the amino acid values<sup>1</sup>. The labelled internal standard used increased the precision of the method and simplified the samples injection. The method is a minim invasive, by using very small quantities of blood. Monitoring these diseases is important because once the diagnosis is made and treatment is started in the first few weeks of life, normal brain development is not disturbed or affected.

*This work has been supported by the Romanian Research Foundation (CEEX, project number 166/2006).*

## REFERENCES

- Deng C., Li N., Wang X., Zhang X., Zeng J.: Rapid Commun. Mass Spectrom. 19, 647 (2005).
- Phillips M., Cataneo R. N., Cheema T., Greenberg J.: Clin. Chim Acta., 344, 189 (2004).
- Culea M., Bucur A., Cozar O.: Analele Univ. Vest Timisoara 45, 89 (2004).
- Culea M., Cozar O., Ristoiu D.: JMS 41, 1594 (2006).
- Nagy N., Takats Z., Pollreis F., Szabo T., Vekey K.: Rapid Commun. Mass. Spectrom. 17, 983 (2003).
- Deng C., Yin X., Zhang L., Zhang X.: Rapid. Commun. Mass. Spectrom. 19, 2227 (2005).
- Jouvet P., Hubert P., Saudubray J. M., Rabier D., Man N. K.: Pediatric Res. 58 (2005) 278.
- Shen X., Deng C., Wang B., Dong L.: Anal. Bioanal. Chem. 384, 931 (2006).
- Culea M., Hachey D. L.: Rapid Commun. Mass. Spectrom. 9, 655 (1995).

### L03 MICROWAVE-ASSISTED EXTRACTION OF ORGANIC COMPOUNDS FROM THE BROWN COAL

SILVIA ČUVANOVÁ<sup>a</sup> and MICHAL LOVÁS<sup>a</sup>

<sup>a</sup>*Institute of Geotechnics, Slovak Academy of Sciences, Watsonova 45, 043 53 Košice, Slovakia, [cuvanova@saske.sk](mailto:cuvanova@saske.sk)*

#### Introduction

Microwave heating arises from the ability of some liquids and solids to transform the absorbed electromagnetic energy into heat. The heating effect originates from the microwave electric field which forces dipoles to rotate and ions to migrate; from a slower response of dipoles and ions to follow the rapid reversal of the electric field. The ability of material to increase its temperature under microwave at a given frequency and temperature is referred to the dissipation factor, defined as  $\tan \delta = \epsilon''/\epsilon'$ , where  $\epsilon''$  is the dielectric loss factor related to the efficiency of a medium to convert microwave energy into heat, while  $\epsilon'$  is the dielectric constant measuring the ability of a molecule to be polarised by an electric field. The penetration depth ( $D_p$ ) is the distance from the material surface where the absorbed electric field falls to 1/e of the electric field at the surface. The penetration depth is inversely proportional to the frequency, whereas the greatest heating is achieved at the high frequencies. However, the penetration depth at such frequencies is so low that only the exterior of the material will heat.  $D_p$  is given by (1):

$$D_p = \frac{c}{2\pi \cdot f \sqrt{2\epsilon'}} \cdot \frac{1}{\left[\sqrt{1 + \tan^2 \delta} - 1\right]^{1/2}}, \quad (1)$$

where:  $f$  – frequency [Hz];  $c$  – speed of light [ $\text{ms}^{-1}$ ].

Together with the ability to dissolve reagents and products, the solvent under microwaves can play a more active role. The acceleration of a chemical reaction under microwaves depends on the dielectric properties of the solvent. Solvents that are able to directly absorb microwaves increase the reaction rate of the dissolved reagents. The solvent overheating is a phenomenon frequently observed when microwaves are applied in chemical processes. In the presence of microwaves, common solvents are found to boil at higher temperatures: for dichloromethane the difference is about 15 °C. In closed vessels this increases the pressure of the system.

The microwave applications in mining and process metallurgy have been the subject of many research studies over the past two decades. The microwaves have potential application in mineral processing and extraction of metals such as copper, gold, nickel, cobalt, lead, zinc and manganese<sup>2</sup>, and also for the direct determination of sulphide, pyrite and organic sulphur concentrations in coals of bituminous or sub-bituminous rank<sup>3</sup>.

Microwave-assisted extraction in the closed system has been developed as a means of avoiding the use of large amounts of solvent and to save time. The samples and sol-

vents in the closed system reach temperatures above the boiling points of the solvents at the atmospheric pressure. As results, the extraction of samples can be completed in minutes as opposed to hours necessary when traditional methods are used<sup>4,5</sup>. There are many reports where PAHs are extracted with comparable efficiency to those by using Soxhlet extraction, even for extraction times of less than 30 min<sup>4</sup>.

The microwave heating has been applied to the extraction of organic contaminants such as polycyclic aromatic hydrocarbons, pesticides, polychlorobiphenyls, herbicides, phenols, neutral and basic priority pollutants in various matrices such as sediments, soils, coal or atmospheric particles. The main purposes of the microwave heating are the reduction of extraction time and solvent quantity. The decrease of solvent waste, solvent release into the environment and human exposure is also important.<sup>6–10</sup>

The most common solvents used for the MAE of PAHs from the solid samples are acetone-hexane, dichloromethane, methanol, and methanol-toluene. However, the selection of solvent to extract analyses has to take into consideration the technique which will be used in the final determination. Most solvents or solvent mixtures used for PAHs extraction appear to be perfectly suited for the gas chromatography. But if liquid chromatography will be used, the solvent exchange would be necessary.<sup>7–9,11–15</sup>

Our article presents the influence of conditions of extraction on the occurrence of PAHs in dichloromethane extract.

#### Experimental

##### Sample Characterization

The research was carried out with the samples of the Slovak brown coal from Handlová (West Slovakia) after the hydrocyclone washing<sup>16</sup>. The chemical analysis of studied sample was following: A<sup>d</sup> (Ash) = 9.01 %, M (Moisture) = 7.55 %, C<sup>daf</sup> = 74.86 %, H<sup>daf</sup> = 4.93 %, N<sup>daf</sup> = 0.6 %, (O + S)<sup>daf</sup> = 19.61 %.

##### Instrumentation

CHN analysis was realized using elementary analyser Carlo Erba Model 1106 equipped with the microprocessor and recorder. Helium (purity 99.998 %) was used as the carrier gas; oxygen (99.999%) was used as the oxidative agent and argon created an inert atmosphere during measurement. The chromatographic column was filled with the Porapak QS with granularity 80–100 mesh. The cyclohexanone – dinitrophenylhydrazone (content of N = 20.14 %, C = 51.79 % and H = 5.07 %) was used as the standard material.

The studied sample was pretreated in the mill and then the sample of under 0.5 mm granularity was activated by the grinding using the planetary mill Pulverisette 6 (Fritsch, Germany) in the air atmosphere at the following conditions: granularity of input – 0.5 mm, mass of sample – 20 g, grinding speed – 400 rev min<sup>-1</sup>, time of grinding – 20 minutes.

SEM/EDX analysis was carried out at the Institute of Theoretical and Physical Chemistry – Braunschweig, Germany. It was used JSM – 6400 Scanning microscope (JEOL

LTD., Tokyo Japan) combined with the Microanalysis System Software, EDAX Genesis V2.50.

### Microwave-Assisted Extraction and Analysis

Soxhlet extraction of the coal sample was realized in dichloromethane for 3 days. The microwave-assisted extraction was realized in the microwave Whirlpool at the power 500 W and frequency 2.45 GHz. The extraction was realized in the non-polar solvent of dichloromethane at the boiling point 40 °C (it increases in microwave oven to 55 °C) for the period of 30 minutes. The boiling point of solvent in the microwave was measured using the contactless thermometer Raytek MX4. MAE was also realized in the closed pressure vessels by automatic pressure regulation within range 1.8–2 bar for the period of 20 minutes.

GC-MS analyses were realised in National Water Reference Laboratory for Slovakia in Bratislava. The chromatographic analyses were performed using Agilent 6890 gas chromatograph coupled to Agilent 5973 mass spectrometric detector (USA). Capillary GC analysis was performed on a 30 m × 250 µm I.D.; 0.25 µm  $d_f$  HP-5MS column (Agilent Technologies). Helium was used as a carrier gas. The MSD was used in the scan mode (m/z 40–550) for all samples. Mobile phase was methanol and water Milli-Q. The identification of compounds was performed using mass spectrum libraries Wiley 7n and NIST02, respectively.

The distribution of temperature in the extraction solvent was operated by modeling program Comsol, version 3.3.

## Results

### Microwave Heating of Dichloromethane

Coal pretreatment with dichloromethane has been reported for improvement of selective grindability of organic substances and mineral matters in coal. Table I summarizes the properties of dichloromethane.

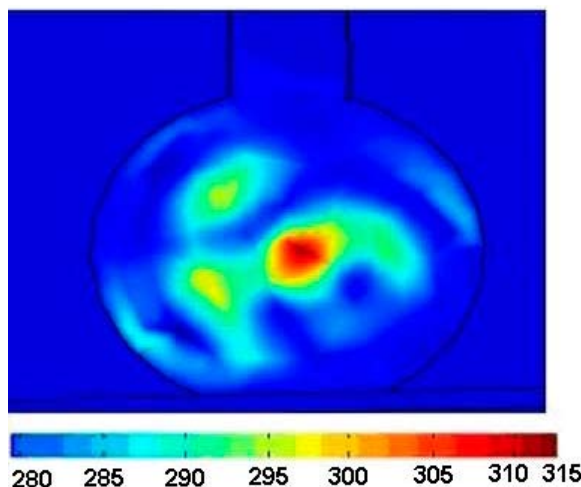


Fig. 1. Distribution of temperature for the microwave heating of dichloromethane after 3 seconds; radius of spherical container is 10 cm

Table I  
The physical properties of dichloromethane

Density [kg m <sup>-3</sup> ]	Diel. const.	Loss factor <sup>17</sup>	Heat capacity [JK <sup>-1</sup> kg <sup>-1</sup> ]	Thermal conduct. [W m <sup>-1</sup> K <sup>-1</sup> ]
1,317.0	8.93	0.042	1,190.0	0.122

The penetration depth calculated according to equation (1) for dichloromethane is 0.16 m.

Commercial final element method based on software COMSOL Multiphysics was used to modeling the dichloromethane microwave heating (Fig. 1). Various steps involved in the modeling with COMSOL software are outlined in Fig. 2.

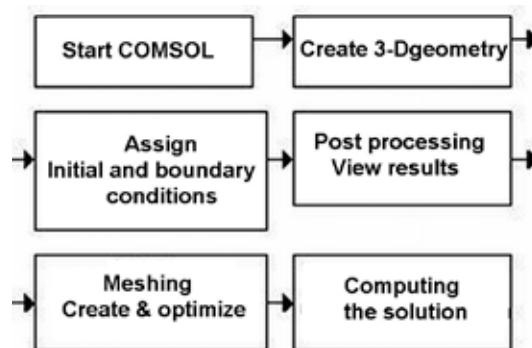


Fig. 2. The COMSOL modeling steps

### Microwave Extraction of Samples in Dichloromethane

Fig. 3. shows the quantity of physically treated brown coal sample after the microwave-assisted extraction in dichloromethane.

The presence of elements typical for the Slovak brown coal (Table II) was confirmed.

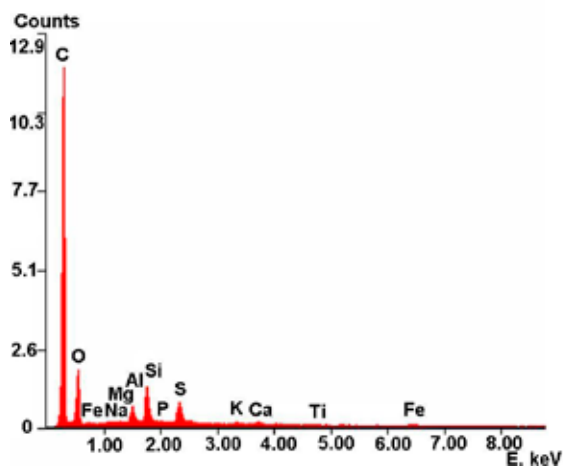


Fig. 3. EDX spectrum of physically treated brown coal sample after the microwave-assisted extraction in dichloromethane

Table II  
Content of elements in the coal sample after the microwave-assisted extraction in dichloromethane

Element	W <sub>t</sub> [%]	A <sub>t</sub> [%]
C	78.52	84.61
O	16.40	13.27
Na	0.14	0.08
Mg	0.08	0.04
Al	0.83	0.40
Si	01.83	0.84
P	0.04	0.02
S	01.15	0.46
K	0.14	0.05
Ca	0.24	0.08
Ti	0.06	0.02
Fe	0.57	0.13

Our attention was intent on the study of influence of Soxhlet and microwave-assisted extraction in the open-vessel and closed-vessel system, respectively.

It was also realized the blank experiment (Fig. 4.). It was prepared with 100 ml Milli Q vody and 10 ml methanol. Then it was mixed 2 hours with the blender Twister.

Fig. 5. shows the chromatogram of coal extract after the Soxhlet extraction in dichloromethane for 72 hours The presence of organic compounds with carbon numbers C15, C20 a C19 was confirmed in the extract after the Soxhlet extraction. All analyzed compounds belong to group of polycyclic aromatic hydrocarbons (Table III).

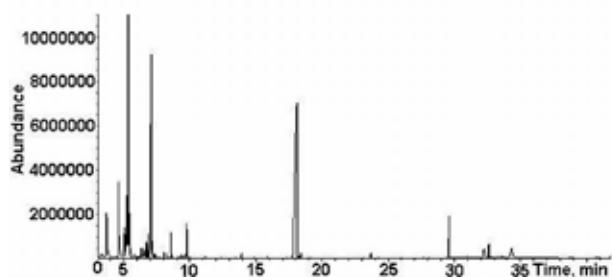


Fig. 4. Typical GC chromatogram of the blank experiment

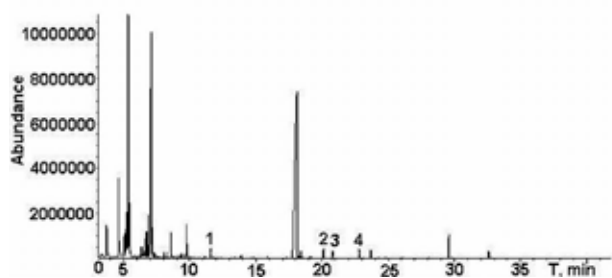


Fig. 5. Typical GC chromatogram of dichloromethane extract of the physically treated brown coal prepared by the Soxhlet extraction; extraction time of 72 hours

Table III  
The composition of the Slovak brown coal extract after the Soxhlet extraction in dichloromethane

Peak number	Ion intensity [m/z]	Formula	Characterization of the compounds
1	198	C <sub>15</sub> H <sub>18</sub>	1,6-dimethyl-4-(1-methylethyl)naphthalene
2	274	C <sub>20</sub> H <sub>34</sub>	4b,8,8-trimethyl-2,10a-(2'-methylethano)-perhydrophenanthrene
3	270	C <sub>20</sub> H <sub>30</sub>	7-izopropyl-1,1,4a-trimethyl-1,2,3,4,4a,9,10,10a-oktahydrophenanthrene
4	252	C <sub>19</sub> H <sub>24</sub>	simonelit

During microwave-assisted extraction in the open-vessel system the extraction time was shortened to 30 minutes at power 500 W and frequency 2.45 GHz. The following organic compounds were identified by GC-MS method: naphthalene and its derivatives with the carbon numbers 14 and 15 (m/z = 184, 198), phenanthrene derivatives with the carbon number 20 (m/z = 274, 276). The presence of benzene derivative C<sub>15</sub>H<sub>22</sub>, indene derivative C<sub>14</sub>H<sub>20</sub> and other naphthalene derivative C<sub>14</sub>H<sub>16</sub> was confirmed as well (Fig. 6., Table IV).

The microwave-assisted extraction in closed-vessel system was realized by pressure 1.8–2 bar for 20 minutes. The temperature was not possible to measure correctly. Fig. 7. shows the representative GC-MS chromatograph of the orga-

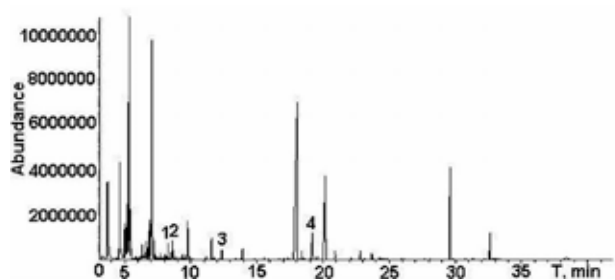


Fig. 6. Typical GC chromatogram of dichloromethane extract of the physically treated brown coal prepared by the microwave-assisted extraction in the open-vessel system; extraction time of 30 minutes

nic compounds occurrence in the microwave extract of coal sample in dichloromethane. The growing of other organic compounds was confirmed. The solvent temperature has the essential influence on number of extracted substances. The temperature is higher by microwave heating in comparison with Soxhlet extraction. Other organic compounds occurred in extract after the microwave-assisted extractions in the closed-vessel system are listed in Table V.

Table IV

The occurrence of other organic compounds in the Slovak brown coal extract after the extraction in dichloromethane; the open-vessel system

Peak number	Ion intensity [m/z]	Formula	Characterization of the compounds
1	202	C <sub>15</sub> H <sub>22</sub>	1-methyl-4-(1,2,2-trimethylcyclopentyl) benzene
2	188	C <sub>14</sub> H <sub>20</sub>	1,1,4,6,7-pentamethyl-2,3-dihydroindene
3	184	C <sub>14</sub> H <sub>16</sub>	1,2,3,4-tetramethylnaphthalene
4	276	C <sub>20</sub> H <sub>36</sub>	2-ethyl-2,4,8,8-tetramethylperhydrophenanthrene

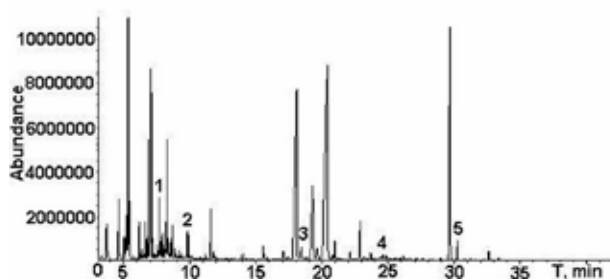


Fig. 7. Typical GC chromatogram of dichloromethane extract of the physically treated brown coal prepared by the microwave-assisted extraction in the closed-vessel system; extraction time of 20 minutes

Table V

The occurrence of other organic compounds in the Slovak brown coal extract after the extraction in dichloromethane; the closed-vessel system

Peak number	Ion intensity [m/z]	Formula	Characterization of the compounds
1	206	C <sub>15</sub> H <sub>26</sub>	alfa-cedrane
2	226	C <sub>16</sub> H <sub>34</sub>	hexadecane
3	272	C <sub>20</sub> H <sub>32</sub>	(5alfa, 9 alfa, 10 beta)-kaur-15-ene
4	234	C <sub>18</sub> H <sub>18</sub>	1-methyl-7-izopropylphenanthrene
5	366	C <sub>26</sub> H <sub>54</sub>	hexakozane

## Conclusions

The focused microwave-assisted extraction in the atmospheric open-vessel systems seems to be a viable alternative

method to Soxhlet extraction for the analysis of organic compounds, mainly polycyclic aromatic hydrocarbons in the coal sample from Handlová. The advantage of using MAE for the coal sample is the reduction of extraction time. The optimized conditions can be applied for extraction with good recoveries and reproducibility. This method can be used in conjunction with GC-MS for the determination of PAHs in the large number of coal samples.

*This work has been supported by the Slovak Research and Development Agency under the contract No. APVV-51-035505 and by the Slovak Grant Agency for Science VEGA, grant No. 2/7163/27. The authors thank to Ing. Peter Tolgyessy, CSc. and Ing. Jarmila Makovinská, CSc. from the National Water Reference Laboratory for Slovakia in Bratislava for their help and advice with the measurements of the GC-MS spectrometry.*

## REFERENCES

- Mingos D. M. P., Baghurst D. R.: *Chem. Soc. Rev.* 20, 1 (1991).
- Al-Harashsheh M., Kingman S. W.: *Hydrometallurgy* 73, 189 (2004).
- Laban K.L., Atkin B. P.: *Fuel* 79, 173 (2000).
- Itoh N., Numata M., Yarita T.: *Anal. Chim. Acta* (2008, in press).
- Karthikeyan S., Balasubramanian R., See S. W.: *Talanta* 69, 79 (2006).
- Letellier, M., Budzinski, H.: *Analisis* 27, 259 (1999).
- Čuvanová S., Lovás M., Turčániová E., Hredzák S.: *The 11th International Conference on Environment and Mineral Processing*, p. 123. Ostrava, 2007.
- Zubrik A., Turčániová E., Ježová V., Čuvanová S., Skybová M.: *J. Alloys Compd.* 434, 837 (2007).
- Zubrik A.: *Dissertation*. Institute of Geotechnics, Slovak Academy of Science in Košice, Košice, Slovakia, 2008.
- Murová I.: *Dissertation*. Institute of Geotechnics, Slovak Academy of Science in Košice, Košice, Slovakia, 2001.
- Pensado L., Casais C., Mejuto C., Cela R.: *J. Chromatogr. A* 869, 505 (2000).
- Fabbri D., Vassura I.: *J. Anal. Appl. Pyrolysis* 75, 150 (2006).
- Liguori L., Heggstad K., T. Hove H., Julshamm K.: *Anal. Chim. Acta* 573-574, 181 (2006).
- Cai O.-Y., Mo C.-H., Wu Q.-T., Zeng Q.-Y.: *Bioresour. Technol.* 99, 1830 (2008).
- Mikošková J., Čáp L., Lemr K.: *Chem. Listy* 98, 85 (2004).
- Hredzák S.: *Gospodarka Surowcami Mineralnymi* 15, 221 (1999).
- Kappe C. O.: *Angew. Chem. Int. Ed.* 43, 6250 (2004).

#### L04 REACTIVITY OF N–NO<sub>2</sub> BONDS IN NITRAMIDES

ZDENĚK FRIEDL<sup>a</sup> and SVATOPLUK ZEMAN<sup>b</sup>

<sup>a</sup>Brno University of Technology, Faculty of Chemistry, Purkyňova 118, 602 00 Brno, Czech Republic

<sup>b</sup>Institute of Energetic Materials, University of Pardubice, 532 10 Pardubice, Czech Republic, friedl@fch.vutbr.cz

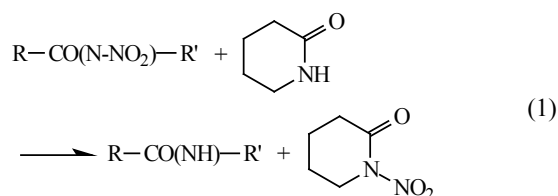
##### Introduction

The highly energetic character of the N–NO<sub>2</sub> group means that *N*-nitro-based energetic materials are of the most powerful explosives available. Different chemical properties of primary and secondary nitramines predetermine the others (e.g. RDX, HMX and HNIW) as the explosives of choice for military use<sup>1</sup>.

Structurally related type of compounds represent nitramides where conjugated C=O group is directly bonded to N–NO<sub>2</sub> grouping. At present the idea of fundamental role of nitro groups is generally accepted<sup>2,3</sup>. The homolytic dissociation of C–NO<sub>2</sub>, N–NO<sub>2</sub> or O–NO<sub>2</sub> represents the primary fission process of energetic materials under thermal, impact, shock and electric spark initiation stimuli. Thus, the relationships exist between characteristics of low-temperature thermal decomposition and detonation characteristics of polynitro compounds<sup>2</sup>.

In the case of polynitro compounds as nitro aromatics, nitramines and nitramides the C–NO<sub>2</sub> or N–NO<sub>2</sub> bond fission is mostly characterized by homolytic *bond dissociation energy*  $BDE(N-NO_2)^{4-12}$ . The theoretical calculations of homolytic  $BDE$  energies are substantially influenced from inadequate treatment of electron correlation. At present the mostly used density functional models with 6-311+G(d,p) basis set provide a much improved description of homolytic  $BDE$  in comparison with Hartree-Fock models. Overall, B3LYP models provide the best results and are quite close to those from the corresponding MP2 models<sup>13,14</sup>.

Recently the elegant method was suggested to overcome this substantial drawback – the isodesmic reaction approach<sup>4,15</sup>. This type of virtual symmetrical chemical equilibria inherently cancels electron correlation effects accompanying homolytic bond dissociation. The application of isodesmic reaction scheme to describe N–NO<sub>2</sub> bond fission leads to the formulation of relative *bond disproportionation energy*  $DISP(N-NO_2)$  described by (1):



The use of closed shells reactants in (1) guarantee that the electron correlation term in bond disproportionation

energy  $DISP(N-NO_2)$  is irrelevant. In view of the difference in cost between theoretical calculations of open shell or neutral molecules, the latter seems the obvious choice for this purpose.

Relating to our results on initiation reactivity<sup>2,3,12</sup> we have recently calculated the theoretical *in silico* bond dissociation energies  $BDE(N-NO_2)$  and bond disproportionation energies  $DISP(N-NO_2)$  for 20 nitramines<sup>16</sup>. The energies obtained were compared with their detonation velocity  $D$  and heat of explosion  $Q_{real}$ .

In this paper we have calculated bond dissociation energies  $BDE(N-NO_2)$  and bond disproportionation energies  $DISP(N-NO_2)$  by B3LYP/6-311+G(d,p) method for 12 nitramides of general formula RN–NO<sub>2</sub> (1-nitropiperidin-2-one as a standard nitramide SN–NO<sub>2</sub>) and the energies obtained were compared with their detonation velocities  $D$ .

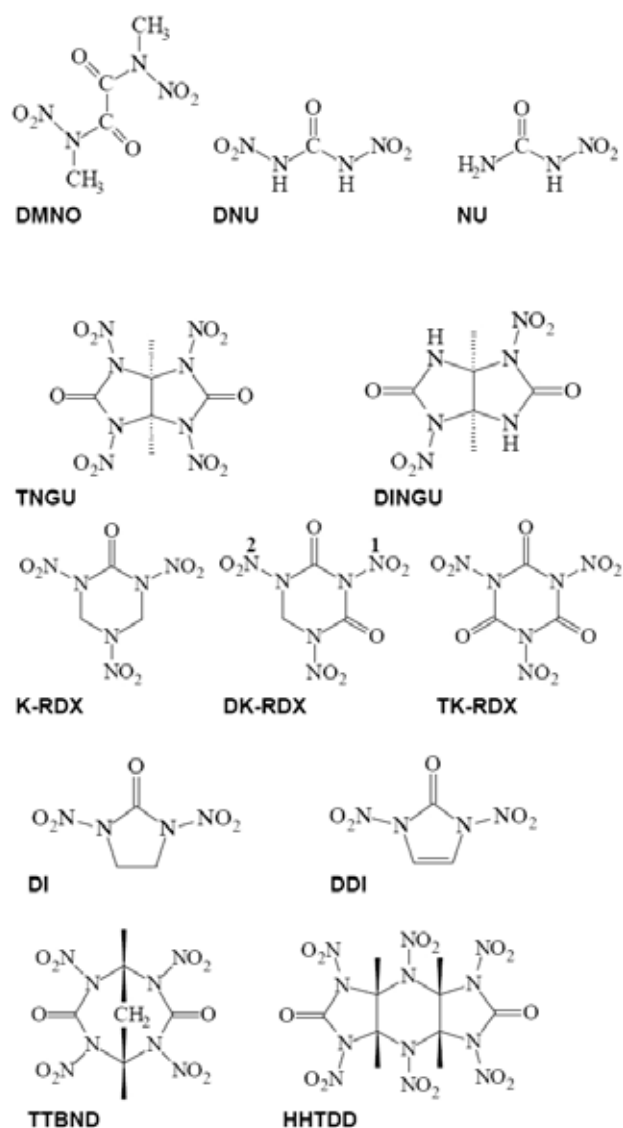


Fig. 1. The chemical structures and names of nitramides studied with numbering of respective NO<sub>2</sub> groups

## Experimental

### Calculations

The calculations of bond dissociation energies  $BDE(N-NO_2)$  and bond disproportionation energies  $DISP(N-NO_2)$  were performed by B3LYP/6-311 + G(d,p) method<sup>17</sup>. The calculations by total optimization gave the equilibrium geometries in the gas phase at 0 K. The optimized structures of 13 nitramides and related amides were verified by normal mode frequency analysis to exclude imaginary frequencies for the remaining  $3N-6$  vibrational degrees of freedom. The relevant data are summarized in Table I.

Table I

Calculated bond dissociation energies  $BDE(N-NO_2)$ , bond disproportionation energies  $DISP(N-NO_2)$  and detonation velocities  $D$  of nitramides studied

Name	BDE DISP [kJ mol <sup>-1</sup> ]	D [kms <sup>-1</sup> ]
DMNO	177.67–18.98	7.20
DNU	171.20–38.55	8.32
NU	207.18–35.44	8.35
TNGU	151.96–40.96	8.86
DINGU	173.20–3.80	8.04
K-RDX	152.39–25.24	9.01
DK-RDX N1	161.89–59.79	8.62
N2	155.12–27.06	8.62
TK-RDX	135.04–98.16	7.85
DI	164.50–2.90	7.99
DDI	252.28–20.30	8.30
TTBND	158.16–38.70	8.72
HHTDD	150.16–31.47	9.26
NPO	173.99–0.00	(3.65)

The chemical structures and names of nitramides studied with numbering of respective  $NO_2$  groups are given in Fig. 1.

DMNON, *N,N'*-dimethyl-*N,N'*-dinitroethanediamide, DNU *N,N'*-dinitrourea, NU *N*-nitrourea, TNGU 1,3,4,6-tetranitro-tetrahydroimidazo[4,5-d]imidazole-2,5-(1*H*,3*H*)-dione, DINGU 1,4-dinitrotetrahydroimidazo[4,5-*d*]imidazole-2,5-(1*H*,3*H*)-dione, K-RDX 1,3,5-trinitro-1,3,5-triazinane-2-one, DK-RDX 1,3,5-trinitro-1,3,5-triazinane-2,4-dione, TK-RDX 1,3,5-trinitro-1,3,5-triazinane-2,4,6-trione, DI 1,3-dinitroimidazolidin 2-one, DDI 1,3-dinitro-1,3-dihydro-2*H*-imidazol-2-one, TTBND 2,4,6,8-tetranitro-2,4,6,8-tetraazabicyclo[3.3.1]nonane-3,7-dione, HHTDD 1,3,4,5,7,8-hexanitrooctahydrodiimidazo[4,5-*b*:4,5-*e*]pyrazine-2,6-(1*H*,3*H*)-dione, NPO 1-nitropiperidin-2-one

### Detonation Parameters

The values of detonation velocities  $D$  were calculated using the known relationships of Rothstein & Petersen<sup>18,19</sup>. Summary of calculated values is given in Table I.

## Results

From the published papers<sup>2,3,20,23,24</sup> it follows that logical relationships exist between the characteristics of low-temperature thermal decomposition and those of initiation and detonation, respectively. The homolytic character of primary fission in both the detonation and low-temperature thermal decompositions of energetic materials (for relevant quotations, see ref.<sup>21</sup>) was a motive factor for using the Evans–Polanyi–Semenov equation<sup>25</sup> (E–P–S) to study the chemical micro-mechanism governing initiation of energetic materials in the following form:

$$E_a = \alpha Q + \beta \quad (2)$$

Application of the definition relationship<sup>26</sup> between detonation velocities and heats of explosion  $Q$  leads to the Eq. (3):

$$Q = \frac{D^2}{2(\gamma^2 - 1)}, \quad (3)$$

where  $\gamma$  is the polytropy coefficient which transforms Eq. (2) into Eq. (4) named in the previous paper<sup>23</sup>

$$E_a = aD^2 + b \quad (4)$$

as a modified E–P–S equation. The original E–P–S describes a relationship between activation energies  $E_a$  of the most substitution reactions of free radicals and corresponding heats of reaction  $\Delta H$  of narrow sets of substance structures<sup>25</sup>. The equation documents that the strength of bond being split is a decisive factor in the given reaction.

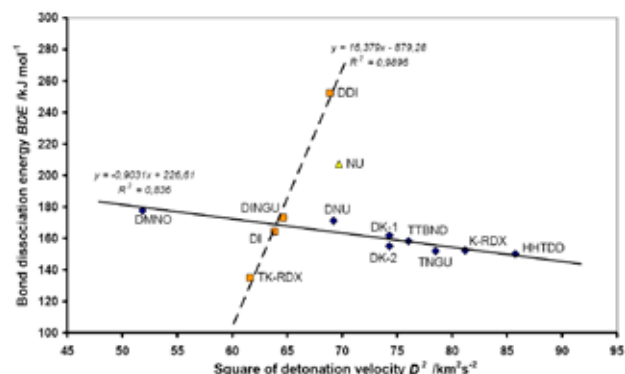


Fig. 2. Relationship between bond dissociation energy  $BDE(N-NO_2)$  and square of detonation velocity  $D^2$  of nitramides studied

In both equations (2) and (4) the energy,  $E$ , can be the activation energy of thermal decomposition ( $E_a$ )<sup>3,23,27</sup>, the slope  $E_a R^{-1}$  of the Kissinger relationship<sup>3,20,24</sup>, the energy of electric spark  $E_{ES}$ , drop energy  $E_p$ , it may be substituted by the charge  $q^N$  at nitrogen atom of the most reactive nitro group in the molecule<sup>3,20,24</sup>, by the net charge of this nitro group<sup>23</sup>, or by the half-wave polarographic potential<sup>20</sup>. Sub-

stitution of the energy  $E$  in Eq. (4) by the BDE energy leads to Fig. 2.

Fig. 2. presents the relationships between dissociation energies  $BDE(N-NO_2)$  and square of detonation velocities  $D^2$ . The dominant relationship with the slope of  $-0.90$  describes the generally expected indirect rule of proportion between ease of bond fission and detonation velocity. This relationship is valid from polycyclic nitramide HHTDD till the open structure of DMNO. Nevertheless, nitramides DDI and TK-RDX, which are strictly planar and highly conjugated fail the general relationship but create a new line with the positive slope of 16.38. Similarly NU miss the plot due to its different structure.

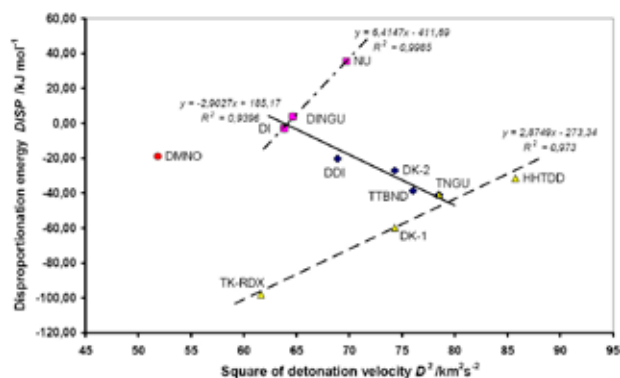


Fig. 3. Relationships between bond disproportionation energies  $DISP(N-NO_2)$  and square of detonation velocity  $D^2$  of nitramides studied

Similarly, a substitution of the energy,  $E$ , in Eq. (4) by the bond disproportionation  $DISP$  energy leads to Fig. 3. Differentiation of the studied nitramides in the sense of Eq. (4) is more pronounced and corresponding relationships are closer as in the case of Fig. 2. TK-RDX and DK1-RDX are nitramides with specific group  $(C=O)-(N-NO_2)-(C=O)$  and make relationship with similar positive slope as nitramides containing  $NH-(C=O)-(N-NO_2)$  group, i.e., DINGU and NU. According to the Fig. 3. the remaining cyclic nitramides are differentiated into line with negative slope  $-2.90$ . Alternative expansion of this plot should probably be relationship comprising nitramides from DMNO via DK2-RDX, TNGU to HHTDD resembling the correlation of BDE in Fig. 2. Considering the detonation of nitramides studied as a “zero order” reaction, then the relationships in Figs. 2. and 3. partly reminder the LFER approach, i.e., correlation of rate constants with Hammett substituent parameters<sup>28</sup>.

## Conclusions

The homolytic dissociation of  $N-NO_2$  bond represents the primary fission process of both secondary nitramines and nitramides under thermal, impact, shock and electric spark initiation stimuli. This bond fission is characterized by homolytic bond dissociation energies  $BDE(N-NO_2)$ . The theoretical calculations of  $BDE$  energies are substantially influenced from inadequate treatment of electron correlation. Recently the

alternative method was suggested to overcome this substantial drawback – the bond separation approach described by an isodesmic reaction  $RN-NO_2 + SN-H \rightarrow RN-H + SN-NO_2$  where  $SN-NO_2$  is a standard nitramide (NPO). This type of virtual symmetrical chemical equilibrium, characterized as bond disproportionation reactions, inherently cancel the electron correlation effects accompanying homolytic bond dissociation. The  $BDE$  energies correlate generally tightly with detonation velocities  $D$  of nitramides studied. The analysis of the relationship for  $DISP(N-NO_2)$  leads to finding that the resulting correlations of  $D^2$  values with these energies somewhat remind analogous relationships between the rate and Hammett constants (detonation is taken as a “zero order” reaction in this case). It seems that the mutual correlation of  $D^2$  with  $BDE(N-NO_2)$  values is more limited by molecular structure than a similar correlation with  $DISP(N-NO_2)$  energies.

*This work has been supported by the project of the Ministry of Education, Youth and Sports of the Czech Republic MSM 00221627501.*

## REFERENCES

1. Agrawal J. P., Hodgson R. D.: *Organic Chemistry of Explosives*. Wiley, Chichester 2007.
2. Zeman S., in: *Energetic Materials* (Politzer P., Murray J.S., eds.), part 2, p. 25. Elsevier, Amsterdam 2003.
3. Zeman S.: *J. Hazard. Mater.* 132, 155 (2006).
4. Hehre W. J., Radom L., Schleyer P. v.R., Pople J. A.: *Ab Initio Molecular Orbital Theory*. Wiley, New York 1986.
5. Wiener J. J. M., Murray J. S., Grice M. E., Politzer P.: *Mol. Phys.* 90, 425 (1997).
6. Harris N. J., Lammertsma K.: *J. Am. Chem. Soc.* 119, 6583 (1997).
7. Rice B. M., Sahu S., Owens F. J.: *J. Mol. Struct.* 583, 69 (2002).
8. Zhao Q., Shaowen Z., Li Q. S.: *Chem. Phys. Lett.* 407, 105 (2005).
9. Shao J., Cheng X., Yang X.: *Struct. Chem.* 16, 457 (2005).
10. Su X., Cheng X., Liu Y., Li Q.: *Int. J. Quant. Chem.* 107, 515 (2006).
11. Shao J., Cheng X., Yang X.: *Struct. Chem.* 17, 547 (2006).
12. Zeman S., Pelikán V., Majzlík J., Friedl Z.: *Centr. Eur. J. Energ. Mater.* 3, 27 (2006).
13. Wiener J. J. M., Politzer P.: *THEOCHEM* 427, 171 (1998).
14. Hehre W. J.: *A Guide to Molecular Mechanics and Quantum Chemical Calculations*. Wavefunction, Irvine 2003.
15. Hehre W. J., Ditchfield D., Radom L., Pople J.: *J. Am. Chem. Soc.* 92, 4796 (1970).

16. Friedl Z., Zeman S., in: *Theory & Practice of Energetic Materials* (Wang Y., Huang P., Li S., eds.), vol. VII, p. 410. Science Press, Beijing/New York 2007.
17. TITAN v.1.0.8. Wavefunction, Schrödinger, Irvine 2000.
18. Rothstein L. R., Petersen R.: *Propellants Explos.* 4, 56 (1979).
19. Rothstein L. R.: *Propellants Explos.* 6, 91 (1981).
20. Zeman S., in: *Structure and Bonding*, vol. 125, *High Energy Density Materials* (Klapötke T., ed.), p. 195, Springer, New York 2007.
21. Zhang C., Shu Y., Huang Y., Zhao X., Dong H.: *J. Phys. Chem. B* 109, 8978 (2005).
22. Zhang C., Shu Y., Wang X.: *J. Energ. Mater.* 23, 107 (2005).
23. Zeman S.: *Thermochim. Acta* 384, 137 (2002).
24. Zeman S.: in: *Theory & Practice of Energetic Materials* (Wang Y., Huang P., Li S., eds.), vol. VI, p. 452. Science Press, Beijing/New York 2005.
25. Semenov N. N.: *Some problems of chemical kinetics and of reaction capability*. USSR Acad. Sci., Moscow 1958.
26. Andreev S. G., Babkin A. V., Baum F. A., Imkhovik N. A., Kobylkin I. F., Kolpakov S. V., Ladov V. I., Odintsov V. A., Orlenko L. P., Okhitin V. N., Selivanov V. V., Solovov V. S., Stanyukovich K. P., Chelyshev V. P., Shekhter B. I.: *Fizika vzryva*. Fizmatlit, Moscow 2002.
27. Pepekin V. I., Makhov N. M., Lebedev Yu. A.: *Dokl. Akad. Nauk SSSR* 230, 852 (1977).
28. Exner O.: *Correlation Analysis of Chemical Data*. Plenum Press, New York 1988.

## L05 XRD, FT-IR AND DTA STUDY OF SOOT OBTAINED FROM PYROLYSIS OF USED TIRES

SLAVOMÍR HREDZÁK, SILVIA ČUVANOVÁ and JAROSLAV BRIANČIN

*Institute of Geotechnics of the Slovak Academy of Sciences, Watsonova 45, 043 53 Košice, Slovak Republic, hredzak@saske.sk*

### Introduction

Processing of used tyres by application of pyrolysis can be considered as an advanced and environmentally friendly method. It is concerned thermal degradation of substances by heating in atmosphere without oxygen or atmosphere with decreased content of oxygen. The pyrolysis of used tyres usually results in the following products: pyrolytic oil (35 %) pyrolytic gas (20–25 %), solid residuum containing pyrolytic soot (33 %) and steel wires (10–12 %). The mass yields of pyrolytic products depend on composition of feed to pyrolysis and mainly on the temperature of pyrolytic process<sup>1, 2, 3</sup>.

Thus, the composition of soot coming from a pilot pyrolytic plant for processing of crushed used tires in Slovak leaching works – Chemistry, Inc. Hnúšťa has been studied. The specimens were prepared using a dry low intensity magnetic separation to remove the residues of thin steel wires and other Fe-bearing phases. The products of magnetic separation were subjected to XRD study. Non-magnetic product was analysed using FT-IR and DTA.

The research on grain size composition and treatment of pyrolytic soot is referred in report<sup>4</sup>. The paper<sup>5</sup> deals with the XRD study, analysis of magnetic fractions as well as of material balance of iron and combustible matter at magnetic separation of pyrolytic soot. A detailed study on phase composition of soot magnetic product is introduced in paper<sup>6</sup>.

FT-IR spectra of various types of commercial soot are different in intensity of absorption band, but their position is identical: 3,435  $\text{cm}^{-1}$ , 2,943  $\text{cm}^{-1}$ , 2,860  $\text{cm}^{-1}$ , 1,600  $\text{cm}^{-1}$ , 1,335–1,000  $\text{cm}^{-1}$  and 755–684  $\text{cm}^{-1}$ . This fact is caused by difference in grain size and specific surface<sup>7,8</sup>.

The study of clean carbon blacks and modified soot is reported in papers<sup>9,10,11,12</sup>. The following values of vibrations are introduced: 3,434.7  $\text{cm}^{-1}$ , 1,728.2  $\text{cm}^{-1}$ , 1,711.7  $\text{cm}^{-1}$ , 1,591  $\text{cm}^{-1}$ , 1,278.9  $\text{cm}^{-1}$ , 1,228.9  $\text{cm}^{-1}$ , 1,119.1  $\text{cm}^{-1}$  and 614.3  $\text{cm}^{-1}$ .

The paper<sup>13</sup> describes the synthesis of carbon materials from organic precursors. Prepared carbon materials had absorption lines: 3,423  $\text{cm}^{-1}$ , 1,579  $\text{cm}^{-1}$ , 1,578  $\text{cm}^{-1}$ , 1,509  $\text{cm}^{-1}$ , 1,383  $\text{cm}^{-1}$ , 1,382  $\text{cm}^{-1}$ , 1,343  $\text{cm}^{-1}$ , 1,191  $\text{cm}^{-1}$ , 1,183  $\text{cm}^{-1}$ , 1,159  $\text{cm}^{-1}$ , 841  $\text{cm}^{-1}$ , 798  $\text{cm}^{-1}$ , 693  $\text{cm}^{-1}$ , 692  $\text{cm}^{-1}$ , 624  $\text{cm}^{-1}$  and 620  $\text{cm}^{-1}$ .

Frequencies of vibrations for graphite, amorphous carbon and refined single-wall carbon nanotubes are reported in paper<sup>14</sup>. As to graphite, two weak vibration at 1590  $\text{cm}^{-1}$  and 868  $\text{cm}^{-1}$  are reported<sup>14,15</sup>.

### Techniques and Equipments

#### Magnetic Separation

The specimen of deferrized soot was prepared by dry low-intensity high gradient magnetic separation using an universal laboratory magnetic separator JONES (Fig. 1), in a cassette located between of its poles. The cassette was equipped by two finely grooved plates, made of carbon-free iron owing to ensuring of required magnetic field parameters. The separation was performed at the induction of 0.15 T. The induction has been examined at the top of grooves by tesla-meter with Hall's sensing head.

Magnetic product was screened by dry way on the sieve with a mesh size of 0.3 mm. Thus, steel wires (M-W) and grainy product (M-G) have been obtained. The both products were analyzed separately.

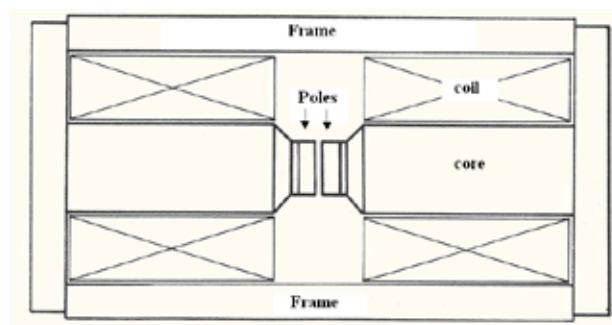


Fig. 1. Design of the JONES separator

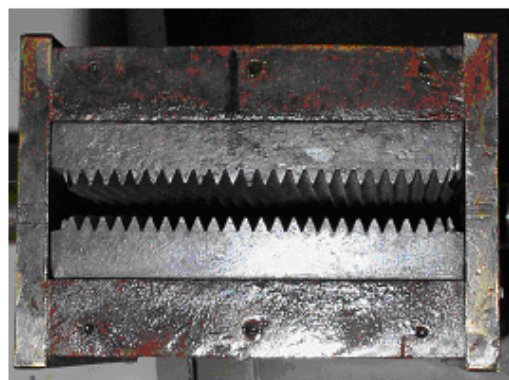


Fig. 2. The cassette equipped by grooved plates

### Material and Products Analyses

After determination of mass yields the products of separation were subjected to chemical analyses and measurements of volume magnetic susceptibility. On the basis of mass yields and chemical analyses the recoveries of observed components into products separation were calculated according to the method of classical material balance.

Loss on ignition (LOI) at 900 °C and  $\text{SiO}_2$  content were assayed gravimetrically. Other elements have been determined by atomic absorption spectroscopy using the device VARIAN with accessories: Fast Sequential AAS AA240FS, Zeeman AAS AA240Z with Programmable Sample

Dispenser PSD120, Graphite Tube Atomizer GTA120 and Vapor Generation Accessory VGA-77.

C, H and N were determined in the Geoanalytical laboratories of the State geological institute of Dionýz Štúr, Spišská Nová Ves using an elementary analysis with thermal conducting detector.

The volume magnetic susceptibility measured using the Kappabridge KLY-2, Geofyzika Brno. The following conditions were applied: a magnetic field intensity of  $300 \text{ Am}^{-1}$ , a field homogeneity of 0.2 %, an operating frequency of 920 Hz at measurement range of device  $-1,999 \times 10^{-6}/+650,000 \times 10^{-6}$  SI unit.

The XRD study of magnetic separation products was performed using the device DRON-UM1 with goniometer GUR-8 at following conditions: radiation  $\text{CuK}\alpha$ , Cu-filter, voltage 30 kV, current 20 mA, step of goniometer  $2^\circ \text{ min}^{-1}$ . The device is equipped by evaluating program developed by PETRA-ARTEP, Ltd. Košice, which operates on the application interface Control WEB2000.

FT-IR spectra were measured by means of spectrometer AVATAR 330 FT-IR ThermoNicolet. KBr tablet technique was applied. Prepared tablets has a diameter of 13 mm.

The tablet consisted of 0.2 g KBr and 0.002–0.003 g of studied specimen (pyrolytic soot and flaky graphite). One tablet was also prepared with half charge of soot. The conditions of measuring were as follows: a range of  $4,000\text{--}400 \text{ cm}^{-1}$ , 64 scans, a resolution of  $4 \text{ cm}^{-1}$ .

Differential thermal analysis was carried out using Derivatograph-C (MOM) equipped by evaluating software WINDER. The measurement has been performed in natural atmosphere up to  $1,000 \text{ }^\circ\text{C}$  at a temperature gradient of  $10 \text{ }^\circ\text{C min}^{-1}$ .

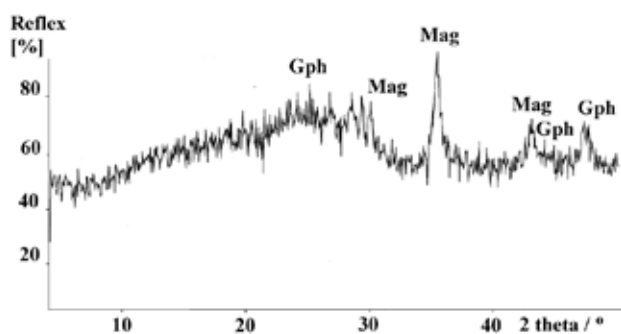


Fig. 3. XRD pattern of M-G product

Table I  
Quality and material balance of separation products

Product	Yield [%]	$\kappa$	Content [%]				Recovery [%]			
			LOI	Fe	Zn	S	LOI	Fe	Zn	S
M-W	1.21	852,267	0.00	98.40	0.22	0.00	0.00	45.93	0.07	0.00
M-G	1.81	107,074	59.60	23.50	2.54	2.83	1.27	16.34	1.19	2.13
N	96.98	1,412	86.72	1.01	3.92	2.43	98.73	37.78	98.74	97.87
feed	100.00	13,620	85.18	2.60	3.85	2.40	100.00	100.00	100.00	100.00

$\kappa$  – volume magnetic susceptibility ( $10^{-6}$  SI unit), LOI – loss on ignition

## Results

### Magnetic Separation

The results of magnetic separation are introduced in Table I. Thus, in such way, a 62.22 % of Fe was removed from soot, whereas obtained Fe-bearing products, namely M-W (steel wires) and M-G (grainy product), attain the Fe content of 98.40 % and 23.50 %, respectively. Naturally, the content of iron clearly corresponds with the value of volume magnetic susceptibility of obtained products. Undesirable elements such as zinc and sulphur, coming from additives at tires production, are bonded with combustible matter of soot. Similarly, a 37.78 % of Fe at a content of 1.01 % remains in deferrized soot.

More detailed chemical composition of defferized soot is given in Table II and III. Thus, under application of dry low-intensity high-gradient magnetic separation the product with carbon content of 80.5 % can be won.

Table II

Composition of deferrized soot

LOI	Fe	Zn	S	$\text{SiO}_2$	Ca	Sum
86.72	1.01	3.92	2.43	4.12	1.13	99.33

Table III

CHN elementary analysis of deferrized soot

C	H	N	R <sup>a</sup>	C/H <sup>b</sup>
80.50	1.80	0.30	17.40	3.75

<sup>a</sup>Difference  $R = 100\% - C(\%) - H(\%) - N(\%)$

<sup>b</sup>Ratio C/H is related to atomic weight ratio

### XRD Study of Magnetic Separation Products

The diffractograms of grainy magnetic product (M-G) and defferized soot are introduced in Fig. 3 and Fig. 4, respectively.

Magnetite and graphite were identified in grainy magnetic product. The defferized soot contains the following mineral phases:

- Gph1 – Graphite – hexagonal,  $a_0 = 2.463$ ,  $c_0 = 6.714$ ,
- Gph2 – Graphite – hexagonal,  $a_0 = 2.456$ ,  $c_0 = 6.696$ ,
- Lon – Lonsdaleite – hexagonal,  $a_0 = 2.52$ ,  $c_0 = 4.12$ ,
- (high pressure modification of carbon),
- Cal – Calcite –  $\text{CaCO}_3$ ,
- Ran – Rankinite –  $\text{Ca}_3\text{Si}_2\text{O}_7$ .

The presence of two forms of graphite is approved by its forked peaks. An enhanced background in the both samples indicates an occurrence of amorphous or cryptocrystalline, primarily carbon phase.

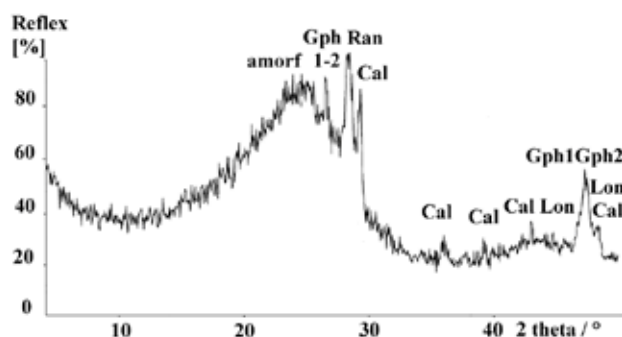


Fig. 4. XRD pattern of deferrized soot

#### FT-IR Study of Deferrized Soot

The FT-IR spectra of deferrized soot are illustrated in Fig. 5 and Fig. 6, respectively. For comparison a FT-IR spectrum of flaky graphite is introduced in Fig. 7. The interpretation of obtained spectra of soot can be as follows:

- 3,431–3,424  $\text{cm}^{-1}$  –  $\nu$  (OH), valence vibrations of –OH bonds, intramolecular H–bond<sup>7</sup>. Vibrations of water, coming from tablet preparation. This band is very conspicuous.
- 2,976–2,852  $\text{cm}^{-1}$  –  $\nu_{\text{as}}$ (CH<sub>3</sub>), group –(C)–CH<sub>3</sub>, valence vibrations of C–H bonds of alkanes, for which is typical forked band in the range of 2,980–2,850  $\text{cm}^{-1}$ .
- 2,064  $\text{cm}^{-1}$  –  $\nu$  (C≡C), group –C≡C–H, very small peak, at larger charge of specimen more visible, it is on the border of belt of the valence vibrations of C≡C bonds. Regarding chemical composition of studied soot it is probably concerned the bond of carbonyl group >C=O with metal. Typical band is in the range of 2,100–2,000  $\text{cm}^{-1}$ .
- 1,635  $\text{cm}^{-1}$ , or more precisely 1,650–1,600  $\text{cm}^{-1}$  at larger charge –  $\nu$  (C=C), group –C=C–C=C–, valence vibrations of conjugated C=C bonds, often two bands, weaker at 1,650  $\text{cm}^{-1}$ , stronger at 1,605  $\text{cm}^{-1}$ . About of 1,600  $\text{cm}^{-1}$  there are also vibration of aromatic C=C bonds and water.
- 1,448–1,350  $\text{cm}^{-1}$  – valence vibration of C–O bonds in the groups COOH.
- 1,107–1,049  $\text{cm}^{-1}$  – valence vibration of C–C bonds.
- 800–700  $\text{cm}^{-1}$  – vibrations of aromatic C=C bonds.

The strong vibration at 1,420  $\text{cm}^{-1}$  as well as weak vibrations at 890–880  $\text{cm}^{-1}$  and 700  $\text{cm}^{-1}$  were also investigated in soot specimen, i.e. all in the fingerprint region (1,500–400  $\text{cm}^{-1}$ ). They can be considered as the peaks of calcite<sup>17</sup>, which was also detected by XRD study.

Authors<sup>14,15</sup> describe weak vibrations for graphite at 1,590  $\text{cm}^{-1}$  and 868  $\text{cm}^{-1}$ . These vibrations were also recorded in studied specimens and in the case of flaky graphite

spectrum, several additional peaks were also detected, probably rests of flotation agents.

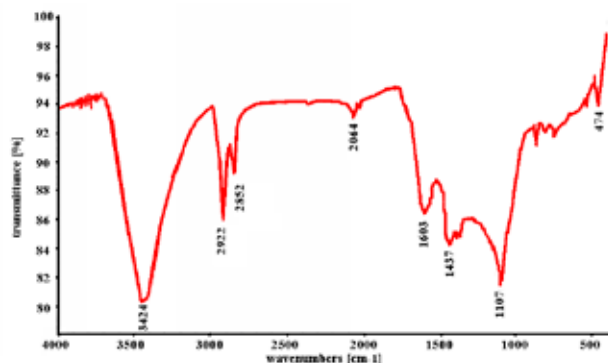


Fig. 5. FT-IR spectrum of deferrized soot

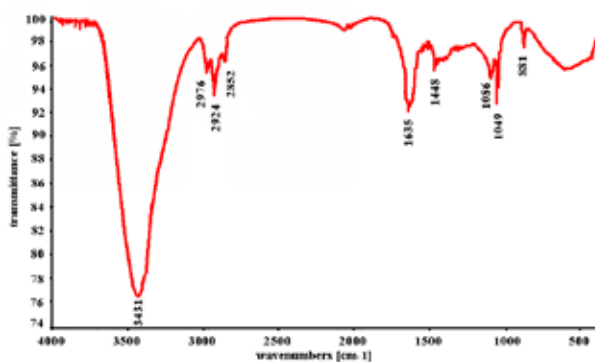


Fig. 6. FT-IR spectrum of deferrized soot – half charge

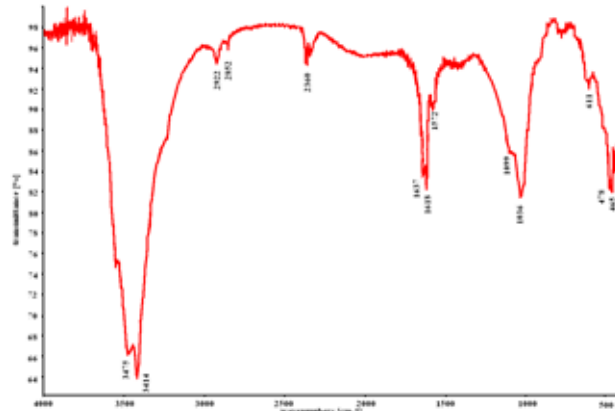


Fig. 7. FT-IR spectrum of flaky graphite

Authors<sup>14</sup> give the following values of vibrations for amorphous carbon: 1,587  $\text{cm}^{-1}$  (middle intensity), 1,250  $\text{cm}^{-1}$  (strong intensity), further without description of intensity: 1,188  $\text{cm}^{-1}$ , 1,168  $\text{cm}^{-1}$ , 1,127  $\text{cm}^{-1}$ , 1,090  $\text{cm}^{-1}$  and 1,045  $\text{cm}^{-1}$ . These vibrations were also observed in spectra of deferrized soot (Fig. 5 and 6). Thus, with regard to results of chemical and XRD analyses, it can be pointed to fact that amorphous carbon occurs in soot.

Subsequently, interpretation of given FT-IR spectra in correlation with chemical analyses can be amended as follows: bands in the region of  $1,150\text{--}1,000\text{ cm}^{-1}$  probably pertain to valence vibrations of  $\text{C--SO}_2\text{--C}$  (also in the region of  $1,376\text{--}1,300\text{ cm}^{-1}$ ) and  $\text{Si--O--Si}$  bonds<sup>18</sup>. A small, but visible peak in the area of  $740\text{--}690\text{ cm}^{-1}$  testifies to a presence of valence bond  $\text{C--S}$ <sup>18</sup>. In the region of  $500\text{--}400\text{ cm}^{-1}$ , namely  $474\text{ cm}^{-1}$  in Fig. 5, there are reported valence vibration of  $\text{Si--O--Si}$  bonds by authors in papers<sup>18,19</sup>. Similarly as to the region of  $500\text{--}400\text{ cm}^{-1}$  other authors<sup>20</sup> introduce for  $\text{Zn--O}$  bonds vibrations at  $532\text{ cm}^{-1}$  and  $473\text{ cm}^{-1}$ , what corresponds with the spectra of studied soot.

#### DTA Study of Defferized Soot

DTA and TG curves are illustrated in Fig. 8. The total mass loss is running about of 85 %, which is in accordance with LOI introduced in Table I and II, respectively.

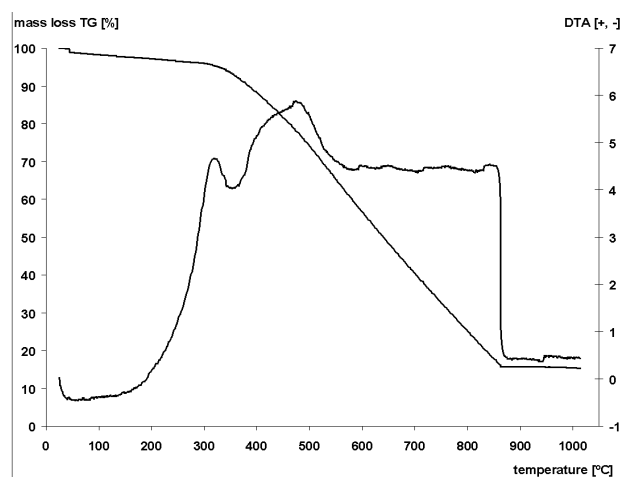


Fig. 8. DTA and TG curves of defferized soot

As to the course of DTA curve a giant exothermic effect can be observed in a temperature interval of  $300\text{--}860\text{ °C}$ . This effect has three tops, namely at  $323, 481$  and  $848\text{ °C}$ . The tops are probably connected with an occurrence of several phases of carbon and/or differences in grain sizes of burning soot.

#### Conclusion

The study of soot coming from pyrolysis of used tires was performed with the aim to verify the possibilities of its treatment and an application in various branches of industry as a secondary raw-material. Special attention was paid to defferized soot.

XRD analysis showed an occurrence of two forms of graphite, lonsdaleite, calcite and rankinite in such soot.

Using FT-IR spectroscopy, graphite and amorphous carbon were identified. Vibrations of functional group of alkanes, alkenes, alkynes and aromatic hydrocarbons have been also observed. Owing to presence of aromatic hydrocarbons bonds it is needed to mention paper<sup>21</sup>, where authors studied bonds of carbon in commercial and pyrolytic soot.

Thus, these carbon blacks are different in the occurrence of aromatic hydrocarbons. Commercial soot, applied in tires production as filler, does not contain any aromatic hydrocarbons and carbon content is higher by 10 %, then in pyrolytic soot. It usually attains 90–97 %.

Other chemical components such as S, Zn, Ca, and  $\text{SiO}_2$  determined in pyrolytic soot coming from original fillers and modifiers added to tire mixtures to obtain required properties.

Finally, studied pyrolytic soot containing of 80.5 % C is not suitable for application in tires production, because carbon content over 95 % is desired. This defferized pyrolytic soot can be used as a filler to asphalt mixture on surface of roads, also in shoe manufacturing industry and generally in production of rubber with lower quality.

*This work was supported by the Slovak Research and Development Agency on the basis of the contract No. APVV-51-035505 and Slovak Grant Agency for the VEGA projects No. 1/4193/07 and 2/7163/27.*

#### REFERENCES

- Sharma V. K., Fortuna F., Mincarini M., Berillo M., Cornacchia G.: *Appl. Energy* 65, 381 (2000).
- Sharma V. K., Mincarini M., Fortuna F., Cognini F., Cornacchia G.: *Energy Convers. Manage.* 39, 511 (1998).
- Chang, Y. M.: *Resour. Conserv. Recycl.* 17, 125 (1996).
- Hredzák S. a kol.: Research report No. 2004SP26, Institute of Geotechnics of the Slovak Academy of Sciences, Košice, 2005.
- Hredzák S., Maceková J., Jakabský Š., Lovás M., Čuvánová S.: *Proc. of the Wastes Recycling X: Deferrization of pyrolytic soot.* (Fečko P. ed.), p. 115. Ostrava 2006.
- Hredzák S., Matik M., Štefušová K., Maceková J.: *Proc. of the 16<sup>th</sup> symposium on Ecology in selected agglomerations of Jelšava-Lubenik and Central Spiš: To occurrence of magnetite in pyrolytic soot.* (Hredzák S., Bindas E. eds.), p. 209. Hrádok 2007.
- Rositani F., Antonucci P. L., Minutoli M., Giordano N.: *Carbon* 25, 325 (1987).
- O'Reilly J. M., Mosher R. A.: *Carbon* 21, 47 (1983).
- Pena J. M., Allen N. S., Edge M., Liauw C. M., Hoon S. R., Valange B., Cherry R. I.: *Polym. Degrad. Stab.* 71, 153 (2001).
- Pena J. M., Allen N. S., Edge M., Liauw C. M., Valange B.: *Polym. Degrad. Stab.* 72, 31 (2001).
- Pena J. M., Allen N. S., Edge M., Liauw C. M., Valange B., Santamaria F.: *Polym. Degrad. Stab.* 74, 1 (2001).
- Pena J. M., Allen N. S., Edge M., Liauw C. M., Valange B.: *Dyes Pigm.* 49, 29 (2001).
- Cudzilo S., Huczko A., Pakula M., Biniak S., Swiatkowski A., Szala M.: *Carbon* 45, 103 (2007).
- Bantignies J. L., Sauvajol J. L.: *Phys. Rev.* B74, 195, 425 (2006).
- Kuhlmann U., Jantoljak H., Pfänder N., Bernier P., Journet C., Thomsen C.: *Chem. Phys. Lett.* 294, 237 (1998).

16. Patrik Kania: Infrared spectroscopy. [http://www.vscht.cz/anl/lach1/7\\_IC.pdf](http://www.vscht.cz/anl/lach1/7_IC.pdf)
17. <http://lms.vscht.cz/Zverze/Knihovna.htm>
18. Oréface R. L, Henchb L. L., Brennan A. B.: *J. Braz. Chem. Soc.* 11, 78 (2000).
19. Russell J. D.: *Clay Miner.* 14, 127 (1979).
20. Kwon Y. J., Kima K. H., Limb C. S., Shim K. B.: *J. Ceram. Process. Res.* 3, 146 (2002).
21. Roy C., Chala A., Darmstadt H.: *J. Anal. Appl. Pyrolysis* 51, 201 (1999).

## L06 DETERMINATION OF THE YIELD OF SODA-ANTHRAQUINONE SEMICHEMICAL PULP FROM HARDWOOD MIXTURE

MICHAL LETKO, ERIKA NOVÁKOVÁ and MILAN VRŠKA

*Department of Chemical Technology of Wood, Pulp and Paper, Faculty of Chemical and Food Technology, Slovak University of Technology, Radlinského 9, 812 37, Bratislava, Slovakia, michalletko@stuba.sk*

### Introduction

In cooperation with the NovaCell project, a central European NSSC mill, Kappa Štúrovo in Slovakia, has converted to sulphur-free production during 2004. It is a new and sulphur free process concept for manufacturing of chemical and semi chemical fibres. The starting point for the development of NovaCell process has been a 2-stage cooking process, consisting of a mild pre-hydrolysis stage with AQ in aqueous environment followed by a cooking stage with alkali. New technology consumes a cooking liquor compound from sodium hydroxide and sodium carbonate for delignification. SAQ pulp is made from mixture of three hardwood species – hornbeam, birch and poplar.

The first results for different wood resources indicated a great potential to reduce the wood consumption at a given production rate or conversely, at a given wood consumption level, the pulp production can be increased considerably compared to the Kraft process. Therefore one of the Novacell aims is high yield, higher than a modern kraft. A higher pulp yield will also contribute to a better use of the capital employed in the pulp mills<sup>1</sup>.

Wood is the dominant cost factor for a pulp mill. Pulp yield has a major impact on the competitiveness of a mill<sup>2</sup>. In order to optimize pulp yield, for example by changing the operating conditions, a mill must be able to monitor the yield accurately. Traditionally, pulp yield is estimated based on wood usage and pulp sales data covering a period of 3–6 months to eliminate the mill operation dynamics. However, this approach can not be used to monitor yield changes occurring for brief periods, e.g., during evaluation of process modifications<sup>3</sup>. There are two general approaches available to measure mill pulp yield: the direct and indirect methods. In the direct pulp measurement method the yield is determined from the wood and pulp mass or mass flow rates. The indirect pulp yield measurement methods rely on measurement of pulp or spent pulping liquor properties to determine the yield using pre-established “calibration curves”. The semichemical SAQ pulp yield is estimated by methodology developed by Duranti<sup>4</sup> and improved by Kovács and Pavlik<sup>5</sup>. It is based on dependence of semichemical pulp yield in % from specific mass according wood species charge. Woitkovich pointed out the importance of knowing the relationship between pulp properties and yield and using of indirect methods for unmeasurability of yield and measurability of physical properties<sup>6</sup>. Since there is not an explicit relationship between yield

and inputs, our aim was to find a mathematical relationship between yield and charge of different species of hardwoods and charge of alkali. We had a concept of a usable equation for industry, in particular for the Smurfit Kappa Štúrovo mill. There are still problems for technologists at the place.

We would like to consider which of the parameters is ruling and statistically significant. By means of mixed cooking we managed to study not only total yield but also yields of individual species of wood. This allows to compare the rate of cooking and reciprocal influences<sup>7</sup>.

### Experimental

#### Materials

For the experiment we used chips from Smurfit Kappa Štúrovo a.s. woodyard. Chips from three species of hardwoods (hornbeam, birch, poplar) were used for cooking SAQ semichemical pulp. Dry matter of the chips before cooking (hornbeam = 93.5 %, birch 94 %, poplar = 94.5 %) and their fractionation have been defined. Screenings from sieve with 0.705 cm mesh were used for cooking.

The cooking liquor was mixed from black and green liquor from Smurfit Kappa Štúrovo a.s. Acid-base titration was used for determination of sodium hydroxide and sodium carbonate.

Green liquor:

concentration: NaOH = 27.94 g dm<sup>-3</sup> as Na<sub>2</sub>O  
Na<sub>2</sub>CO<sub>3</sub> = 71.14 g dm<sup>-3</sup> as Na<sub>2</sub>O  
Total alkali = 99.08 g dm<sup>-3</sup> as Na<sub>2</sub>O

Black liquor:

concentration: Na<sub>2</sub>CO<sub>3</sub> = 48.67 g dm<sup>-3</sup> as Na<sub>2</sub>O  
NaOH = 0 g dm<sup>-3</sup> (consumed)  
Total alkali = 48.67 g dm<sup>-3</sup> as Na<sub>2</sub>O

#### Cooking

Cooking was carried out in a 1 dm<sup>3</sup> autoclaves electrically heated in silicone oil. 100 g of oven-dry chips with hydromodule (liquor/wood rate) 3 were added. The charge of anthraquinone was 0.5 % for oven-dry wood. Cooking temperature was 170 °C for 60 minutes (cooking time).

Cooking curve was recorded by help of a digital thermometer. Alkali charge was calculated from determined sodium hydroxide in green liquor.

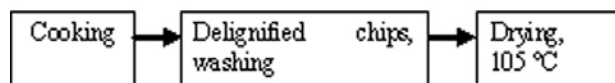


Fig. 1. Experimental procedures

When mixed cooking is carried out, reduction of liquor concentration is followed by the influence of more accelerated cooking of some species. However, this effect changes the conditions for other ones. This is why we wanted both total and partial yield of each wood specie. The same conditions have been provided for each wood in autoclave (separated by permeable barrier). It was entered with stainless steel bars. Calculated and weighed volumes of chips were put into

stainless container gradually. Each specie was covered with stainless steel bar. Full cooking container was inserted into autoclave and flooded with the volume of green liquor as shown in Table II. The volume was topped up to 300 ml with black liquor. When oil in boiler reached 170 °C, the prepared autoclaves were inserted. It is possible to cook three autoclaves in our boiler.

After 60 minutes the autoclaves were removed from the boiler and cooled down. Then, the autoclaves were opened and each wood specie had been washed for 48 hours in permeable polyamide bags. After cooking the liquor was taken for analysis. Washed chips were dried at 105 °C. Oven-dry chips were weighed and the yield was determined gravimetrically.

### Experimental Design

Central composite rotatable design (CCRD) was used in this study<sup>8</sup>. The design consists of a three-factored ( $n = 3$ ) factorial design with two levels. The levels, codes and interval of variation of the independent variables are given in the Table I, while the treatment combinations with responses are presented in Table III. The process variables considered were charge of hornbeam (16.4–70 g), birch/poplar ratio (0.16–1.84) and charge of alkali expressed as  $\text{Na}_2\text{O}$  (6.7–7.7 %). Center composite design was used to show the effect of charge of different hardwood and alkali charges on the pulp yield in 20 runs of which 6 were for the center point, and 14 were for noncenter point with axial distance of 1.6818 ( $\alpha = 2^{n/4}$ ). The following second order polynomial response surface model (1) was fitted to each of the response variable where  $b_0$ ,  $b_i$ ,  $b_{ii}$ , and  $b_{ij}$  are the constant, linear, quadratic and cross-product regression coefficients, respectively,  $X_i$ 's are the coded independent variables of  $X_1$  (hornbeam, g),  $X_2$  (ratio birch/poplar) and  $X_3$  (alkali charge, %).

$$Y = b_0 + \sum_{i=1}^3 b_i X_i + \sum_{i=1}^3 b_{ii} X_i^2 + \sum_{i \neq j=1}^3 b_{ij} X_i X_j \quad (1)$$

Table I  
Coded and uncoded levels of three variables used in cooking of hardwood mixture

Variables		Levels					Semi-range
		-1.682	-1	0	1	1.682	
Hornbeam [g]	X1	16.4	30	50	70	70	20
Birch/Poplar	X2	0.16	0.5	1	1.5	1.84	0.5
$\text{Na}_2\text{O}$ [%]	X3	6.7	6.9	7.2	7.5	7.7	0.3

A three-dimensional response surface and contour plots of independent variables and their interactions were generated using the Statgraphics plus. Optimization of SAQ cooking was aimed at establishing appropriate levels within the independent variables such as charge of hornbeam, birch/poplar ratio and alkali charge.

Table II  
Real quantities for responsible levels used in cooking of hardwood mixture

Variables	Levels				
	-1.682	-1	0	1	1.682
Hornbeam [g]	16.4	30	50	70	88.6
Birch [g]	6.9	16.7	25	30	32.4
Poplar [g]	43.1	33.3	25	20	17.6
Charge of green green liquor [ml]	240	247	258	268	276

### Results

The effect of hornbeam, birch/poplar ratio and alkali charges on the yield was investigated using the CCRD statistical model. The observations for total yield, hornbeam yield, birch yield and poplar yield with different combinations of the process parameters are presented in Table III. Response surface analysis was applied to the experimental data using Statgraphic plus. The second-order polynomial response surface model (1) was fitted to each of the response variable (Y). Estimated regression coefficients of the quadratic polynomial models for the response variables, along with the corresponding  $R^2$  and P-values, are given in Table IV. The coefficient of determination ( $R^2$ ) values of all responses are quite high ( $>0.8$ ) The highest (nearly 0.9) in case of total yield and the lowest in case of yield of birch.

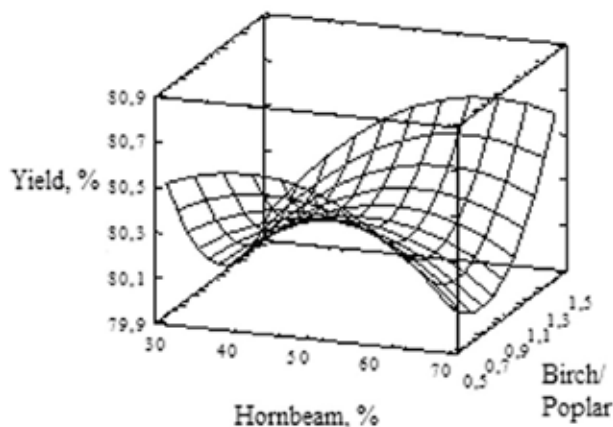


Fig. 2. Saddle 3D response surface of the effect of hornbeam charge and birch/poplar ratio on total yield of SAQ semichemical pulp from hardwood mixture when the alkali charge was constant 7.2 % as  $\text{Na}_2\text{O}$

By analysis of solid residue after delignification according to treatment combinations of experiments of CCRD the values of yields were obtained. Predictive equation (2) for total yield of SAQ pulp was acquired from non-linear regression analysis.

Assessment of the effect of individual regression coefficients claimed that alkali charge has the most significant influence on pulp yield; negative sign indicates that this influence is negative. Its influence is statistically significant

in all cases (P-value is less than 0.05). Negative effect of this trend is demonstrated in combinations with other parameters (in particular hornbeam charge). However, this impact is not always statistically significant.

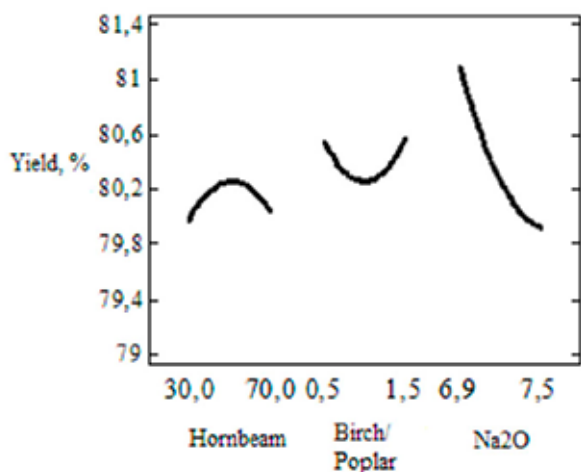


Fig. 3. Influence of variables on total yield of SAQ semichemical pulp from hardwood mixture

The second important factor which can influence the yield of semichemical pulp is the birch/poplar ratio in the processed mixture. Moreover, the yield will be influenced mainly by poplar charge in the mixture which was cooked at the slowest rate in our conditions (Table III). Its effect is

negative for total yield and for poplar yield. Approximate poplar yield is not more than 2 % compared to semichemical pulp from birch and hornbeam.

Optimal values of yields and the conditions in which it is possible to get them can be read from local maximums and minimums shown in Fig. 3. Dominant position of the effect of alkali charge is confirmed by the drop of yield in dependence upon of 1 % alkali charge. The effect of other parameters is within several few tenths of percent. Generally, the results give numerous possibilities and combinations how to evaluate the effect of individual variables on the monitored result, in this case the yield. The canonical analysis indicated that the predicted response surface is a saddle shaped as depicted in Fig. 2.

Since the method applied is taken after preliminary analysis for determine optimal process parameters to acquire the desired (min, max) result, in Table V a combination of optimal parameters for acquirement of maximum yield is presented. In our case it is not clear whether maximum yield is the suitable result. It is necessary to compare and evaluate the other qualitative parameters, for example chemical composition.

$$Y = 225.84 + 0.34X_1 - 3.04X_2 - 40.46X_3 - 0.00061X_1^2 + 1.19X_2^2 + 2.83X_3^2 + 0.02X_1X_2 - 0.08X_2X_3 - 0.04X_1X_3 \quad (2)$$

Table III

Treatment combinations for SAQ cooking with 3 variable 2<sup>nd</sup>-order response surface model designs

Runs	Coded variables			Un-coded variables			Response			Total yield
	X <sub>1</sub>	X <sub>2</sub>	X <sub>3</sub>	Hornbeam	Birch/Poplar	Na <sub>2</sub> O	Yield of hornbeam	Yield of birch	Yield of poplar	
1	0	0	0	50	1	7.2	78.5	80.9	80.0	79.8
2	0	0	0	50	1	7.2	80.4	80.8	80.4	80.5
3	1.682	0	0	88.6	1	7.2	79.8	77.2	84.2	80.4
4	-1.682	0	0	16.4	1	7.2	80.5	80.1	82.1	80.9
5	0	1.682	0	50	1.84	7.2	78.9	80.1	81.6	80.2
6	0	-1.682	0	50	0.16	7.2	79.1	78.6	80.7	79.5
7	0	0	0	50	1	7.2	78.8	80.8	79.6	79.7
8	1	1	-1	70	1.5	6.9	79.1	78.9	80.0	79.3
9	0	0	0	50	1	7.2	79.6	79.6	82.0	80.4
10	0	0	-1.682	50	1	6.7	79.8	80.0	81.2	80.3
11	-1	-1	-1	30	0.5	6.9	79.0	75.7	83.2	79.3
12	0	0	0	50	1	7.2	79.0	80.4	80.8	80.1
13	-1	1	1	30	1.5	7.5	79.7	78.8	82.5	80.3
14	0	0	0	50	1	7.2	79.2	78.0	80.0	79.1
15	1	-1	-1	70	0.5	6.9	80.6	80.0	81.5	80.7
16	0	0	1.682	50	1	7.7	79.0	78.4	82.0	79.8
17	1	1	1	70	1.5	7.5	77.7	77.8	82.5	79.3
18	-1	1	-1	30	1.5	6.9	78.7	78.1	79.6	78.8
19	-1	-1	1	30	0.5	7.5	77.0	77.4	80.9	78.4
20	1	-1	1	70	0.5	7.5	77.6	77.0	77.5	78.0

Table IV

Estimated coefficients for determination of semichemical pulp yield and P-values of statistical significance

Estimated coefficients	Influenced parameter	Total yield		Yield of hornbeam		Yield of birch		Yield of poplar	
		Estimate	P-value	Estimate	P-value	Estimate	P-value	Estimate	P-value
b <sub>0</sub>		225.84		198.77		254.98		224.064	
b <sub>1</sub>	X <sub>1</sub>	0.34	0.7415	0.53	0.4328	0.314	0.544	0.184	0.4989
b <sub>2</sub>	X <sub>2</sub>	-3.04	0.8957	2.39	0.7966	5.142	0.650	-16.44	0.6543
b <sub>3</sub>	X <sub>3</sub>	-40.46	0.0001*	-35.43	0.0004*	-49.32	0.001*	-36.7497	0.0017
b <sub>11</sub>	X <sub>12</sub>	-0.00061	0.0202*	-0.0003	0.2433	-0.001	0.048*	-0.00069	0.0459
b <sub>22</sub>	X <sub>22</sub>	1.19	0.0076*	0.58	0.1728	1.82	0.013*	1.1559	0.0387
b <sub>33</sub>	X <sub>32</sub>	2.83	0.0172*	2.58	0.0392*	3.484	0.065	2.425	0.1025
b <sub>12</sub>	X <sub>1</sub> X <sub>2</sub>	0.02	0.0666	-0.034	0.0280*	0.031	0.155	0.0763	0.0009
b <sub>23</sub>	X <sub>2</sub> X <sub>3</sub>	-0.08	0.9269	-0.25	0.7812	-1.417	0.320	1.417	0.2216
b <sub>13</sub>	X <sub>1</sub> X <sub>3</sub>	-0.04	0.0599	-0.065	0.0146*	-0.035	0.320	-0.027	0.3423
r <sub>2</sub>		88.70		84.26		81.88		85.42	

\* value is statistically significant if P&lt;0.05

Table V

Optimal values for maximal yield

	Optimal values			
	Total	Hornbeam	Birch	Poplar
Yield [%]	83.62	82.77	84.12	84.55
Hornbeam [%]	83.64	83.64	72.41	51.61
Ratio birch/poplar	1.84	0.39	1.79	0.16
Na <sub>2</sub> O [%]	6.70	6.70	6.70	6.70

### Conclusions

Because yields of different wood species were monitored in cooking of mixed hardwoods in addition to total yield, we are able to assess the changes of individual species when delignification is influenced by changes in alkali concentration. It varies according to the rate of delignification of individual wood species. It is possible that quickly delignified wood reduces the alkali concentration. Consequently, alkali concentration is not sufficient for wood with slower delignification. Again, this rate is more reduced with decreasing alkali concentration.

By the yields comparison of investigated wood species we found out that in mixed cooking dawns the slowest drop of yield in the case of poplar. Throughout the range upper yield up to 2 % was established in the all range. Birch and hornbeam wood mass drops were almost equal.

The information about yields of individual wood species from mixed cooking were processed to the following dependence (equation): yield = f(wood charge, alkali charge). It can be said on the basis of the coefficients in the equation

that alkali and poplar charges show the highest effect on pulp yield. The effect of hornbeam charge in hardwood mixture was insignificant.

*We thank Slovak Grant Agency (Project VEGA 1/0770/08) for its financial support. The authors express their thanks to E. Szabó and M. Babinec from Smurfit Kappa Sturovo a.s. for cooperation.*

### REFERENCES

1. Stigsson L., Berglin N., Olm L., Tormund D., Tomani P., Hakansdotter-Palm L., Delin L.: *SPCI Conference: Sulphur-free pulping – The Novacell Process*. Stockholm, 2005.
2. Van Heiningen A.R.P., Gao Y., Da Silva Perez D.: *7th EWLP Conference*, p. 63. Turku, Finland, 2002.
3. Easty D. B., Malcolm E. W.: *Tappi J.* 65, 78 (1982).
4. Duranti D., Colapietro M.: *Cellulosa Carta* 18, 3 (1967).
5. Kovacs V., Pavlik S.: *Papir Celuloza* 37, 39 (1982).
6. Woitkovich P.C.: *Mechanical pulping. Annual research review*. Project 3716, pp. 49-80. Inst. Paper Sci. Technol. Atlanta, Georgia 1991.
7. Letko M.: *Diploma thesis*, FCHPT-STU, Bratislava, Slovakia, 2007.
8. <http://www.itl.nist.gov/div898/handbook/>. NIST/SEMATECH e-Handbook of Statistical Methods. 14. February 22, 2005.

## 5.2. Posters

### P01 LITHIUM BROMIDE MEDIATED SYNTHESIS AND X-RAY ANALYSIS OF BISARYLMETHYLIDENES OF PIPERIDINONE SYSTEM

M. SAEED ABAEE<sup>a</sup>, MOHAMMAD M. MOJTAHEDI<sup>a</sup>, ROHOLAH SHARIFI<sup>a</sup>, A. WAHID MESBAH<sup>a</sup> and WERNER MASSA<sup>b</sup>

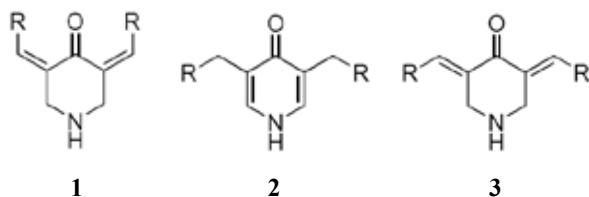
<sup>a</sup>Department of Organic Chemistry, Chemistry & Chemical Engineering Research Center of Iran, P.O. Box 14335–186, Tehran, Iran,

<sup>b</sup>Fachbereich Chemie der Philipps-Universität Marburg, Hans-Meerwein-Strasse, D-35032 Marburg, Germany, abae@ccerci.ac.ir

#### Introduction

Bis(arylmethylidene)cycloalkanones as very important biologically active intermediates<sup>1</sup>, are generally synthesized via aldol condensation of homocyclic ketones with aromatic aldehydes<sup>2</sup>. So far, several procedures have appeared in the literature for the synthesis of these compounds using Lewis acid catalysis<sup>3</sup>, solid-supported reactions<sup>4</sup>, ionic liquids<sup>5</sup> microwave irradiation<sup>4a</sup>, and ultrasound mediation<sup>4b</sup>.

In contrast, on the heterocyclic counter part much less development is achieved. In this regard, we recently disclosed Lewis acid catalyzed synthesis of several novel bisarylmethylidene derivatives of pyranone<sup>6</sup>, thiopyranone<sup>7</sup>, piperidinone<sup>8</sup>, dioxanone<sup>9</sup> and cyclohexenone<sup>10</sup> structures using very straight forward synthetic methods. The structure of these products was assigned logically based on their spectroscopic characterization. However, to distinguish between the possible isomers (Scheme 1) and to verify the proposed geometry we decided to determine the crystal structure of representative compounds.



Scheme 1

In the present article, a convenient and rapid procedure is offered for the synthesis of bis(arylmethylidene)piperidin-4-ones under catalysis of LiBr which has found many applications as a mild Lewis-acid in recent years to ease up various synthetic organic transformations.<sup>11</sup> The X-ray structure analysis of the *p*-methoxyphenyl derivative confirms the presence of exocyclic double bonds in the products in *Z-Z* configuration **3** (Scheme 1).

#### Experimental

##### General

Reactions were monitored by TLC. NMR spectra were obtained on a FT-NMR Bruker Ultra Shield™ (500 MHz) as CDCl<sub>3</sub> or DMSO-*d*<sub>6</sub> solutions and the chemical shifts were expressed as  $\delta$  units with Me<sub>4</sub>Si as the internal standard. All chemicals and reagents were purchased from commercial sources.

##### Typical Procedure

A mixture of **4** (Table II) (5.0 mmol), an aldehyde (5.0 mmol), LiBr (0.5 mmol), and Et<sub>2</sub>NH (10.0 mmol) in CH<sub>2</sub>Cl<sub>2</sub> (15 ml) was stirred in a flask. Complete disappearance of the starting materials was observed within 2–3 hours by TLC. The mixture was diluted by dichloromethane and washed twice by water. The organic phase was dried over Na<sub>2</sub>SO<sub>4</sub>, the solvent was removed at reduced pressure and the product was precipitated after removal of the volatile portion. The structures of the products were assigned by spectroscopic methods.

##### Spectral Data

**3a**: IR [cm<sup>-1</sup>]: (KBr)  $\nu$  3,235 (NH), 1,665 (C=C), 1,593 (C=O); <sup>1</sup>H NMR [ppm]: (CDCl<sub>3</sub>)  $\delta$  1.68 (s, 1H, NH), 4.21 (s, 4H, H<sub>2</sub>C–N–CH<sub>2</sub>), 7.40–7.48 (m, 10H, Ar), 7.86 (s, 2H, CH=C); <sup>13</sup>C NMR [ppm]: (CDCl<sub>3</sub>)  $\delta$  48.6 (NCH<sub>2</sub>), 128.9, 129.5, 130.9, 135.4, 135.6, 136.4, 188.4 (C=O).

**3b**: IR [cm<sup>-1</sup>]: (KBr)  $\nu$  3,289 (NH), 1,657 (C=C), 1,579 (C=O); <sup>1</sup>H NMR [ppm]: (CDCl<sub>3</sub>)  $\delta$  1.74 (s, 1H, NH), 2.43 (s, 6H, CH<sub>3</sub>), 4.18 (s, 4H, H<sub>2</sub>C–N–CH<sub>2</sub>), 7.26 (d, *J* = 8 Hz, 4H, Ar), 7.32 (d, *J* = 8 Hz, 4H, Ar), 7.82 (s, 2H); <sup>13</sup>C NMR [ppm]: (CDCl<sub>3</sub>)  $\delta$  21.9 (CH<sub>3</sub>), 48.6 (NCH<sub>2</sub>), 129.7, 131.1, 132.9, 134.8, 136.3, 139.8, 188.4 (C=O).

**3c**: IR [cm<sup>-1</sup>]: (KBr)  $\nu$  3,242 (NH), 1,667 (C=C), 1,509 (C=O); <sup>1</sup>H NMR [ppm]: (CDCl<sub>3</sub>)  $\delta$  1.72 (s, 1H, NH), 3.90 (s, 6H, OCH<sub>3</sub>), 4.19 (s, 4H, H<sub>2</sub>C–N–CH<sub>2</sub>), 6.98 (d, *J* = 9 Hz, 4H, Ar), 7.40 (d, *J* = 9 Hz, 4H, Ar), 7.81 (s, 2H, CH=C); <sup>13</sup>C NMR [ppm]: (CDCl<sub>3</sub>)  $\delta$  48.6 (NCH<sub>2</sub>), 55.8 (OCH<sub>3</sub>), 114.5, 128.4, 132.9, 133.6, 136.1, 160.7, 188.3 (C=O).

**3d**: IR [cm<sup>-1</sup>]: (KBr)  $\nu$  3,301 (NH), 1,657 (C=C), 1,584 (C=O); <sup>1</sup>H NMR [ppm]: (CDCl<sub>3</sub>)  $\delta$  1.77 (s, 1H, NH), 4.15 (s, 4H, H<sub>2</sub>C–N–CH<sub>2</sub>), 7.35 (d, *J* = 8.5 Hz, 4H, Ar), 7.43 (d, *J* = 8.5 Hz, 4H, Ar), 7.78 (s, 2H, CH=C); <sup>13</sup>C NMR [ppm]: (CDCl<sub>3</sub>)  $\delta$  48.5 (NCH<sub>2</sub>), 129.3, 132.1, 134.0, 135.1, 135.6, 135.7, 187.9 (C=O).

**3e**: IR [cm<sup>-1</sup>]: (KBr)  $\nu$  3,240 (NH), 1,668 (C=C), 1,585 (C=O); <sup>1</sup>H NMR [ppm]: (DMSO-*d*<sub>6</sub>)  $\delta$  3.40 (s, 1H, NH), 4.14 (s, 4H, H<sub>2</sub>C–N–CH<sub>2</sub>), 7.37 (d, *J* = 8 Hz, 4H, Ar), 7.60 (d, *J* = 8 Hz, 4H, Ar), 7.64 (s, 2H, CH=C).

**3f**: IR [cm<sup>-1</sup>]: (KBr)  $\nu$  3,350 (NH), 1,650 (C=C), 1,605 (C=O); <sup>1</sup>H NMR [ppm]: (CDCl<sub>3</sub>)  $\delta$  1.70 (s, 1H, NH), 3.43 (s, 4H, H<sub>2</sub>C–N–CH<sub>2</sub>), 3.74 (s, 12H, OCH<sub>3</sub>), 3.88 (s, 6H, OCH<sub>3</sub>), 6.13 (s, 4H, Ar), 7.70 (s, 2H, CH=C); <sup>13</sup>C NMR [ppm]: (CDCl<sub>3</sub>)  $\delta$  54.2 (NCH<sub>2</sub>), 55.7 (OCH<sub>3</sub>), 55.9 (OCH<sub>3</sub>), 90.8, 107.2, 129.8, 134.9, 159.6, 162.4, 188.0 (C=O).

**3g**: IR [cm<sup>-1</sup>]: (KBr)  $\nu$  3,291 (NH), 1,647 (C=C), 1,581 (C=O); <sup>1</sup>H NMR [ppm]: (CDCl<sub>3</sub>)  $\delta$  1.85 (s, 1H, NH), 4.22 (s, 4H, H<sub>2</sub>C–N–CH<sub>2</sub>), 7.19 (dd,  $J$  = 4, 4.5 Hz, 2H), 7.38 (d,  $J$  = 4 Hz, 2H), 7.60 (d,  $J$  = 4.5 Hz, 2H), 7.98 (s, 2H, CH=C); <sup>13</sup>C NMR [ppm]: (CDCl<sub>3</sub>)  $\delta$  48.2 (NCH<sub>2</sub>), 127.5, 128.6, 131.3, 133.0, 133.6, 139.1, 187.0 (C=O).

Table I  
Crystal and experimental data for **3b**

Empirical formula	C <sub>21</sub> H <sub>21</sub> NO <sub>3</sub>
Formula weight	335.39
Temperature	153(2) K
Wavelength	0.71073 Å
Habitus, color	needle, light-yellow
Crystal size	0.39 × 0.12 × 0.06 mm <sup>3</sup>
Crystal system	orthorhombic
Space group	Cmc2 <sub>1</sub> , Z = 4
Unit cell dimensions	a = 37.748(5) Å b = 7.3077(10) Å c = 6.0658(9) Å
Volume	1,673.3(4) Å <sup>3</sup>
Density (calculated)	1.331 mg m <sup>-3</sup>
Absorption coefficient	0.089 mm <sup>-1</sup>
F(000)	712
Diffractometer type	IPDS-II
Theta range for data collection	2.16 to 27.09 °
Index ranges	-48 ≤ h ≤ 48, -9 ≤ k ≤ 9, -7 ≤ l ≤ 7
Reflections collected	6,300
Independent reflections	1,023 [R(int) = 0.1296]
Completeness to theta = 26.30 °	99.6 %
Observed reflections	619 [I > 2σ(I)]
Refinement method	Full-matrix least-squares on F <sup>2</sup>
Data/restraints/parameters	1,023/1/121
Goodness-of-fit on F <sup>2</sup>	0.826
R indices (all data)	R1 = 0.0756, wR2 = 0.0854
Final R indices [I > 2σ(I)]	R1 = 0.0396, wR2 = 0.0762
Largest diff. peak and hole	0.130 and -0.187 e.Å <sup>-3</sup>

#### X-ray Crystal Structure Analysis

A crystal of **3b** was investigated on an IPDS II area detector system (Stoe) at -120 °C using MoK $\alpha$ -radiation. Crystal and experimental data are given in Table I.

The structure was solved by direct methods in space group Cmc2<sub>1</sub> and refined using the SHELX97 programs<sup>12</sup> with anisotropic displacement parameters for all C and O atoms. All hydrogen atoms were located from a difference Fourier map but H4 at N4 only was refined. The others were kept riding on idealized positions with isotropic displacement parameters taken as 1.2U<sub>eq</sub> (1.5U<sub>eq</sub> for CH<sub>3</sub>) of their bonding

partners. No absorption or extinction correction was applied. The absolute structure was not determined, the Friedel pairs were merged. Crystallographic data (excluding structure factors) for the structure reported in this paper have been deposited with the Cambridge Crystallographic Data Center as supplementary publication no. CCDC-689654. Copies of the data can be obtained free of charge on application to CCDC, 12 Union Road, Cambridge CB2 1EZ, UK [Fax: int. Code + 44(1223)336-033; E-mail: deposit@ccdc.cam.ac.uk or via www.ccdc.cam.ac.uk/conts/retrieving.html]

#### Results

An equimolar mixture of piperidin-4-ones **4** and an aldehyde (as listed in Table II) was treated with LiBr (10 % mol) and Et<sub>3</sub>NH in dichloromethane. Complete conversion of the starting materials to the desired product was observed within 2–3 hours as reactions were monitored by TLC. Control experiments confirmed the combined promoting and catalytic effects of LiBr; an alternative reaction in the absence of the catalyst led to formation of less than 10 % of the product after 24 hours.

The structure of the products was assigned with spectroscopic methods and compared with the literature data. In order to verify this structure, a single crystal of **3b** was prepared and investigated by X-ray diffraction. The result, as depicted in Fig. 1, clearly supports the proposed structure with exocyclic double bonds C2–C5 and C2'–C5'.

Table II  
LiBr catalyzed aldol condensation reactions of **4**

ArCHO	Product	M.P.[°C]	Yield[%]	
benzaldehyde	<b>3a</b>	175–177	92	
( <i>p</i> -MeO)benzaldehyde	<b>3b</b>	196–197	93	
( <i>p</i> -Me)benzaldehyde	<b>3c</b>	180–181	90	
( <i>p</i> -Cl)benzaldehyde	<b>3d</b>	192–194	88	
( <i>p</i> -Br)benzaldehyde	<b>3e</b>	207–208	87	
2,4,6-(MeO <sub>3</sub> )C <sub>6</sub> H <sub>2</sub> CHO	<b>3f</b>	198–199	88	
2-thiophenecarbaldehyde	<b>3g</b>	205–206	91	

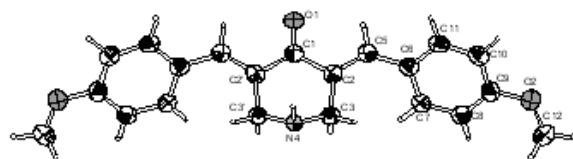


Fig. 1. Structure of **3b** at 153 K in the crystal. Displacement ellipsoids at 50% probability level. Bond lengths C1–C2 1.486(4), C2–C3 1.521(4), C2–C5 1.340(4) Å

### Conclusions

In summary, a LiBr promoted aldol condensation of piperidin-4-ones **4** with various aldehydes was carried out within few hours. Reactions proceeded with catalytic amounts of the Lewis acid, and use of harsh conditions and tedious work up procedures were avoided. High yields of the products and rapid completion of the reactions are among other advantages of this methodology. The proposed structure was confirmed by single crystal X-ray diffraction analysis.

*This work has been partially supported by the Ministry of Science, Research, and Technology of Iran.*

### REFERENCES

- (a) Deli J., Lorand T., Szabo D., Foldesi A.: *Pharmazie* **39**, 539 (1984).;  
(b) Guilford W. J., Shaw K. J., Dallas J. L., Koovakkat S., Lee W., Liang A., Light D. R., McCarrick M. A., Whitlow M., Ye B., Morrissey M. M.: *J. Med. Chem.* **42**, 5415 (1999).
- (a) Hathaway B. A.: *J. Chem. Educ.* **64**, 367 (1987);  
(b) Zheng M., Wang L., Shao J., Zhong Q.: *Synth. Commun.* **27**, 351 (1997);  
(c) Iranpoor N., Kazemi E.: *Tetrahedron* **54**, 9475 (1998);  
(d) Nakano T., Migita T.: *Chem. Lett.* 2157 (1993).
- (a) Wang L., Sheng J., Tian H., Han J., Fan Z., Qian C.: *Synthesis* 3060 (2004);  
(b) Sabitha G., Reddy K. K., Reddy K. B., Yadav J. S.: *Synthesis* 263 (2004);  
(c) Iranpoor N., Zeynizadeh B., Aghapour A. J.: *Chem. Res.* 554 (1999);  
(d) Zhu Y., Pan Y.: *Chem. Lett.* 668 (2004);  
(e) Abaee M. S., Mojtahedi M. M., Sharifi R., Zahedi M. M., Abbasi H., Tabar-Heidar K.: *J. Iran Chem. Soc.* **3**, 293 (2006).
- (a) Wang J., Kang L., Hu Y., Wei B.: *Synth. Commun.* **32**, 1691 (2002);  
(b) Li J., Yang W., Chen G., Li T.: *Synth. Commun.* **33**, 2619 (2003).
- (a) Zheng X., Zhang Y.: *Synth. Commun.* **33**, 161 (2003);  
(b) Hu X., Fan X., Zhang X., Wang J.: *J. Chem. Res.* 684 (2004);  
(c) Zhang X., Fan X., Niu H., Wang J.: *Green Chemistry* **5**, 267 (2003).
- (a) Abaee M. S., Mojtahedi M. M., Zahedi M. M., Bolourtchian M.: *Synth. Commun.* **36**, 199 (2006);  
(b) Abaee M. S., Mojtahedi M. M., Zahedi M. M., Sharifi R.: *Heteroatom Chem.* **18**, 44 (2007).
- (a) Abaee M. S., Mojtahedi M. M., Zahedi M. M.: *Synlett* 2317 (2005);  
(b) Abaee M. S., Mojtahedi M. M., Zahedi M. M., Mesbah A. W., Ghandchi N. M., Massa W.: *Synthesis* 3339 (2007).
- Abaee M. S., Mojtahedi M. M., Sharifi R., Zahedi M. M.: *Heterocycl. Chem.* **44**, 1497 (2007).
- Abaee M. S., Mojtahedi M. M., Hamidi V., Mesbah A. W., Massa W.: *Synthesis*, in press.
- Abaee M. S., Mojtahedi M. M., Zahedi M. M., Sharifi R., Mesbah A. W., Massa W.: *Synth. Commun.* **37**, 2949 (2007).
- (a) Mojtahedi M. M., Akbarzadeh E., Sharifi R., Abaee M. S.: *Org. Lett.* **9**, 2791 (2007);  
(b) Bailey W. F., Luderer M. R., Jordan K. P.: *J. Org. Chem.* **71**, 2825 (2006);  
(c) Shao L. X., Shi M.: *Synlett* 1269 (2006);  
(d) Rudrawar S.: *Synlett* 1197 (2005) and references cited therein.
- Sheldrick G. M.: SHELXS-97 and SHELXL-97, Programs for the solution and refinement of crystal structures, University of Göttingen, 1997.

## P02 NOVEL DIKETOPYRROLOPYRROLES FOR MOLECULAR OPTICAL AND ELECTRICAL DEVICES

PAVEL BEDNÁŘ<sup>a</sup>, OLDŘICH ZMEŠKAL<sup>a</sup>, MARTIN WEITER<sup>a</sup>, MARTIN VALA<sup>a</sup> and JAN VYŇUCHAL<sup>b</sup>  
<sup>a</sup>Brno University of Technology, Faculty of Chemistry, Purkyňova 118, Brno 612 00, Czech Republic,  
<sup>b</sup>VUOS a.s., Rybitvi 296, Ribitvi 533 54, Czech Republic,  
 bednar-p@fch.vutbr.cz

### Introduction

Diketopyrrolopyrroles (DPPs) and variously substituted analogues represent class of low molecular materials with large  $\pi$ -conjugated system (Fig. 1). Diketopyrrolopyrroles exhibits excellent photostability, heat and weather fastness. Furthermore, some of their physical properties such as absorption in visible area of light and high values of photoluminescence quantum yields together with semi-conducting properties are of considerable research interest.

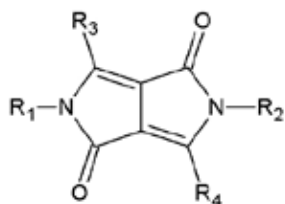


Fig. 1. General formula of DPPs

The characterization of new derivatives of diketopyrrolopyrrole with different substitution and determination of their potential use in optoelectronics was the main goal of our work.

### Experiments

We studied thirty derivatives of DPPs which were synthesized in VUOS a.s. However, only three materials along with the basic derivative (DPP04) are discussed in this paper (Table I).

The basic material DPP04 is insoluble in solvents with low polarity e.g. chloroform or toluene and only spectrally

Table I  
DPP derivatives used in experiments

DPP	R <sub>1</sub> , R <sub>2</sub>	R <sub>3</sub> , R <sub>4</sub>
DPP04	–H	
DPP10	–C <sub>4</sub> H <sub>9</sub>	
DPP12	–C <sub>7</sub> H <sub>15</sub>	
DPP29	–C <sub>4</sub> H <sub>9</sub>	

soluble in dimethylsulphoxide (DMSO). This material is therefore not usefull in spin-coating, dip or drop casting methods. The nitrogens of the basic DPP structure (R<sub>1</sub>, R<sub>2</sub>) were alkylated to increase the solubility in solvents like chloroform and toluene.

The substitution of piperidine groups on phenyl groups was used for modification of all properties.

The studied materials were characterized by optical and electrical methods. The absorbance and photoluminescence spectra of these materials in dimethylsulphoxide and thin layers spin-coated on the SiO<sub>2</sub> glass were analysed. The photoluminescence quantum yield of DPPs dissolved in dimethylsulphoxide was also determined.

The electrical measurements were obtained on sandwich structures, consisting of the transparent indium-tin oxide electrode (ITO) on glass, spin-coated PEDOT interlayer from water dispersion, spin-coated soluble DPP material, evaporated tris(8-hydroxyquinoline) (Alq<sub>3</sub>) interlayer and finalized by evaporation of the aluminium electrode.

The PEDOT (polystyrenesulfonate/poly-(2,3-dihydrothienol-(3,4b)-1,4-dioxin) interlayer was used for the decrease of the energy barrier for the hole injection and in a similar manner the Alq<sub>3</sub> interlayer was used for injection of electrons.

The current-voltage and electroluminescence characterizations were performed in vacuum at room-temperature.

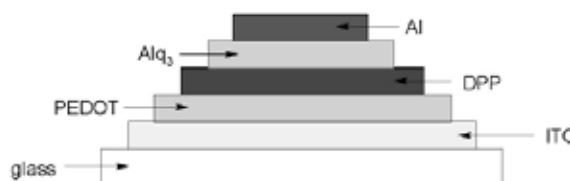


Fig. 2. Sandwich structure for electrical and optoelectrical measurement

### Results

The normalized absorbance and photoluminescence spectra of DPP solutions in DMSO are depicted on Fig. 3. The basic optical properties of DDP solutions are summarized in Table II.

The  $\lambda_{\text{Abx, max}}$  is a wavelength of absorbance maximum in a visible area of light, the  $\epsilon_{\text{max}}$  is the molar absorption coefficient at this wavelength and the  $\lambda_{\text{PL, max}}$  is the wavelength of the photoluminescence maximum.

The absorbance spectra and the calculations (Table II) show that the alkylation of nitrogens of basic DPP structure cause hypsochromic shift and change of the shape of the spectra and decrease the molar absorption coefficient. But these changes don't depend on length of alkyl chain. The substitution of piperidinyl groups on phenyls contributed to the large bathochromic shift and increased the molar absorption coefficient.

The photoluminescence spectra and calculations give the results that the alkylation's of nitrogen's caused the change of

Table II  
Basic optical properties of DPPs soluted in DMSO

DPP	$\epsilon_{\max}$ [l mol <sup>-1</sup> cm <sup>-1</sup> ]	$\lambda_{\text{Abx,max}}$ [nm]	$\lambda_{\text{PL,max}}$ [nm]	QY
DPP04	34,300	507	516	0.74
DPP10	18,500	467	530	0.69
DPP12	19,500	466	529	0.77
DPP29	42,400	536	599	0.41

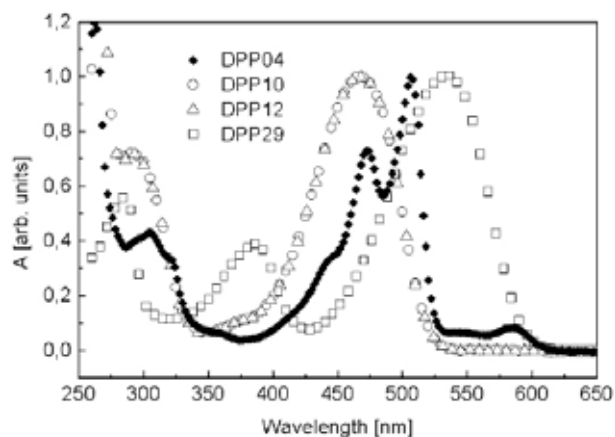


Fig. 3. Normalized absorbance spectra of DPPs in DMSO solutions

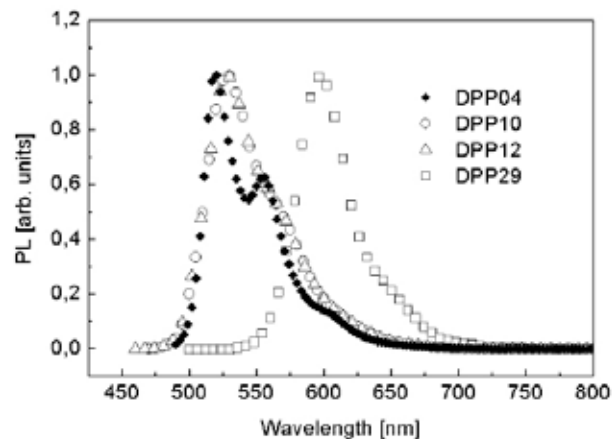


Fig. 4. Normalized photoluminescence spectra of DPPs in DMSO solutions

shape of the spectra but it does not depend on length of alkyl chain. The substitution of piperidinyl groups on phenyls contributed to the large bathochromic shift again and the substitution decreased the photoluminescence quantum yield.

The electroluminescence spectra show that the electroluminescence does not essentially depend on length of used

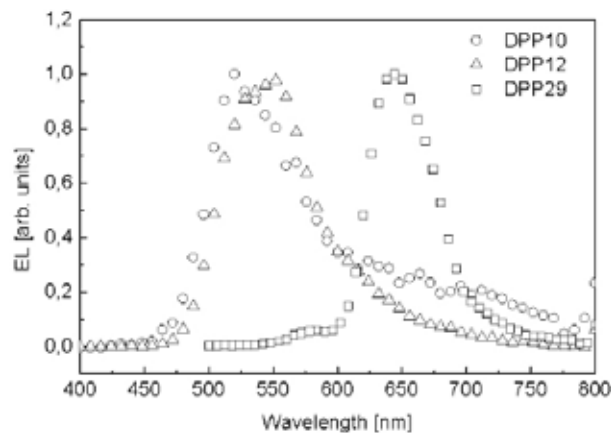


Fig. 5. Normalized electroluminescence spectra

alkyl chain. The substitution of piperidine groups on phenyls had the similar effect analogous to absorbance or photoluminescence spectra and contributed to the large bathochromic shift.

### Conclusions

This work was focused on study of number of diketopyrrolopyrroles with different substitution on nitrogens of basic skeleton of DPP and on phenyl groups.

The absorbance and photoluminescence spectra of DPPs in DMSO solutions give the result that the alkylation of nitrogens of the basic DPP structure changes the spectra, but the length of used alkyl chain doesn't have influence on the change.

The substitution of piperidinyl on phenyl groups (material U29) contributed beside the bathochromic shift of all types of spectra to the increase of molar absorption coefficient and to the substantial decrease of photoluminescence quantum yield.

The all OLED prototypes showed significant electroluminescent behavior and the utilized DPP materials are of new perspective and future development. However, the electroluminescence depends on many parameters and the optimization of multilayered structure is necessary to obtain efficient light emitting diode.

*This work was supported by the Ministry of Industry and Trade of the Czech Republic project FT-TA3/048 and by Grant Agency of Academy of Science by project A401770601.*

### REFERENCES

- Alp S., Ertekin K., Horn M., Icli S.: *Dyes Pigment.* 60, 103 (2006).
- Mizuguchi J.: *J. Phys. Chem.* 104, 1817 (2000).

**P03 DIAGNOSIS OF CIRRHOSIS BY GC/MS**CORNELIA MESAROS, MONICA CULEA and  
ANDREEA IORDACHE*Babes-Bolyai University, Str. Kogalniceanu, nr.1, 3400 Cluj-Napoca, Romania,  
mculea@phys.ubbcluj.ro***Introduction**

Caffeine test consists in caffeine oral intake followed by measurements of blood, saliva, labelled CO<sub>2</sub> in the exhalation air, urine caffeine or metabolites<sup>1,2</sup>. The pharmacokinetic parameters of caffeine, clearance and half-life time, were usually studied by HPLC and immunoassay methods and by GC/MS<sup>3</sup>. Clearance of caffeine is a quantitative test of hepatic function, because caffeine is metabolized by the hepatic P-450 cytochrome oxidase system. Caffeine, 1,3,7-trimethylxanthine, has been introduced as a compound for measuring the metabolic capacity of the liver, being well tolerated when administered orally.

The aim of the present investigation was to validate a rapid GC/MS method for plasma caffeine level determination for the characterization of some pharmacokinetic parameters in children. The application of the method on hepatitis and cirrhosis is tested.

**Experimental****Chemicals and Reagents**

Caffeine as a sterile caffeine sodium benzoate solution in water for injection use containing 125 mg of caffeine and 125 mg of sodium benzoate per 1 ml ampoule was obtained from pharmacy. All other reagents were from Merck (Germany). <sup>15</sup>N-theophylline, 74,2 atom % <sup>15</sup>N, labeled at the nitrogen in the position 7, synthesized in the National Institute for Research and Development for Isotopic and Molecular Technology Cluj-Napoca, was used as internal standard

**Equipment**

A Hewlett Packard (Palo Alto, CA, USA) 5989B mass spectrometer coupled to a 5890 gas chromatograph were used in the conditions: EI mode, electron energy 70 eV, electron emission 300 μA and ion source temperature 200 °C, selected ion monitoring (SIM) mode. The GC/MS interface line was maintained to 280 °C, and quadrupole analyser at 100 °C. The gas chromatograph-mass spectrometer (GC/MS) assay used a HP-5MS fused silica capillary column, 30m × 0.25 mm, 0.25 μm film-thickness, programmed from 200 °C to 250 °C at a rate of 10 °C min<sup>-1</sup>, the flow rate 1 ml min<sup>-1</sup>, with helium 5.5 as carrier gas. Injector temperature was 200 °C.

**Extraction Procedure**

0.5 ml of plasma containing caffeine was placed into a 5 ml screw-cap vial and 5 μl of internal standard <sup>15</sup>N-theophylline, 1 ml of the extraction solvent, chloroform: isopropanol 20:1 (v/v) and 0.2 g NaCl were added. After mechanical

mixing for 1 min, the sample was centrifuged for 3 min. 3 μl of the organic layer (lower layer) were injected into the GC.

**Method validation**

The method was validated in the range 0–20 μg ml<sup>-1</sup> caffeine. Known amounts of caffeine 3, 5, 10, 15, 20 μg ml<sup>-1</sup> and 10 μg of <sup>15</sup>N-theophylline were taken through above procedure. The regression curve, plotted as peak-area ratio of m/z 194 to m/z 181 versus caffeine concentration, gave the following linearity parameters: slope 0.5082, intercept -0.0528, r = 0.98.

Table I

Precision and accuracy of the method

Concentration added [μg ml <sup>-1</sup> ]	n	Concentration measured [μg ml <sup>-1</sup> ]	RSD [%]	Accuracy [%]
3	5	3.1	2.96	3.36
5	7	5.5	5.06	10.0

Precision gave R.S.D values lower than 5% for 5 μg ml<sup>-1</sup> (n = 7) and lower than 3 % for 3 μg ml<sup>-1</sup> (n = 5). Accuracy showed values lower than 10 % (Table I). Each value was obtained as an average between two measurements of the same sample. The limit of detection was 0.1 μg ml<sup>-1</sup> caffeine in blood sample, signal to noise ratio 4:1.

**Population**

Caffeine concentration measurements were performed in 32 hospitalized children suffering of hepatic dysfunctions and controls. Three different groups were studied: A, formed by 19 children with hepatitis aged 3–15 years old, B, consisting from 5 children with cirrhosis, aged between 5–12 years old, and C, 8 children as control aged between 5–15 years old. The main dose was 4 mg kg<sup>-1</sup>, p.o., for all groups. Blood samples were taken, at 0, 30 min, 1, 3, 6, 9 and 12 h. Blood samples were drawn into heparinized plastic tubes and immediately centrifuged. Plasma was stored at -20 °C. Written informed consents were obtained from each subject parent prior to this study.

**Calculation**

Regression curves obtained by the GC/MS method in the SIM mode were used for pharmacokinetic parameters study. Caffeine elimination constant was calculated as follows:

$$k_{el} = (\ln C_1 - \ln C_2) / \Delta t, \quad (1)$$

where C<sub>1</sub> = higher caffeine blood concentration, C<sub>2</sub> = lower caffeine blood concentration and Δt = the time elapsed between venous blood samples

Two points caffeine clearance was calculated as Cl = k<sub>el</sub> · V<sub>d</sub> and caffeine half-life as t<sub>1/2</sub> = ln 2 / k<sub>el</sub>, using a constant volume of distribution (V<sub>d</sub>) of 0.6 liters per kg body weight.

Clearance values calculated as dose/area under curve (AUC) were compared with the two-points values.

### Results

Caffeine clearance, measured in patients with cirrhosis and chronic hepatitis, was reduced and half live time was increased in children with liver disease as compared with control. The decreased metabolism observed in patients with various forms of liver disease was correlated to the disease status. Plasma concentrations of caffeine were measured in 19 patients with chronic hepatitis and 5 patients with cirrhosis and in 8 healthy subjects after caffeine ( $4 \text{ mg kg}^{-1} \text{ p. o.}$ ) loading. The correlations of total body clearance between two-point study (sampling times 1 h and 9 h) and seven-point study (sampling times 0, 0.5, 1, 3, 6, 9, 12 h) were highly significantly,  $r = 0.94$ ,  $p$  less than 0.001. These findings suggest that caffeine pharmacokinetic parameters can be estimated using two-point blood sampling procedure and GC/MS determination, following a single load. The elimination half-life ( $t_{1/2}$ ) of caffeine was significantly longer in cirrhotic patients than in the other two groups and clearance was substantially reduced in these patients. The higher concentrations of caffeine obser-

ved in the first hour after caffeine loading in hepatitis (Fig. 1.) compared with controls could be a possible test for hepatitis when very precise and accurate methods as isotopic dilution GC/MS are used. Significant changes (Student's paired t-test  $p < 0.01$ ) were observed in caffeine metabolism in children with decompensate cirrhosis.

The clearance values of  $0.55 \pm 0.41 \text{ ml min}^{-1} \text{ kg}^{-1}$  and half-life times of  $19.11 \pm 14.9 \text{ h}$  are changed because of the reduction in "functioning hepatocyte mass". The control values for clearance and half-life time were of  $1.36 \pm 0.23 \text{ ml min}^{-1} \text{ kg}^{-1}$  and  $t_{1/2} = 5.23 \pm 0.85 \text{ h}$  ( $n = 8$ ). Patients with noncirrhotic liver disease showed intermediate values ( $\text{Cl} = 1.19 \pm 0.45 \text{ ml min}^{-1} \text{ kg}^{-1}$  and  $t_{1/2} = 6.62 \pm 2.37 \text{ h}$ ) but higher values of caffeine plasma concentrations especially in the first hour after dose.

### Conclusions

The method is simple, precise and rapid, useful in the analysis of xanthines. Isotopic labeled internal standard used avoids metabolites overlapping. The elimination half-life ( $t_{1/2}$ ) of caffeine was significantly longer in cirrhotic patients and clearance was substantially reduced than in control. Caffeine pharmacokinetic parameters can be estimated using two-point blood sampling procedure by GC/MS determination, following a single load. The higher concentrations of caffeine observed in the first hour in hepatitis compared with controls could be a possible test for hepatitis.

*This work has been supported by the Romanian Research Foundation (CEEX, project number 166/2006).*

### REFERENCES

1. Park G. J., Katelaris P. H., Jones D. B., Seow F., le Cou-  
teur D. G., Ngu M. C.: *Hepatology*, 38, 1227 (2003).
2. Wittayalertpanya S., Mahachai V.: *J. Med. Assoc. Thai.*  
84, 189 (2001).
3. Culea M., Palibroda N., Panta Chereches P., Nanulescu  
M.: *Chromatographia*, 53, 387 (2001).

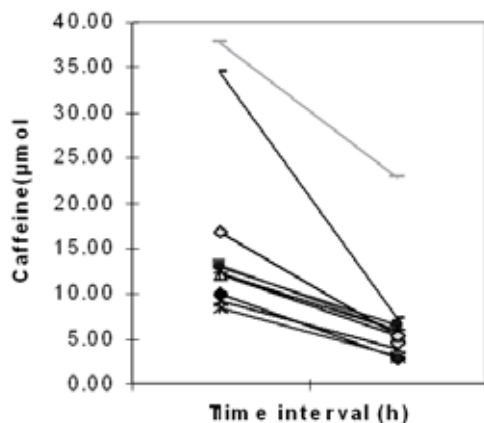


Fig. 1. Caffeine plasma concentrations at time interval (1 h and 9 h) in hepatitis ( $n = 19$ )

## P04 LEUKOTRIENE QUANTITATION BY GC-MS

MONICA CULEA, EUGEN CULEA, PARASCHIVA  
CHERECHES-PANTA and ADELA PINTEA

Babes-Bolyai University, Str. Kogalniceanu, nr. 1, 3400  
Cluj-Napoca, Romania  
mculea@phys.ubbcluj.ro

### Introduction

Quantitation of eicosanoid levels in biological systems is important for understanding of their role in cell function or pathological and for diagnosis. Leukotrienes quantitation is limited by sensitivity of the method. Gas chromatography – mass spectrometry (GC-MS) provides a sensitive and specific method when proper derivatization method is used.

Bronchoscopy with bronchoalveolar lavage is the gold standard to assess airway inflammation but invasiveness makes it unethical especially in children. The exhaled leukotriene B<sub>4</sub> (LKB<sub>4</sub>) is elevated in asthmatic children compare with control. LKB<sub>4</sub> is a non-invasive marker for airway inflammation in asthmatic children<sup>1,2</sup>.

A preliminary work is described for GC-MS use for quantitative determination of LKB<sub>4</sub> in exhaled breath content.

### Experimental

Gas chromatography was performed on a 5% phenyl methylpolysiloxane column (30 m × 0.25 mm I.D., 0.25 μm film thickness) operated in a suitable temperature program. Helium carrier gas was of 1 ml min<sup>-1</sup>. Ionization was performed by electron impact (EI) and detection in SIM mode. Arachidonic acid was used as internal standard.

### Exhaled Breath Condensate Collection

A condensing chamber (Ecoscreen II, Germany) was used to obtain exhaled breath condensate (EBC). 1.5 ml of EBC was obtained after 15 minutes of breath through a mouthpiece connected to the condenser. Samples were stored at –80 °C before measurements.

Patients with asthma were recruited from Pediatric Clinic III of Cluj-Napoca. The preliminary study was for 3 patients with asthma and 3 controls.

### GC-MS Method

LKB<sub>4</sub> and arachidonic acid, the internal standard, were analyzed by GC-MS after derivatization with ethylchloroformate and liquid-liquid extraction. A modified method was used<sup>2</sup>. Reagents were from Merck (Germany). Standards containing different concentration of LKB<sub>4</sub> and the same concentration of arachidonic acid (IS) were prepared in water. Deactivation of all glass surfaces, injector liner and vials, was made with 10% dichlorodimethylsilan in hexane for 30 minutes.

500 μl EBC, 1 μg arachidonic acid (IS), 20 μl ethylchloroformate and 40 μl pyridine were shaken few second

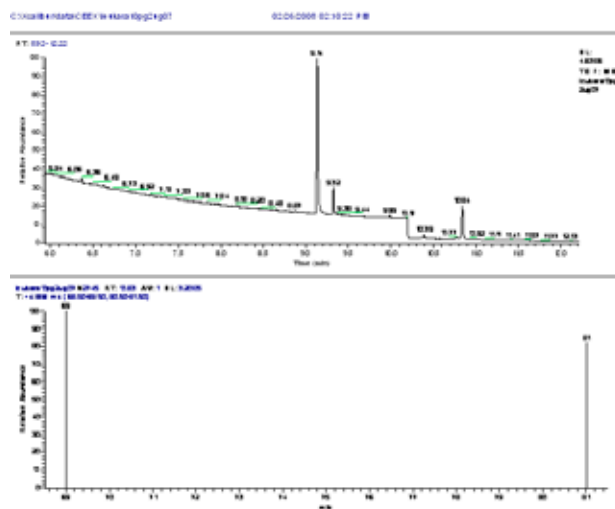


Fig. 1. SIM chromatogram for arachidonic acid ethyl ester, the internal standard, elution time 9.33 min, and derivatized LKB<sub>4</sub>, elution time 10.85 min: The ions m/z 69 and 81 are used in SIM mode for LKB<sub>4</sub>. The distilled water (500 μl) was spiked with 1 μg arachidonic acid and 10 pg LKB<sub>4</sub>

for evaporating CO<sub>2</sub>. 0.25 ml chloroform, 0.5 ml sodium carbonate-bicarbonate solution were shaken 30 seconds. After 2 minutes of phase equilibrium, 3 μl of the lower phase was injected into the fused silica capillary column in the split-less mode. Injector temperature was 280 °C. Gas chromatography was performed on a 5% phenyl methylpolysiloxane column (30 m × 0.25 mm I.D., 0.25 μm film thickness) operated in the following temperature program: initial temperature 80 °C (1.5 min), then increased with a rate of 28 °C min<sup>-1</sup> at 315 °C and kept 5 minutes. The ion current chromatogram for the two compounds is presented in Fig. 1. The selected ions were m/z 79 for arachidonic acid derivative and m/z 69, 81 for LKB<sub>4</sub> derivative. The mass spectra for the two derivatized compounds are presented in the Figs. 2. and 3.

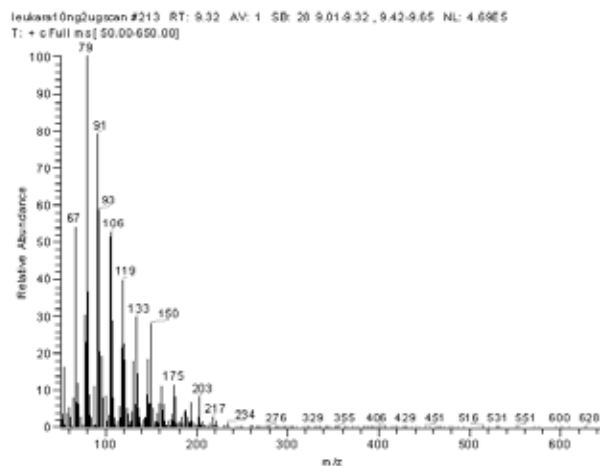


Fig. 2. The mass spectrum of arachidonic acid ethyl ester (9.33 min), M = 332

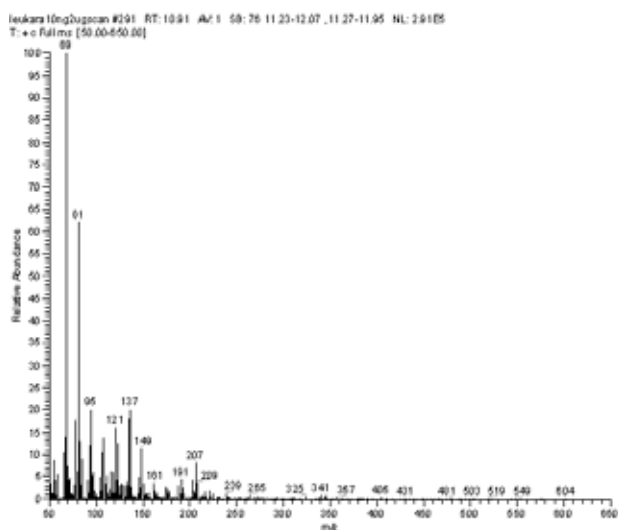


Fig. 3. The mass spectrum of leukotriene B4 ethyl ester (10.85 min)

Helium carrier gas flow was of  $1 \text{ ml min}^{-1}$ . Ionization was performed by electron impact (EI) and detection in SIM mode.

### Results

The method provided good response linearity and precision ( $<30\%$  C.V.) in the range  $1\text{--}400 \text{ pg ml}^{-1}$ , necessary to analyse leukotriene B4 in exhaled air. Arachidonic acid was used as internal standard because its structure is similar to leukotrienes, is undetectable in EBC without addition of arachidonic acid and is stable in aqueous solution.

The linearity of the method was studied in the range  $1\text{--}400 \text{ pg ml}^{-1}$ . The regression curve obtained was:

Table I  
LKB4 in EBC values in asthmatic and control children

Patient	LKB <sub>4</sub> [ $\text{pg ml}^{-1}$ ]	RSD [%]
1	178.2	32
2	219.5	47
3	315	35
Controls (n = 3)	78	36

$y = 0.0027x + 0.4038$ , with a regression coefficient of  $r = 0.99$ . The detection limit was of  $1 \text{ pg ml}^{-1}$ , at a signal-to-noise of 5.

The method was applied for few cases of patients and controls. The different values of LKB4 were significant higher in asthmatic children than in healthy children.

Measurements of exhaled LKB4 are important for identifying the children with no respiratory symptoms but having inflammations which may require therapy.

### Conclusions

The LKB4 was detectable in exhaled breath condensate. GC-MS non-invasive method showed significant increased value for LKB4 in children with asthma than in healthy control.

*This work has been supported by the Romanian Research Foundation (CEEX, project number 166/2006).*

### REFERENCES

- Shirley M. A., Murphy R. C.: *J. Biol. Chem.* 265, 16288 (1990).
- Cap P., Chladek J., Pejhal F., Maly M., Petru V., Barnes P. J., Montuschi P.: *Thorax* 59, 265 (2004).

## P05 CHARACTERIZATION OF OLIGOSACCHARIDES USING ESI-MS IN PRESENCE OF ANIONS

RICHARD ČMELÍK and JANETTE BOBÁĽOVÁ

*Institute of Analytical Chemistry of the ASCR, v. v. i., Department of Proteomics and Glycomics, Veveří 97, 60200 Brno, Czech Republic, cmelik@iach.cz*

### Introduction

Knowledge of oligosaccharide sequence, inter-residual linkages, and branching are essential for understanding their biological functions and technological properties. Electrospray ionization (ESI) mass spectrometry (MS) has become one of the most important tool for structural analysis of carbohydrates<sup>1</sup>.

For the analyses of oligosaccharides, the fragmentation of sodium or lithium adducts are commonly used to elucidate its structure, while the negative mode approach give more detailed<sup>2</sup> or complementary information. However, neutral oligosaccharides typically produce low signals of  $[M-H]^-$  ions. An alternative way of charging a molecule to render it detectable in negative-ion mode is via either derivatization or the addition of an ammonium salt<sup>3</sup>. In the latter case, various anions ( $A^-$ ) can be added in order to increase the response of saccharides to induce formation of stable and abundant anionic adducts  $[M + A]^-$ .

### Experimental

Dextran 1000 (DEX) and ammonium salts were purchased from Fluka (Buchs, Switzerland), whereas low glucose syrup (LGS) was from Amylon (Havlíčkův Brod, Czech Republic). Maltooligosaccharides (MOS) were obtained from Sigma (St. Louis, USA). Oligosaccharides were dissolved at  $30 \mu\text{g ml}^{-1}$  in methanol/water (1 : 1, v/v) containing different concentration (0, 3, 30, 100, 300  $\mu\text{M}$ ) of ammonium salts (bicarbonate, bisulfate, chloride, and nitrate).

ESI-MS/MS experiments were performed using a Esquire LC instrument (Bruker Daltonik, Germany) equipped with an ESI ion source. Samples were infused into the mass spectrometer at a flow rate of  $3 \mu\text{l min}^{-1}$  via a metal capillary held at high voltage ( $-3.5 \text{ kV}$ ). Other potentials were modified and optimized before each experiment. Nitrogen was used as a drying ( $5 \text{ dm}^3 \text{ min}^{-1}$ ,  $250 \text{ }^\circ\text{C}$ ) and nebulizing gas (14 psi).

### Results

In this study, we reported the comparison of the malto- and isomaltooligosaccharides mixtures (MOS, LGS, and DEX) using negative-ion ESI MS. Oligosaccharide samples were analyzed without additives, as well as after the addition of different amount of the ammonium salts. The effect of anion type and concentration in MS spectra have been investigated.

All oligosaccharide mixtures revealed two dominant ion series,  $[\text{Glc}_x-H]^-$  and  $[\text{Glc}_x-H-120]^-$ . Small amount of  $[\text{Glc}_x-H+H_2O]^-$  (for LGS),  $[\text{Glc}_x-H-60]^-$  (DEX), as well  $[\text{Glc}_x-H-60-H_2O]^-$  (LGS, MOS) ions were also observed. In general, higher oligomers ( $x \geq 5$ ) formed deprotonated molecules in preference to fragments; lower oligomers were rather detected as  $[\text{Glc}_x-H-120]^-$  ions. MS spectra of LGS dominated by  $[\text{Glc}_x-H]^-$  (up to  $x = 5$ ) or  $[\text{Glc}_x-H+H_2O]^-$  ions.

The MS spectra of samples containing ammonium chloride showed  $[\text{Glc}_x+Cl]^-$  ion series. At low nozzle-skimmer voltages under the conditions of high salt concentration (100 or 300  $\mu\text{M}$ ), preferential production of  $[\text{Glc}_x+Cl]^-$  was observed. The application of ammonium nitrate gave nitrate adducts of oligosaccharides. At the highest concentration of nitrate, the  $[\text{Glc}_x+NO_3]^-$  ions dominated. The ratio of deprotonated molecule to adducts (chloride of nitrate) and then that of  $[\text{Glc}_x-H-120]^-$  (respectively  $[\text{Glc}_x-H+H_2O]^-$  for LGS) to adducts decreased with increasing concentration of appropriate anion (Fig. 1). In both cases, the addition of anion dopant resulted in significantly simplified spectra and enhanced sensitivity and resolution.

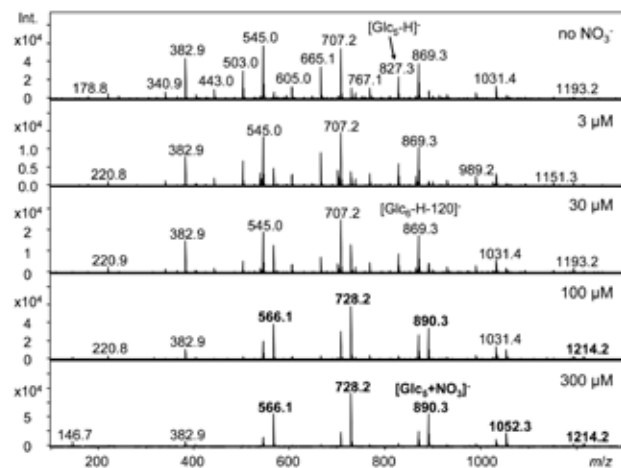


Fig. 1. MS spectra of DEX at the different concentration of  $NO_3^-$

The behavior of bisulfate differed from the above mentioned anions. The abundance of  $[\text{Glc}_x+HSO_4]^-$  reached the maximum levels at the concentration of 30 and 100  $\mu\text{M}$  of bisulfate, then  $HSO_4^-$  and  $H_3S_2O_8^-$  ions substantially increased.  $NH_4HCO_3$  did not form observable adducts.

The influence of the particular studied anions on distribution of oligosaccharide derived ions is shown in Fig. 2 and Table I.

Tandem MS ( $MS^2$ ) spectra generated from chloride and nitrate adduct ions of the same sample showed fragmentation pattern very similar to that for  $[\text{Glc}_x-H]^-$ , whereas a higher abundance of fragment ions was detected. On the other hand, attempts to fragment bisulfate adducts failed in all cases. Besides dominant fragments  $[\text{Glc}_y-H]^-$  and  $[\text{Glc}_y-H-120]^-$  ( $y \leq x$ ), the differences in  $MS^2$  spectra have been observed for

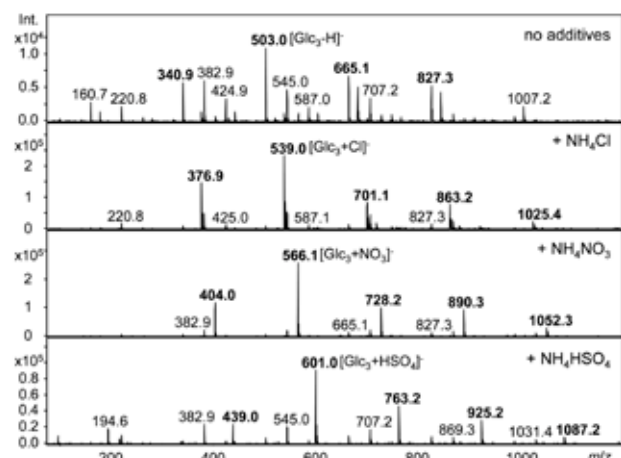


Fig. 2. MS spectra of LGS with and without the addition of salts (300  $\mu\text{M}$ )

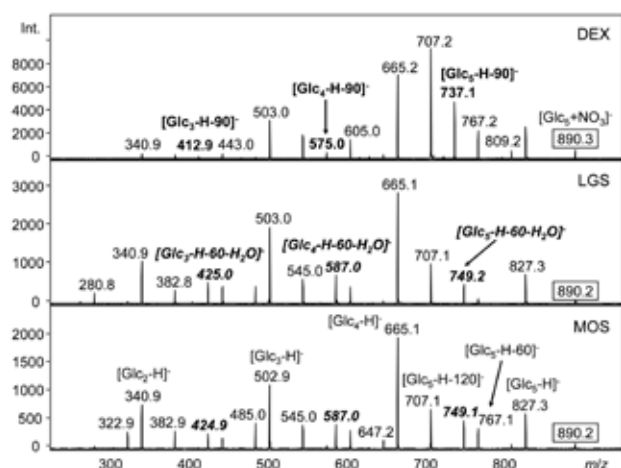


Fig. 3. MS<sup>2</sup> spectra of nitrate adducts  $[\text{Glc}_x + \text{NO}_3]^-$  of DEX, LGS, and MOS

particular oligosaccharide samples. The linkage included in DEX were reflected in specific cross-ring fragments  $[\text{Glc}_y\text{-H-90}]^-$ , while the presence of  $[\text{Glc}_y\text{-H-60-H}_2\text{O}]^-$  appeared to be characteristic for MOS and LGS (Fig. 3).

These observations are in agreement with the fact that DEX and MOS/LGS represent isomeric glucans differing in the prevalent  $\alpha$ -(1  $\rightarrow$  4), respectively  $\alpha$ -(1  $\rightarrow$  6) glycosidic linkage.

Table I  
Abundant ions observed in the MS spectra of DEX, LGS and MOS with and without salts

Ion series	Range of the observed ion series – DP (x)			Salt
	DEX	LGS	MOS	
$[\text{Glc}_x\text{-H}]^-$	1–7	1–6	1–7	–
$[\text{Glc}_x\text{-H} + \text{H}_2\text{O}]^-$	–	4–6	–	–
$[\text{Glc}_x\text{-H-60}]^-$	3–6	–	–	–
$[\text{Glc}_x\text{-H-60-H}_2\text{O}]^-$	–	2–6	3–7	–
$[\text{Glc}_x\text{-H-120}]^-$	2–7	2–5	2–8	–
$[\text{Glc}_x + \text{Cl}]^-$	2–7	2–6	2–8	$\text{Cl}^-$
$[\text{Glc}_x + \text{NO}_3]^-$	2–7	2–6	2–8	$\text{NO}_3^-$
$[\text{Glc}_x + \text{HSO}_4]^-$	3–7	2–6	3–7	$\text{HSO}_4^-$

### Conclusions

In the ESI negative-ion mass spectra, oligosaccharides were stabilized by adduct formation  $[\text{M} + \text{A}]^-$  with several anions ( $\text{A} = \text{NO}_3, \text{Cl}$ ). The analogous molecular mass distributions of presented glucose oligomers were obtained, whereas the adducts appeared in mass spectra in higher abundances relative to  $[\text{M-H}]^-$ . In addition, the in-source fragmentation was suppressed.

MS<sup>2</sup> experiments enable to distinguish  $\alpha$ -(1  $\rightarrow$  4) and  $\alpha$ -(1  $\rightarrow$  6) linkages on the base of specific diagnostic product ions. A fragmentation of  $[\text{Glc}_x + \text{Cl}]^-$  and  $[\text{Glc}_x + \text{NO}_3]^-$  ion adducts was found to be suitable for structural determination of (iso)maltooligosaccharides because more prominent cross-ring fragmentation was observed.

*This work was supported by the Project No. 2B06037 from the Ministry of Education, Youth and Sports of the Czech Republic and Institutional Research Plan AV0Z40310501.*

### REFERENCES

- Harvey D. J.: *Proteomics* 5, 1774 (2005).
- Garozzo D. Giuffrida M., Impallomeni G.: *Anal. Chem.* 62, 279 (1990).
- Jiang Y., Cole R. B.: *J. Am. Soc. Mass Spectrom.* 16, 60 (2005).

**P06 A NEW APPROACH TO PROTEIN ENZYMATIC DIGESTION FOR FAST PROTEIN IDENTIFICATION BY MATRIX-ASSISTED LASER DESORPTION/IONIZATION TIME-OF-FLIGHT MASS SPECTROMETRY**

FILIP DYČKA, MARKÉTA LAŠTOVIČKOVÁ and JANETTE BOBÁLOVÁ

*Institute of Analytical Chemistry of the ASCR, v.v.i., 602 00 Brno, Veveří 97, Czech Republic, bobalova@iach.cz*

**Introduction**

The combination of protein separation by polyacrylamide gel electrophoresis with mass spectrometric analysis of proteins digested enzymatically in-gel is a very powerful tool for protein identification in complex biological systems. Recently several approaches have been developed for fast protein digestion. One approach is the use of modified trypsin for in-gel digestion of proteins instead of native trypsin<sup>1</sup>. Other promising approaches include microwave technology<sup>2–4</sup> or ultrasonic assisted protein enzymatic digestion<sup>5</sup>. The traditional sample preparation for protein identification through peptide formation is time-consuming procedure therefore we have studied and compared the variable performances of the fast enzymatic digestion of proteins using the different techniques. Most important, the new approach of protein digestion takes minutes, in contrast to several hours required by conventional methods.

The aim of this study was to demonstrate the usefulness of fast methods to apply microwave and ultrasonic device to in-gel digestion.

**Experimental**

**Protein Separation**

0.5 mg of bovine serum albumin (BSA) (Roche Diagnostics GmbH, Mannheim, Germany) was resuspended in 1 ml of sampling buffer (Laemmli Sample Buffer (Bio-Rad) with  $\beta$ -mercaptoethanol, 19:1). SDS-PAGE separation was performed on 12 % 1-D SDS PAGE gel. The visualization was carried out by Coomassie Brilliant Blue (CBB) G-250.

**In-gel Digestion**

The BSA bands separated by 1-D GE were excised manually, cut into pieces and in-gel digestion procedure was performed to the three BSA samples<sup>6</sup> following the protocols outlined in Table I.

**Protein Identification**

Obtained peptides were analyzed by MALDI-TOF/TOF MS (Applied Biosystems 4700 Proteomics Analyzer). This TOF/TOF instrument is equipped with Nd/YAG laser, 355 nm.  $\alpha$ -Cyano-4-hydroxycinnamic acid (CHCA; 8 mg ml<sup>-1</sup>, 0.1 % trifluoroacetic acid/acetonitrile (1:1, v/v)) was used as a MALDI matrix.

Table I

In-gel preparation, digestion, and peptide extraction using conventional, microwave (MW) and ultrasonic methods

Protocol	Solution	Convent. [min]	MW [min]	Ultrasonic [min]
Reduce	10 mM dithiothreitol.	45	45	45
Alkylate	55 mM iodoacetamide.	30	30	30
Wash	50% ACN in 0.1 M ammonium bicarbonate.	30	30	30
Rehydrate	12.5 ng $\mu$ l <sup>-1</sup> of trypsin in 50mM ammonium bicarbonate, 5mM calcium chloride.	45	45	45
Digest	12.5 ng $\mu$ l <sup>-1</sup> of trypsin in 50mM ammonium bicarbonate, 5mM calcium chloride.	16 h	4	10
Extract	0.1% TFA, 50% ACN.	30	30	30
Total time		19 h	3 h, 4 min.	3 h, 10 min.

**Results**

BSA was used as model protein to study the in-gel digestion. Three BSA samples excised from 1-D SDS PAGE gel (Fig. 1) were subjected to in-gel digestion with trypsin using conventional method, microwave irradiation and sonication in order to compare speed and convenience of new approaches.

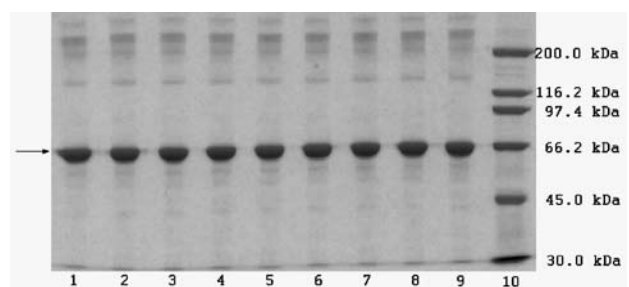


Fig. 1. 1-D SDS PAGE separation of BSA (lane 1–9). Molecular weight markers are in lane 10. Protein bands marked by arrow were further in-gel digested by the standard, microwave or ultrasonic method and identified by mass spectrometry

The gel particles with trypsin were incubated for 16 h at 37 °C, put into a microwave for 4 min at 350 W or put into an ultrasonic bath for 10 min at power 35 W. After in-gel digestion the peptide fragments were purified by ZipTipC<sub>18</sub> and directly spotted on the sample plate of the MALDI-TOF/TOF MS. Finally, CHCA was applied to each spot prior to acquiring mass spectra.

The mass spectra of tryptic peptides of BSA are shown in Fig. 2.A for conventional method, Fig. 2.B for the microwave method and Fig. 2.C for the ultrasonic method. The peptide peak patterns were almost the same for microwave and ultrasonic method, indicating that the digested peptide fragments

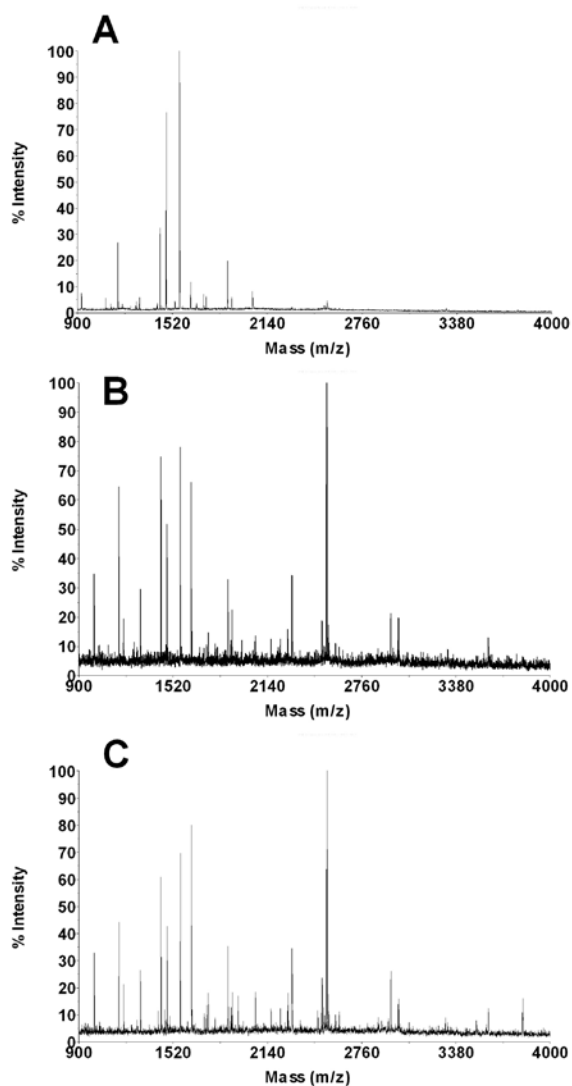


Fig. 2. The MALDI-TOF mass spectra of BSA. The spectra were obtained after in-gel digestion: A – using conventional method; B – microwave method; C – ultrasonic method. CHCA was used as a matrix

from two methods were similar. More relevant changes were observed between traditional method and new fast approaches. Protein identification was performed by searching the peptide masses against the NCBI nr sequence database using the MASCOT search program. The methods using microwave and ultrasonic technologies gave slightly more matched tryptic fragments than the conventional method. The highest number of matched peptide and the highest score gave the method using ultrasonic device. Considering the required reaction time for the conventional method is much longer, the new methodic approaches apparently led to higher efficiency for in-gel digestion.

### Conclusions

This work reports fast digestion procedures and protein identification based on the use of microwave and ultrasonic technology. These alternative methodologies can be an important advancement in proteomic research.

*This work was supported by the Grant Agency of the Academy of Sciences of the Czech Republic No. IAA600040701 and Research Plan of Institute of Analytical Chemistry of the ASCR, v.v.i. (AV0Z40310501).*

### REFERENCES

1. Havlis J., Thomas H., Sebel M., Shevchenko A.: *Anal. Chem.* **75**, 1300 (2003).
2. Juan H. F., Chang S. C., Huang H. C., Chen S. T.: *Proteomics* **5**, 840 (2005).
3. Pramanik B. N., Mirza U. A., Ing Y. H., Liu Y.-H., Bartner P. L., Weber P. C., Bose A. K.: *Protein Sci.* **11**, 2676 (2002).
4. Sun W., Gao S., Wang L., Chen Y., Wu S., Wang X., Zheng D., Gao Y.: *Mol. Cell. Proteomics* **5**, 769 (2006).
5. Rial-Otero R., Carreira R. J., Moro A. J., Santos H. M., Vale G., Moura J. L., Capelo J. L.: *J. Chrom. A* **1166**, 101 (2007).
6. Shevchenko A., Wilm M., Vorm O., Mann M.: *Anal. Chem.* **68**, 850 (1996).

**P07 THE  $^{13}\text{C}$  AND  $^{119}\text{Sn}$  NMR SPECTRA OF SOME TRIORGANOTIN-(IV)-N,N-DIETHYL-DITHIOCARBAMATES USED AS WOOD PRESERVATIVES**

JURAJ KIZLINK<sup>a</sup> and LADISLAV REINPRECHT<sup>b</sup>

<sup>a</sup>Faculty of Chemistry, Brno University of Technology, Purkyňova 118, 612 00 Brno, Czech Republic,

<sup>b</sup>Faculty of Wood Sciences and Technology, TU Zvolen, Masarykova 24., 960 53 Zvolen, Slovak Republic, kizlink@fch.vutbr.cz

**Introduction**

The organotin compounds (OTCs), mainly triorganotin compounds are very effective against fungi and were widely used for all kinds of wood preservation<sup>1</sup>. They are nowadays already less used to their leaking into the sweet water (brooks, lakes, rivers), but more used for sea water. OTCs are very well soluble in organic solvents and on the other hand have very low solubility in water. Many of them are irritant and harmful for human skin and some are also phytotoxic agents. For their relatively high toxicity and eco-toxicity their application is limited and are often replaced by other organic compounds now<sup>2,3</sup>. For this purpose the new groups of the OTCs on the base of substituted dithiocarbamic acid were synthesised and tested<sup>4,5,6</sup>. Till this time no cancerogenity among known OTCs was observed and reported.

**Experimental**

The various trialkyl-, triaryl- and triaralkyl-tin-(IV)-N,N-diethyldithiocarbamates were synthesized from corresponding trialkyl-, triaryl- and triaralkyl-tin-(IV)-chlorides (Merck s.r.o. Brno, CZ) and sodium N,N-diethyldithiocarbamate under trade name Kupral (Lachema a.s. Brno, CZ)

in ethanol or isopropanol, sometimes with methylethylketone in mixture. After removing solvent, the products as oil residue were filtrated with diatomace powder as additive throw the sinter-glass filter No. 3, under pressure of motor vacuum pump<sup>4,5</sup>.

All these compounds were tested as wood preservatives against rot – caused by wood destroying fungi *Coniophora puteana*, *Coriolus versicolor*, *Serpula lacrymans* and against moulds.

**Results and Discussion**

The best antifungal results were obtained with the trialkyltin-(IV)-compounds in the order of R in the  $\text{R}_3\text{Sn}$ -group: methyl- and butyl-, comparable with commercial abroad widely used tributyltin-(IV)-naphtenate (TBTN) used as standard<sup>4-9</sup>. The lower efficacy was when R = cyclohexyl- or phenyl-, otherwise if R = benzyl-, the efficacy was very poor<sup>6</sup>.

Besides these organotin-N,N-diethyldithiocarbamates we have tested also other organotin fungicides. A very good result was obtained with the compound tributyltin amidosulfonate (TBTAS), which was even comparable to the most effective, formerly commercialy produced and used bis-tributyltin oxide (TBTO) as hexabutyl-distannoxane and very effective against the  $\text{g}^+$  bacteria *Streptococcus aureus*. However, this volatile compound is already out of use from technical praxis for its high toxicity and is also included in the severe poisons<sup>10,11</sup>.

The diagrams of the biocidal efficacy for fungicides and photos of testing method (poisoned soil method) are presented on the poster at 4<sup>th</sup> Meeting on Chemistry & Life.

The  $^{13}\text{C}$  and  $^{119}\text{Sn}$  NMR spectra of these compounds were also measured on the JEOL spectrometer JNM-FX 100 (Japan) at 25.047 and 37.14 MHz at 300 K. The che-

Table I

$^{13}\text{C}$  and  $^{119}\text{Sn}$  NMR shifts for organotin compounds type  $\text{R}_3\text{SnSC}(\text{S})\text{N}(\text{C}_2\text{H}_5)_2$  at 300 K

Compound R	Solvent	$\delta(^{119}\text{Sn})$	$\delta(^{13}\text{C})/(\text{nJ}(^{119}\text{Sn}, ^{13}\text{C}), \text{Hz})$								Ref.
			C-1	C-2	C-3	C-4	C-5	CS	CH <sub>2</sub>	CH <sub>3</sub>	
$\text{C}_6\text{H}_5$ -phenyl-	$\text{CDCl}_3$	-189.8	142.54 (604.2)	136.50 (47.6)	128.31 (62.3)	128.85 (13.4)	–	–	50.44	12.05	12
n- $\text{C}_4\text{H}_9$ -n-butyl-	neat	12.0	17.48 (352.8)	28.71 (22.0)	26.90 (66.0)	13.58 (<5)	–	196.73	49.25	11.86	13
n- $\text{C}_4\text{H}_9$ -n-butyl-	$\text{CDCl}_3$	23.4	17.50 (350.2)	28.74 (20.6)	26.98 (67.4)	13.58 (<5)	–	197.11	49.39	11.75	13
n- $\text{C}_4\text{H}_9$ -n-butyl-	pdpv	14.4	18.21 (356.1)	29.38 (22.0)	27.51 (67.4)	14.00 (<5)	–	197.46	49.86	12.30	13
n- $\text{C}_4\text{H}_9$ -n-butyl-	hmpa	-19.0	18.62 (413.2)	28.34 (24.9)	26.64 (76.2)	13.13 (<5)	–	198.58	48.17	11.55	13
$\text{CH}_2=\text{CH}$ -vinyl-	$\text{CDCl}_3$	-202.1	140.01 (587.6)	134.86 (–)	–	–	–	195.35	49.91	11.83	15
$\text{C}_6\text{H}_5\text{CH}_2$ -benzyl-	$\text{CDCl}_3$	-92.6	26.45 (303.3)	140.53 (41.5)	127.60 (30.8)	128.13 (17.6)	123.63 (22.0)	195.58	49.80	11.83	14
c- $\text{C}_6\text{H}_{11}$ -cyklohexyl-	$\text{CDCl}_3$	-28.3	35.94 (337.0)	33.30 (17.6)	30.60 (67.4)	28.33 (<5)	–	198.81	50.85	13.47	14

mical shifts were determined relative to a suitable signal of solvent<sup>12–15</sup> as CDCl<sub>3</sub> (77.00 ppm), pentadeuteriopyridine (pdpy) (149.90 ppm), hexadeuteriodimethyl sulphoxide (hdso) (39.60 ppm) and hexamethylphosphor triamide (hmpa) (36.00 ppm) respectively by known method.<sup>12–16</sup> Achieved results are presented in the Table I.

### Conclusion

Organotin compounds having three direct tin-carbon bonds have high biocidal activity<sup>10,17</sup>, so they are useful as disinfectants and antimicrobial agents for paper, textiles, wood and even for masonry and stonework.<sup>18–20</sup> Their highest consumption nowadays is as antifouling paints for the wood seawater vessels against the marine organisms immersion.

*This work was supported by Grant No. I/4377/07 in SR.*

### REFERENCES

1. Kizlink J.: Chem. Listy 86, 178 (1992).
2. Paulus W.: *Microbicides for the Protection of Materials*, Chapman and Hall, London 1993.
3. Cooney J. J., Wuertz S.: J. Ind. Microbiol. 4, 375 (1989).
4. Kizlink J.: J. Oil Colour Chem. Assoc. 74, 329 (1991).
5. Kizlink J., Rattay V., Košík M.: J. Oil Colour Chem. Assoc. 76, 468 (1993).
6. Kizlink J., Fargašová A., Reinprecht L.: Drevársky výskum 41, 19 (1996).
7. Reinprecht L., Kizlink J.: Acta Fac. Xylol. Zvolen 38, 75 (1996).
8. Kizlink J., Fargašová A.: CHEMagazín 7, 16 (1997).
9. Reinprecht L., Kizlink J.: Drevársky výskum 44, 67 (1999).
10. Kizlink J.: Chem. Papers 55, 53 (2001).
11. Kizlink J.: CHEMagazín 13, 20 (2003).
12. Holeček J., Nádvořník M., Handlíř K., Lyčka A.: J. Organometal. Chem. 241, 177 (1983).
13. Nádvořník M., Holeček J., Handlíř K.: J. Organometal. Chem. 275, 43 (1984).
14. Lyčka A., Jirman J., Koloničný A.: J. Organometal. Chem. 333, 305 (1987).
15. Handlíř K., Holeček J.: Inorg. Chim. Acta 150, 287 (1988).
16. Gielen M., Willem R., Wrackmeyer B.: *Advanced Applications of NMR to Organometallic Chemistry*, Wiley, New York 1996.
17. Fargašová A.: Bull. Environ. Contam. Toxicol. 60, 9 (1998).
18. Sjoestroem E., Alén R.: *Analytical Methods in Wood Chemistry – Pulping and Papermaking*, Springer, Berlin 1999.
19. Ambrožová V.: *Nátěry dřeva*, Grada Publishing, Praha 2000.
20. Vitvar P.: *Přehled a charakteristika chemických prostředků proti biotickým škůdcům, ohni a povětrnostním vlivům*, Výzkumný a vývojový ústav dřevařský (VVUD), Praha 2000 and 2003 (handbooks).

## P08 PREPARATION OF DIMETHYL CARBONATE FROM METHANOL AND CARBON DIOXIDE – THE REMOVAL OF REACTION WATER BY OLEFINS

JURAJ KIZLINK

*Faculty of Chemistry, Brno University of Technology, Purkyňova 118, 612 00 Brno, Czech Republic, kizlink@fch.vutbr.cz*

### Introduction

The development of suitable methods based on the carbon dioxide for the synthesis of various organic products is very attractive now. Carbon dioxide is in the last twenty years very significant waste, which is responsible for the greenhouse effect formation<sup>1</sup>. The preparation of dimethyl carbonate (DMC) is one of many reactions for the utilization of carbon dioxide together with methanol as significant product for various uses<sup>2</sup>, nowadays also as additive for engine fuels<sup>3</sup>.

The one-pot synthesis of DMC from carbon dioxide and methanol has become attractive due to the low cost of the starting materials, but the DMC yield by this way is relatively low, due to the fact that carbon dioxide is highly thermodynamically stable and kinetically inert compound and due to the deactivation of catalysts induced by water formation in the reaction process<sup>4,5</sup>.

The main catalyst system is based on the organotin (IV) compounds, especially on the dialkyltin dialkoxides<sup>6,7</sup>. It has been also reported, that DMC can be synthesized in the presence of tin (IV) and titanium (IV) alkoxides<sup>8</sup>, similar organotin compounds<sup>9–11</sup> and also metal (Hg, Mg, Zn) acetates or some other (Co, Mn, Ni) acetates<sup>12</sup>. The values of temperatures, pressures and times range between 130–180 °C, 0.5–3.0 MPa, 2–12 hours respectively<sup>12</sup>.

The first way is the use of the special catalyst systems, which are effective in spite of the reaction water is presented. The modified ZrO<sub>2</sub> catalysts promoted with phosphoric acid were used<sup>13–15</sup>. This catalyst was prepared by calcining of commercially available ZrO<sub>2</sub>. It was found, that the DMC formation rate was strongly dependent on the structure of zirconia catalyst and it was very dependent on the calcination temperature. It was also observed and reported, that during the reaction the dimethyl ether (DME) was formed on various types of oxide catalysts (Al<sub>2</sub>O<sub>3</sub>, SiO<sub>2</sub>, CeO<sub>2</sub>, GeO<sub>2</sub>, TiO<sub>2</sub>, ZrO<sub>2</sub> a.s.o.). The other catalytic systems are based on H<sub>3</sub>PW<sub>12</sub>O<sub>40</sub>/Ce<sub>x</sub>Ti<sub>1-x</sub>O<sub>2</sub> compound<sup>17</sup>, H<sub>3</sub>PW<sub>12</sub>O<sub>40</sub>/ZrO<sub>2</sub> system<sup>18</sup>, Cu-Ni/VSO system<sup>5,19</sup>, H<sub>3</sub>PO<sub>4</sub>/V<sub>2</sub>O<sub>5</sub> system<sup>4</sup> and mixtures of methyl iodide, tetrabutylammonium bromide and often potassium carbonate<sup>20</sup>. The formation of DME decreased by the high (super-critical) pressure of carbon dioxide<sup>10,20,21</sup>.

The main issue is the formation of water, which can terminate this reaction in the equilibrium and also destroy the catalysts. The removal or utilization of reaction water is the important problem for this DMC preparation. Desiccants used as „water traps“ were quite effective, but also very expensive.

As desiccants were applied CaCl<sub>2</sub> compound<sup>22</sup>, Na<sub>2</sub>SO<sub>4</sub>, MgSO<sub>4</sub> salts<sup>6</sup>, 2,2-dimethoxypropane (DMP) compound<sup>23</sup>, acetals<sup>24</sup>, dicyclohexylcarbodiimide (DCC) compound<sup>7,8</sup>, trimethyl phosphate (TMP) compound<sup>8</sup>, molecular sieves<sup>25</sup> and some epoxides as ethylene oxide (EO) named oxirane<sup>26,27</sup> and styrene oxide (SO) compound<sup>28</sup>.

The second way as the novel reaction route for DMC preparation is the removal of reaction water by means of olefins. These olefins in the reaction mixture under catalysts based on the metal oxides and zeolites in the H<sup>+</sup>-form can react with reaction water into corresponding alcohols. The relatively high temperatures of about 180–200 °C were necessary for ethylene, when part of DMC formed was also decomposed. Better was propylene at 150–180 °C, when isopropanol was formed and the best was isobutylene at about 130–150 °C, when *tert*-butanol was formed. The formation of methyl *tert*-butylether (MTBE) was also observed (high octane additive for engine petrol). For industry, the petroleum C<sub>4</sub>-isobutylene gas fraction from the production of the MTBE is for lower price here more suitable.

The reaction mechanism is explained often by means of NMR method mainly in the following references.<sup>10–11,29,30</sup>

### Experimental

All reactions were carried in a stainless autoclave reactor with inner volume about 100 ml with vertical magnetic stirring<sup>2</sup> or horizontal shaking with electrical heating. Catalysts were prepared from commercial items (Reachim, Moscow, SU) according to references<sup>5,6,7</sup>. All zeolites were from the refinery Slovnaft a.s. (Bratislava, SK). Carbon dioxide and olefins were pure, min. 98% grade (Messer).

The products were analysed by GC-method with butanol, octane or toluene as internal standards, according to previous references.<sup>6–8</sup>

### Results and Discussion

The best results by the first way with the zirconia catalysts were conversion 20 % and selectivity 80 % and so the yields up to 16 %. By the second way with olefins the conversion was about 70 %, selectivity about 8 % for ethylene, 11 % for propylene and 15 % for isobutylene, so the yields were about 5–11 %. The main problem was here the stirring of the catalysts. The contact between reaction liquids and catalysts must be effective. The addition of large amounts of desiccants e.g. DMP, TMP is not effective because of decreasing the DMC and increasing the DME formation rate.

### Conclusion

The one-pot synthesis of DMC from methanol and carbon dioxide is very interesting process for the utilization of carbon dioxide. The very interesting way is here the utilization of water stable catalysts such as various metal (Ce, Ge, Mg, Sn, V, Zn, Zr) oxides. For the removal of reaction water the best way now is the utilization of ethylene oxide, when together with DMC also ethylene glycol and 2-methoxyethanol are produced. The our way for olefins must be yet more

investigated. The intention here is the utilization of carbon dioxide from large bioethanol factory in the Slovak Republic, where emissions of carbon dioxide (purity about 97 % grade) of 40,000 tons per year from the maize starch fermentation as degas waste are released into the atmosphere.

## REFERENCES

1. Yamazaki N., Nakahama S.: *Ind. Eng. Chem. Prod. Res. Dev.* 18, 249 (1979).
2. Sakakura T., Choi J. Ch., Yasuda H.: *Chem. Rev.* 107, 2365 (2007).
3. Aresta M., Dibenedetto A.: *Catal. Today* 98, 455 (2004).
4. Wu X. L., Xiao M., Meng Y. Z., Lu Y. X.: *J. Mol. Catal. A-Chem.* 238, 158 (2005).
5. Wu X. L., Xiao M., Meng Y. Z., Lu Y. X.: *J. Mol. Catal. A-Chem.* 249, 93 (2006).
6. Kizlink J.: *Collect. Czech. Chem. Commun.* 58, 1399 (1993).
7. Kizlink J., Pastucha I.: *Collect. Czech. Chem. Commun.* 59, 2116 (1994).
8. Kizlink J., Pastucha I.: *Collect. Czech. Chem. Commun.* 60, 687 (1995).
9. Sakakura T., Saito Y., Okano M., Choi J. Ch., Sako T.: *J. Org. Chem.* 63, 7095 (1998).
10. Sakakura T., Choi J. Ch., Saito Y., Matsuda T., Sako T.: *J. Org. Chem.* 64, 4506 (1999).
11. Sakakura T., Choi J. Ch., Saito Y., Sako T.: *Polyhedron* 19, 573 (2000).
12. Zhao T., Han Y., Sun Y.: *Fuel Process. Technol.* 62, 187 (2000).
13. Tomishige K., Sakaihoru T., Ikeda Y., Fujimoto K.: *Catal. Letters* 58, 225 (1999).
14. Tomishige K., Ikeda Y., Sakaihoru T., Fujimoto K.: *J. Catalysis* 192, 355 (2000).
15. Ikeda Y., Asadullah M., Fujimoto K., Tomishige K.: *J. Phys. Chem. B* 105, 10653 (2001).
16. Tomishige K., Furusawa Y., Ikeda Y.: *Catal. Letters* 76, 71 (2001).
17. La K. W., Jung J. Ch., Kim H., Baeck S. H., Song I. K.: *J. Mol. Catal. A-Chem.* 269, 41 (2007).
18. Jiang C., Guo Y., Wang C., Hu C., Wu Y., Wang E.: *Appl. Catal. A-Gen.* 256, 203 (2003).
19. Wang X. J., Xiao M., Wang S. J., Lu Y. X., Meng Y. Z.: *J. Mol. Catal. A-Chem.* 278, 92 (2007).
20. Fujita S., Bhanage B. M., Arai M., Ikushima Y.: *Green Chem.* 3, 87 (2001).
21. Hong S. T., Park H. S., Lim J. S.: *Res. Chem. Intermed.* 32, 737 (2006).
22. Jiang Q., Li T., Liu F.: *Chin. J. Appl. Chem.* 16, 115 (1999).
23. Tomishige K., Kunimori K.: *Appl. Catal. A-Chem.* 237, 103 (2002).
24. Choi J. C., He L. N.: *Green Chem.* 4, 230 (2002).
25. Hou Z. S., Han B., Liu Z., Jiang T., Yang G.: *Green Chem.* 4, 467 (2002).
26. Cui H., Wang T., Wang F., Gu Ch., Wang P. Dai Y.: *Ing. Eng. Chem. Res.* 42, 3865 (2003).
27. Cui H., Wang T., Wang F., Gu Ch., Wang P. Dai Y.: *Ing. Eng. Chem. Res.* 43, 7732 (2004).
28. Tian J. S., Wang J. Q., Chen J. Y., Fan J. G., Cai F., He L.N.: *Appl. Catal. A-Gen.* 301, 215 (2006).
29. Holeček J., Nádvořník M.: *J. Organometal. Chem.* 315, 299 (1986).
30. Suciú E. N., Kuhlman B., Knudsen G.: *J. Organometal. Chem.* 556, 41 (1998).

## P09 AMADORI REARRANGEMENT FOR SYNTHESIS OF CHIRAL FRAGMENTS

JANA MARKOVÁ and MILAN POTÁČEK

Department of Chemistry, Masaryk University, Kotlářská 2, 602 00 Brno, Czech Republic, 21510@mail.muni.cz

### Introduction

Amadori rearrangement is a reaction between sugars and amines. The rearrangement is based on the conversion of N-substituted glycosylamines to the N-substituted 1-amino-1-deoxy-2-ketoses. Amadori observed this reaction in years 1926-31. The true structure of the rearranged product exposed Weygand and Kuhn in 1937<sup>1</sup>. Recently, it has been found that Amadori rearrangement takes place in living cells and organisms, where sugars and amino acids coexist. There Amadori rearrangement causes the functional modification of proteins, which are characteristic for diseases *diabetes mellitus* and *arteriosclerosis*<sup>2</sup>. Amadori rearrangement is also known as initial phase of Maillard reaction<sup>3</sup> and plays an important role in the synthesis of osazone, quinoxaline, folic acid and riboflavine<sup>4</sup>.

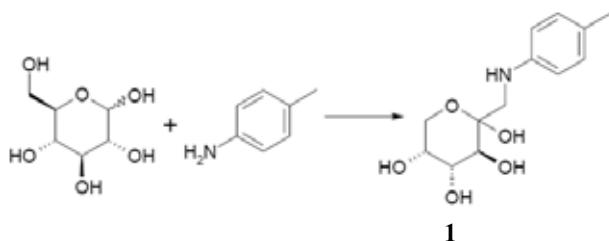
We have investigated conditions for Amadori rearrangement of D-glucose and 5-deoxy-D-xylose with *p*-toluidine, benzylamine and dibenzylamine. 1-Amino-3,4,5,6-tetrahydroxyhexane-2-on and 1-amino-3,4-dihydroxypentane-2-on were prepared by hydrogenolysis of benzyl group on Pd/C. These compounds are to be used for the insertion of stereogenic carbon atoms with hydroxyl groups of sugar to various organic molecules.

### Experimental

Amadori rearrangement is the reaction between sugars and amines in the presence of acid catalyst. The influence of amines and acid on the course of the reaction was investigated. As acid catalysts acetic acid and diethylmalonate were used.

#### Reactions in the Presence of Acetic Acid

The reactions were carried out in water in the presence of 1.4 equiv. of amine and 0.04 equiv. of acetic acid. The reaction mixture was heated at 90 °C for 30 min. Then a mixture of ethanol and diethylether was added and white crystals of the product were obtained after cooling to 3–4 °C for 24 h.



Scheme 1

Reaction of D-glucose with *p*-toluidine

#### Reactions in the Presence of Diethylmalonate

The reactions were carried out in the mixture of ethanol and diethylmalonate. 1.4 equiv of amine was used. After 2 h of reflux diethylether was added to the reaction mixture. White crystals of the product were obtained when the solution was kept at 3–4 °C for 20 h.

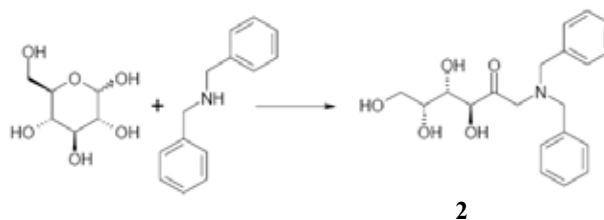
#### Hydrogenolysis of Benzyl Group on Pd/C

Product of Amadori rearrangement with dibenzylamine was hydrogenolysed on 10 % Pd/C in the presence of methanol. Reaction was carried out at room temperature and atmospheric pressure for 16 h. A yellow liquid product was obtained after the filtration and evaporation of solvent from the reaction mixture.

### Results

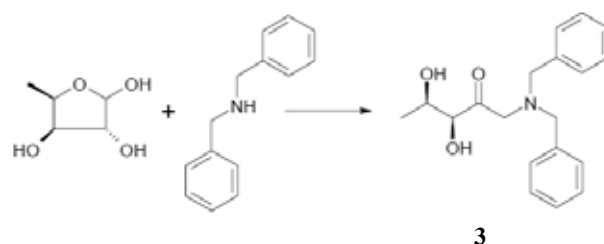
The products of Amadori rearrangement were successfully obtained by the reaction of D-glucose with *p*-toluidine **1** (Scheme 1) and dibenzylamine **2** (Scheme 2).

On the other hand, the reaction of D-glucose with benzylamine does not follow the principles of Amadori rearrangement.



Scheme 2

Reaction of D-glucose with dibenzylamine



Scheme 3

Reaction of 5-deoxy-D-xylose with dibenzylamine

Table I  
Reaction of D-glucose

Amine	D-glucose		
	Catalyst	Product	Yield[%]
benzylamine	CH <sub>3</sub> COOH	glycosylamine	75
	DEM	glycosylamine	90
<i>p</i> -toluidine	CH <sub>3</sub> COOH	Amadori product	61
	DEM	Amadori product	71
dibenzylamine	CH <sub>3</sub> COOH	glycosylamine	65
	DEM	Amadori product	72

Table II  
Reaction of 5-deoxy-D-xylose

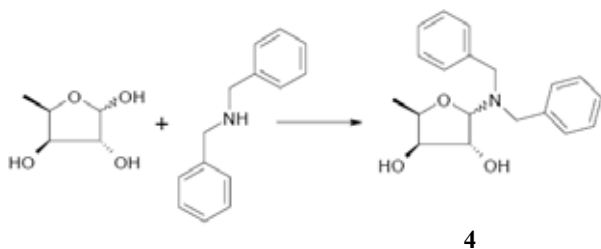
Amine	5-deoxy-D-xylose		Yield [%]
	Catalyst	Product	
benzylamine	CH <sub>3</sub> COOH	glycosylamine	68
	DEM	glycosylamine	86
<i>p</i> -toluidine	CH <sub>3</sub> COOH	glycosylamine	74
	DEM	glycosylamine	78
dibenzylamine	CH <sub>3</sub> COOH	glycosylamine	74
	DEM	Amadori product	51

gement independently on the selection of acid catalyst. The observed results and yields are summarized in Table I.

The required product of Amadori rearrangement of 5-deoxy-D-xylose was obtained only in case of the reaction with dibenzylamine, which was carried out in the presence of diethylmalonate **3** (Scheme 3).

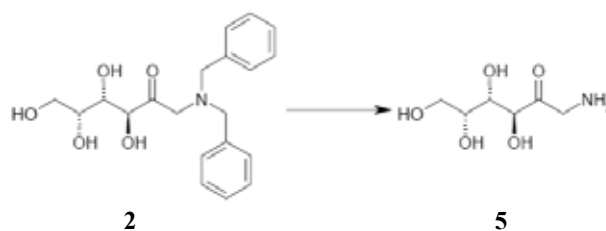
Reactions performed under various conditions yield corresponding glycosylamines only **4** (Scheme 4).

The observed results are summarized in Table II.



Scheme 4  
Glycosylamine of 5-deoxy-D-xylose

The rearrangement of the studied sugars with *p*-toluidine yielded products containing six member ring in its structure **1** (Scheme 1). However, when dibenzylamine was used the open form **2** of the product was obtained (Scheme 2).



Scheme 5  
Hydrogenolysis of the compound **2**

The cyclization of these products does not take place because of sterical hindrance of the large benzyl groups of amine. Both cyclic and open forms of the products were confirmed by <sup>1</sup>H and <sup>13</sup>C NMR spectroscopy.

The product with free amino group **5** was obtained after the hydrogenolysis of compound **2** on Pd/C catalyst (Scheme 5). Compound **5** with unprotected amino group can be then used in further reactions introducing stereogenic centre into an appropriate organic substrate.

### Conclusions

The scope of Amadori rearrangement of D-glucose and 5-deoxy-D-xylose was searched. It was found that the structure of both sugar and amine plays an important role for course of the reaction. The rearrangement takes place more readily and with better yield in the presence of diethylmalonate when compared to acetic acid.

### REFERENCES

- Hodge J. E.: Adv. Carbohydr. Chem. 10, 169, (1990).
- Lederer M. O., Dreibusch C. M., Bundschuh R. M., Carbohydr. Res. 301, 111, (1997).
- Stadler R. H., Blank I., Varga N., Nature 419, 449, (2002).
- Weygand F., Bergmann A., Chem. Ber. 80, 255, (1947).

**P10 EFFICIENT MICROWAVE-ASSISTED  
OXIDATIVE DEPROTECTION OF  
TRIMETHYLSILYL ETHERS WITH CALCIUM  
HYPOCHLORITE UNDER SOLVENT-FREE  
CONDITIONS**

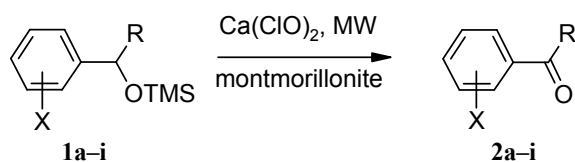
MOHAMMAD M. MOJTAHEDI, M. SAEED ABAEE and  
HASSAN ABBASI

*Chemistry & Chemical Engineering Research Center of Iran,  
P. O. Box 14335–186 Tehran, Iran,  
mojtahedi@ccerci.ac.ir*

**Introduction**

Trimethylsilylation of alcohols is a very common practice in organic synthesis to protect hydroxyl groups<sup>1</sup>. Such maneuver maintains the hydroxyl functionality and prevents its oxidation during reactions. However, sometimes, it is required to convert silyl ethers into their corresponding carbonyl structures. This conversion could be either carried out in a two step desilylation-oxidation process or directly achieved in a one pot reaction. Earlier protocols for such direct oxidations include the use of chromium based procedures<sup>2</sup>, DMSO based reagents<sup>3</sup>, NBS<sup>4</sup>, photochemical conversions<sup>5</sup>, manganese based procedures<sup>6</sup>, and some other different methods<sup>7</sup>. Such processes usually involve the use of harsher reaction conditions, harder work up procedures, and formation of harmful residuals. In recent years, milder reagents and reaction conditions are introduced for direct oxidation of TMS protected alcohols into their corresponding carbonyl analogues<sup>8</sup>. But, introduction of new and efficient methods for oxidative deprotection of trimethylsilyl ethers using inexpensive reagents and under environmentally safe conditions is still considerably attractive.

Calcium hypochlorite is a cheap and mild solid oxidant which can easily be stored<sup>9</sup>, is relatively stable, and has recently been used efficiently for oxidation of various organic functionalities<sup>10</sup>. In continuation of our previous investigations to develop environmentally friendly procedures<sup>11</sup>, we now report a one-pot oxidative deprotection of TMS ethers of benzylic alcohols on a solid support under microwave irradiation (MW) using Ca(ClO)<sub>2</sub> (Scheme 1). As a result, mild transformation of the substrates to their corresponding carbonyl compounds is observed without any undesired over oxidation.



Scheme 1

**Experimental**

**General**

A commercial microwave oven (900 W) was used for irradiation of the reaction mixtures. GC analyses were recor-

ded on a "Fison instrument Gas Chromatograph 8000" equipped with a mass detector "Trio 1000". TMS silyl ethers were prepared according to available procedures<sup>12</sup>. All products are known compounds and are identified by comparison of their physical and spectroscopic data with those of authentic samples<sup>13</sup>.

**Typical Procedure for Oxidative  
Deprotection Reactions**

Montmorillonite K-10 (1.0 g) and calcium hypochlorite (286 mg, 2 mmol) were mixed thoroughly in a mortar. The resulting solid was mixed well with a TMS protected benzylic alcohol (**2a-i**) (2 mmol). The mixture was transferred to a 25 ml beaker and irradiated in microwave oven for the time periods specified in Table I. The progress of the reactions was monitored by TLC or GC. The reaction mixtures were extracted twice by 10 ml portions of diethyl ether. The combined ethereal phases were washed by water and dried over anhydrous calcium chloride. The products were obtained after evaporation of the volatile portion. <sup>1</sup>H NMR and IR spectra of the products were obtained and compared with those of authentic samples.

**Spectral Data**

**2a:** <sup>1</sup>H NMR (CDCl<sub>3</sub>, δ, 80 MHz): 7.42–7.50 (m, 3H), 7.69–7.80 (m, 2H), 9.66 (s, 1H); IR (KBr disk, cm<sup>-1</sup>) 1,703, 2,737, 2,819.

**2b:** <sup>1</sup>H NMR (CDCl<sub>3</sub>, δ, 80 MHz): 6.52 (dd, *J* = 7.5, 15.8 Hz, 1H), 7.20–7.52 (m, 6H), 9.54 (d, *J* = 7.5 Hz, 1H); IR (KBr disk, cm<sup>-1</sup>) 1,681, 2,743, 2,815.

**2d:** <sup>1</sup>H NMR (CDCl<sub>3</sub>, δ, 80 MHz): 7.42 (d, *J* = 8 Hz, 2H), 7.75 (d, *J* = 8 Hz, 2H), 9.91 (s, 1H); IR (KBr disk, cm<sup>-1</sup>) 1,701, 2,785, 2,859.

**2e:** <sup>1</sup>H NMR (CDCl<sub>3</sub>, δ, 80 MHz): 2.36 (s, 3H), 7.20–7.31 (m, 3H), 7.69–7.80 (m, 2H); IR (KBr disk, cm<sup>-1</sup>) 1,682, 3,063.

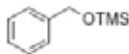
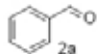

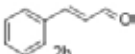
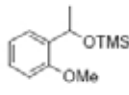
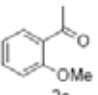
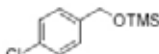
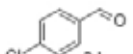
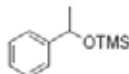
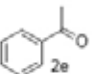
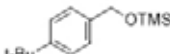
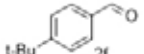
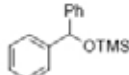
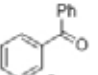
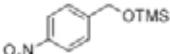
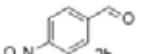
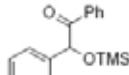
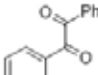
**2i:** <sup>1</sup>H NMR (CDCl<sub>3</sub>, δ, 80 MHz): 7.31–7.61 (m, 6H), 7.65–7.98 (m, 4H); IR (KBr disk, cm<sup>-1</sup>) 1,658, 3,063.

**Results**

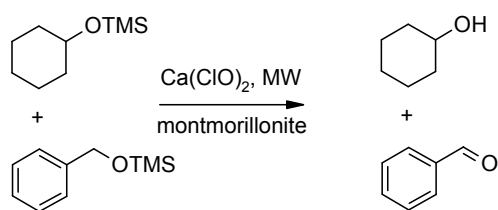
An equimolar mixture of TMS benzylether and Ca(ClO)<sub>2</sub> on montmorillonite K-10 support was subjected to MW irradiation and complete conversion to benzaldehyde (**2a**) was performed within 60 seconds. Extraction of the product by diethyl ether followed by GC analysis showed 97% formation of **2a**. Control experiments conducted in the absence of MW irradiation at elevated or room temperature prolonged the reaction time considerably (Table I, entry 1). TMS ethers of other benzylic alcohols were subjected to the same transformation under three different sets of conditions (entries 2–9). In all cases MW irradiated samples resulted in formation of high to excellent yields of products **2b-i** in less than 2 minutes while lack of irradiation for the same mixtures took much longer time periods for reactions to complete.

The selectivity of the method was examined using an equimolar mixture of benzylsilyl ether and cyclohexylsilyl

Table I  
 Montmorillonite K-10 supported oxidative deprotection of TMS ethers under thermal and MW conditions

Entry	Substrate	Product	Time			Yield [%] <sup>a</sup>			Mp or bp [°C torr <sup>-1</sup> ]	
			Mw [s]	40 °C [h] <sup>b</sup>	RT [h]	Mw [s]	40 °C [h] <sup>b</sup>	RT [h]	Found	Reported <sup>13</sup>
1			60	12	48	97	90	90	177–179	178–179
2			90	12	48	93	88	90	247	248
3			60	12	48	90	87	85	130/18	131/18
4			60	12	48	92	86	85	46–50	45–50
5			90	12	48	93	83	85	19–20	19–20
6			60	12	48	94	89	90	131/25	130/25
7			60	18	60	88	80	83	46–50	47–51
8			90	20	72	87	85	80	103–105	103–106
9			90	20	72	85	81	80	93–95	94–95

<sup>a</sup>Gc yields, <sup>b</sup>refluxing dichloromethane



Scheme 2

Competitive oxidative deprotection of TMS ethers

cyclohexylsilyl ether was only deprotected giving 96 % of cyclohexanol (Scheme 2).

### Conclusions

We presented an efficient, facile, and environmentally safe method for conversion of benzylic silyl ethers to their corresponding carbonyl compounds under solvent-free conditions. Rapid formation of the desired products, no over oxidation reaction, and selective oxidation of benzylic silyl ethers are the advantages of the present method.

ether. Under MW irradiation, formation of benzaldehyde as the sole carbonyl product was observed in 98% yield while

*This work has been partially supported by the Ministry of Science, Research, and Technology of Iran.*

## REFERENCES

- (a) Sartori G., Ballini R., Bigi F., Bosica G., Maggi R., Righi P.: *Chem. Rev.* 104, 199 (2004);  
(b) Lalonde M., Chan T. H.: *Synthesis* 817 (1985);  
(c) Colvin E. W.: *Chem. Soc. Rev.* 7, 15 (1978).
- (a) Baker R., Rao V. B., Ravenscroft P. D., Swain C. J.: *Synthesis* 572 (1983);  
(b) Paquette L. A., Lin H. S., Junn B. P., Coghlan M. J.: *J. Am. Chem. Soc.* 110, 5818 (1988).
- Tolstikov G. A., Miftakhov M. S., Adler M. E., Komissarova N. G., Kuznetsov O. M., Vostrikov, N. S.: *Synthesis* 940 (1989).
- (a) Pinnick H. W., Lajis N. H.: *J. Org. Chem.* 43, 371 (1978);  
(b) Marco I. E., Mekhalfia A., Ollis W. D.: *Synlett* 345 (1990).
- Piva O., Amougay A., Pete J. P.: *Tetrahedron Lett.* 32, 3993 (1991).
- Solladie G., Berl V.: *Synlett* 795 (1991).
- Muzart J.: *Synthesis* 11 (1993).
- (a) Karimi B., Rajabi J.: *Org. Lett.* 6, 2841 (2004);  
(b) Tajbakhsh M., Heravi M. M., Habibzadeh S.: *Phosphorus, Sulfur and Silicon* 178, 361 (2003).  
(c) Tajbakhsh M., Hosseinzadeh R., Niaki M. Y.: *J. Chem. Res.* 508 (2002);  
(d) Hajipour A. R., Mallakpour S. E., Mohammadpoor-Baltork I., Malakoutikhah M.: *Tetrahedron* 58, 143 (2002).
- (a) Hirano M., Yakabe S., Itoh S., Clark J. H., Morimoto T.: *Synthesis* 1997, 1161.  
(b) Hirano M., Yakabe S., Fukami M., Morimoto T.: *Synth. Commun.* 27, 2783 (1997).
- (a) Lewkowski J.: *ARKIVOC* 17 (2001);  
(b) Cottier L., Descotes G., Lewkowski J., Skowroński R., Viollet E.: *J. Heterocycl. Chem.* 32, 927 (1995);  
(c) Nwaukwa S. O., Keehn P. M.: *Tetrahedron Lett.* 23, 35 (1982);  
(d) Nwaukwa S. O., Keehn P. M.: *Tetrahedron Lett.* 23, 3131 (1982);  
(e) Larionov O. V., Kozhushkov S. I., De Meijere A.: *Synthesis* 1916 (2003);  
(f) McDonald C. E., Nice L. E., Shaw A. W., Nestor N. B.: *Tetrahedron Lett.* 34, 2741 (1993);  
(g) Zolfigol M. A., Mallakpour S., Khazaie A., Vaghaie R. G., Torabi M.: *Russ. J. Org. Chem.* 40, 914 (2004);  
(h) Mojtahedi M. M., Saidi M. R., Bolourtchian M., Shirzi J. S.: *Monatsh. Chem.* 132, 655 (2001);  
(i) Inokuchi T., Matsumoto S., Nishiyama T., Torii S.: *J. Org. Chem.* 55, 462 (1990).
- (a) Heravi M. M., Oskooiee H. A., Yazdanpanah S., Mojtahedi M. M.: *J. Chem. Res.* 129 (2004);  
(b) Heravi M. M., Ajami D., Tabar-Heidar K., Mojtahedi M. M.: *J. Chem. Res.* 620 (1998);  
(c) Abaee M. S., Mojtahedi M. M., Zahedi M. M., Bolourtchian M.: *Synth. Commun.* 36, 199 (2006);  
(d) Mojtahedi M. M., Heravi M. M.: *Indian J. Chem. B.* 44, 831 (2005);  
(e) Mojtahedi M. M., Ghasemi M. H., Abaee M. S., Bolourtchian M.: *ARKIVOC* 68 (2005).
- (a) Mojtahedi M. M., Saidi M. R., Bolourtchian M., Heravi M. M.: *Phosphorus, Sulfur and Silicon* 177, 289 (2002);  
(b) Mojtahedi M. M., Abbasi H., Abaee M. S.: *Phosphorus, Sulfur and Silicon* 181, 1541 (2006);  
(c) Mojtahedi M. M., Abbasi H., Abaee M. S.: *J. Mol. Catal. A: Chem.* 250, 6 (2006);  
(d) Mojtahedi M. M., Abaee M. S., Hamidi V., Zolfaghari A.: *Ultrason. Sonochem.* 14, 596 (2007).
- Aldrich Catalogue Handbook of Fine Chemicals, 2007.

## P11 EFFICIENT IONIC LIQUID PROMOTED SYNTHESIS OF BENZOFURANS AT ROOM-TEMPERATURE

ALI SHARIFI, M. SAEED ABAEE, BAHRAM ZAMIRI and MOJTABA MIRZAEI

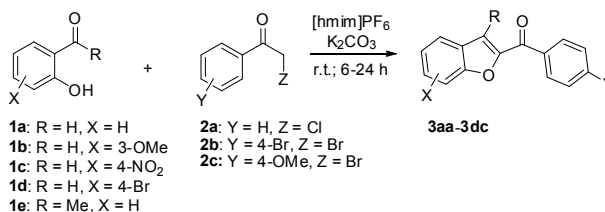
Chemistry & Chemical Engineering Research Center of Iran, P. O. Box 14335–186 Tehran, Iran, sharifi@ccerci.ac.ir

### Introduction

The overwhelming demand to design green and safe chemical procedures in the past three decades has dictated the use of safer and less toxic media with fewer hazards and more environmental compatibility<sup>1</sup>. In this context, ionic liquids have emerged as very powerful substitutes for regular molecular solvents from both economical and environmental points of view<sup>2</sup>. Less volatility, no chance of explosion, thermal stability, and ease of handling are among the reasons to consider ionic liquids as possible environmental benign alternates for conventional solvents. Easy separation of the products from ionic liquids is an additional advantage in many instances. Among various ionic liquids, those based on imidazolium moieties have shown great potential as eco-friendly catalytic systems for room temperature organic transformations<sup>3</sup>.

Benzofuran derivatives constitute highly valuable heterocyclic motifs found in the structure of many natural<sup>4</sup> and synthetic products<sup>5</sup>. Derivatives of these compounds are known to possess important pharmaceutical<sup>6</sup>, antifungal<sup>7</sup>, antitumor<sup>8</sup>, and other bioorganic properties<sup>9</sup>. In addition, benzofurans are used in cosmetic formulations<sup>10</sup> and have the application as synthetic precursors for optical brighteners<sup>11</sup>. Many multi-step synthetic approaches for the construction of the benzofuran ring exist in which the key-step includes dehydrative annulation of phenols bearing appropriate ortho vinylic substituents<sup>12</sup>, intramolecular cyclization of substituted allyl-aryl ethers<sup>13</sup>, cyclization of o-formylphenoxyacetic acids or esters<sup>14</sup>, or ring-closure of arylacetylenes<sup>15</sup>. Perhaps, the most straightforward method for one-pot preparation of benzofuran derivatives is the Rap-Stoermer condensation of salicylaldehyde with  $\alpha$ -haloketones<sup>16</sup> providing the opportunity for the synthesis of a diverse array of benzofuran derivatives in a single step process. The reaction is traditionally carried out under basic conditions in refluxing alcoholic solvents giving low yields of products in many occasions<sup>6–7</sup>. In line with the context of green and sustainable chemistry, several reports are recently released to expand the synthetic applicability of Rap-Stoermer reaction by using microwave irradiation<sup>17</sup>, solvent-free systems<sup>18</sup>, polymer-supported reagents<sup>19</sup>, and solid state synthesis<sup>20</sup>. However, these reactions are still conducted at high temperature<sup>18–19</sup>, require the use of commercially unavailable starting materials<sup>20</sup>, conducted in refluxing solvents<sup>19</sup> or need an external stimulant to proceed<sup>17,20</sup>. In continuation of our previous experiences on environmentally sustainable reactions<sup>21</sup>, we would like to

herein report a novel procedure for efficient Rap-Stoermer condensation of  $\alpha$ -haloketones with various salicylaldehyde derivatives performed at room temperature in the presence of 1-hexyl-3-methyl-1*H*-imidazolium hexafluorophosphate ([hmim]PF<sub>6</sub>) (Scheme 1).



Scheme 1

### Experimental

#### General

Reactions were monitored by TLC and GC. NMR spectra were obtained on a FT-NMR Bruker Ultra Shield™ (500 MHz) or Bruker AC 80 MHz as CDCl<sub>3</sub> solutions and the chemical shifts were expressed as  $\delta$  units with Me<sub>4</sub>Si as the internal standard. GC experiments were carried out using a Fisons 8000 apparatus. All chemicals and reagents were purchased from commercial sources.

#### Typical Procedure for [hmim]PF<sub>6</sub> Mediated Rap-Stoermer Condensations

An equimolar mixture of **1** (5 mmol), **2** (5.5 mmol), and K<sub>2</sub>CO<sub>3</sub> (10 mmol) was added to 7 ml [hmim]PF<sub>6</sub> and the mixture was stirred at room temperature until TLC and GC experiments showed complete disappearance of the starting materials. The mixture was extracted with Et<sub>2</sub>O (3 × 20 ml), the extracts were combined, and the volatile portion was removed under reduced pressure. The product was purified with short column chromatography over silicagel using hexane/EtOAc (7:1). The spectroscopic and physical properties of the products were obtained and compared with those available in the literature.

#### Selected Spectral Data

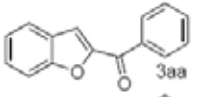
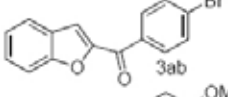
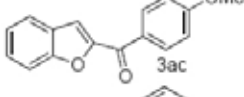
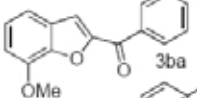
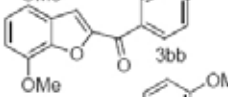
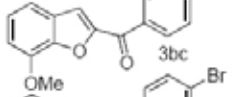
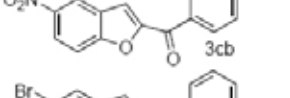
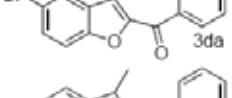
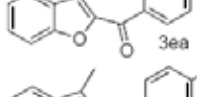
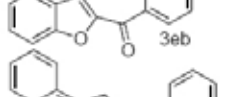
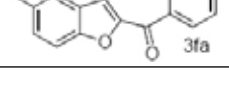
(4-Bromophenyl)(7-methoxybenzofuran-2-yl)methanone (**3bb**). Yellow crystals were obtained in 90% yield, mp 93–95 °C; IR (KBr, cm<sup>-1</sup>) 1,639, 1,554, 1,280, 871; <sup>1</sup>H NMR (CDCl<sub>3</sub>)  $\delta$  4.08 (s, 3H), 7.02 (d, 1H, *J* = 7.8 Hz), 7.30 (dd, 1H, *J* = 7.8, 7.8 Hz), 7.35 (d, 1H, *J* = 7.8 Hz), 7.61 (s, 1H), 7.74 (d, 2H, *J* = 8.41 Hz), 8.03 (d, 2H, *J* = 8.41 Hz); <sup>13</sup>C NMR (CDCl<sub>3</sub>)  $\delta$  56.5, 110.1, 115.4, 116.7, 125.2, 128.5, 128.9, 131.6, 132.3, 136.1, 146.2, 146.5, 152.9, 183.1; MS (70 eV) *m/z* (%): 332, 330 (M<sup>+</sup>), 251, 175, 76. Calcd. For C<sub>16</sub>H<sub>11</sub>BrO<sub>3</sub>: C, 58.03; H, 3.35. Found: C, 58.01; H, 3.47.

(7-Methoxybenzofuran-2-yl)(4-methoxyphenyl) methanone (**3bc**). White crystals were obtained in 80% yield, mp 66–68 °C; IR (KBr, cm<sup>-1</sup>) 1,664, 1,593, 1,315, 1,230, 1,160; <sup>1</sup>H NMR (CDCl<sub>3</sub>)  $\delta$  3.93 (s, 3H), 4.07 (s, 3H), 6.98 (d, 1H, *J* = 7.7 Hz), 7.05 (d, 2H, *J* = 8.8 Hz), 7.26 (dd, 1H, *J* = 7.8, 7.9 Hz), 7.32 (d, 1H, *J* = 7.8), 7.56 (s, 1H), 8.19 (d, 2H,

$J = 8.8$  Hz);  $^{13}\text{C}$  NMR ( $\text{CDCl}_3$ )  $\delta$  55.9, 56.5, 109.8, 114.3, 115.3, 115.8, 125.0, 129.1, 130.2, 132.5, 145.9, 146.5, 153.6, 164.0, 182.8; MS (70 eV)  $m/z$  (%): 282 ( $\text{M}^+$ ), 252, 135. Calcd. For  $\text{C}_{17}\text{H}_{14}\text{O}_4$ : C, 72.33; H, 5.00. Found: C, 72.15; H, 5.12.

(4-Bromophenyl)(3-methylbenzofuran-2-yl)methanone (**3eb**). White crystals were obtained in 78% yield, mp 103–105 °C; IR (KBr,  $\text{cm}^{-1}$ ) 1,643, 1,562, 1,296, 929;  $^1\text{H}$  NMR ( $\text{CDCl}_3$ )  $\delta$  2.71 (s, 3H), 7.39 (d, 1H,  $J = 6.8, 7.8$  Hz), 7.59–7.53 (m, 2H), 7.71 (d, 2H,  $J = 8.5$  Hz), 7.75 (d, 1H,  $J = 7.8$  Hz), 8.03 (d, 2H,  $J = 8.47$  Hz);  $^{13}\text{C}$  NMR ( $\text{CDCl}_3$ )  $\delta$  10.5, 112.7, 122.0, 123.9, 128.0, 128.2, 128.9, 129.6, 131.8, 132.1, 136.9, 148.4, 154.7, 185.0; MS (70 eV)  $m/z$  (%): 315, 314 ( $\text{M}^+$ ), 235, 207. Calcd. For  $\text{C}_{16}\text{H}_{11}\text{BrO}_2$ : C, 60.98; H, 3.52. Found: C, 60.59; H, 3.55.

Table I  
Ionic liquid mediated Rap-Stoermer condensations

Entry	Substrate	Product	Time [h]	Yield [%]
1	<b>1a</b> + <b>2a</b>		6	90
2	<b>1a</b> + <b>2b</b>		24	93
3	<b>1a</b> + <b>2c</b>		24	98
4	<b>1b</b> + <b>2a</b>		24	98
5	<b>1b</b> + <b>2b</b>		6	90
6	<b>1b</b> + <b>2c</b>		24	80
7	<b>1c</b> + <b>2b</b>		24	70
8	<b>1d</b> + <b>2a</b>		6	90
9	<b>1e</b> + <b>2a</b>		24	90
10	<b>1e</b> + <b>2b</b>		24	93
11	<b>2a</b> + 2-hydroxy-1-naphthaldehyde		24	90

<sup>a</sup>Gc isolated yields

## Results

The reaction between  $\alpha$ -chloroacetophenone with salicylaldehyde was investigated under various sets of conditions to find the optimum conditions. A suspension of the two reactants and  $\text{K}_2\text{CO}_3$  in the ionic liquid led to 90% formation of product **3aa** within 6 hours time period (Table I, entry 1). Conduction of the same reaction in the presence of some other ionic liquids ( $[\text{bmim}]\text{PF}_6$ ,  $[\text{hmim}]\text{BF}_4$ ,  $[\text{bmim}]\text{PF}_6$ , or bases ( $\text{Et}_3\text{N}$ ,  $t\text{-BuONa}$ ) led to formation of lower quantities of the product within the same time periods. The product was easily obtained in high purity by a simple diethyl ether. The optimized conditions were employed to investigate the Rap-Stoermer condensation of salicylaldehyde with other substrates bearing electron-withdrawing and electron-releasing groups. Therefore, reactions of **1a** with **2b** (entry 2) and with **2c** (entry 3) gave 93 and 98 % of **3ab** and **3ac**, respectively. The generality of the procedure was shown by subjecting derivatives of *o*-hydroxybenzaldehydes to undergo condensation with different  $\alpha$ -haloacetophenones (entries 4–8). Furthermore, *o*-hydroxyacetophenone (entries 9–10) and 2-hydroxy-1-naphthaldehyde (entries 11) conveniently exhibited similar reactions. In all cases, reactions smoothly reached to completion within 6–24 hours time periods good to excellent yields of the desired products which were separable by simple ethereal extraction.

## Conclusions

In summary, we have developed a novel and general procedure for room-temperature Rap-Stoermer condensation of  $\alpha$ -haloacetophenone with various 2-hydroxyarylaldehydes mediated by  $[\text{hmim}]\text{PF}_6$ . Reactions complete in short time periods in the presence of no external stimulant and the procedure is applicable to both 2-hydroxyacetophenone and 2-hydroxyarylaldehydes. The versatility of the reaction, use of a recyclable media, production of pure single compounds, and easy procedure and work up are among other benefits of the present method.

*This work has been partially supported by the Ministry of Science, Research, and Technology of Iran.*

## REFERENCES

- Lancaster M.: *Green Chemistry: An Introductory Text*, Royal Society of Chemistry, Cambridge, UK 2002.
- (a) Shen Z. L., Ji S. J., Loh T. P.: *Tetrahedron Lett.* **46**, 3137 (2005);  
(b) Yadav J. S., Reddy B. V. S., Eshwaraiah B., Srinivas M., Vishnumurthy P.: *New J. Chem.* **27**, 462 (2003).
- (a) Earle M. J., McCormac P. B., Seddon K. R.: *Green Chem.* **1**, 23 (1999);  
(b) Huddleston J. G., Willauer H. D., Swatloski R. P., Visser A. E., Rogers R. D.: *Chem. Commun.* 1765 (1998);  
(c) Wilkes J. S.: *Green Chem.* **4**, 73 (2002);  
(d) Bradaric C. J., Downard A., Kennedy C., Robertson A. J., Zhou Y.: *Green Chem.* **5**, 143 (2003);

- (e) Sheldon R.: Chem. Commun. 2399 (2001);  
(f) Mojtahedi M. M., Abaee M. S., Abbasi H.: J. Iran. Chem. Soc. 3, 93 (2006).
4. (a) Simpson T. J.: *The Chemistry of Natural Products*, Blackie, London 1985;  
(b) Dean F. M.: *The Total Synthesis of Natural Products*, Wiley, New York 1973, vol. 1, p 513.
5. (a) Katritzky A. R., Ji Y., Fang Y., Prakash I.: J. Org. Chem. 66, 5613 (2001);  
(b) Park K. K., Seo H., Kim J.-G., Suh I.-H.: Tetrahedron Lett. 41, 1393 (2000);  
(c) Nicolaou K. C., Snyder S. A., Bigot A., Pfefferkon J. A.: Angew. Chem. Int. Ed. 39, 1093 (2000);  
(d) Park K. K., Han I. K., Park J. W.: J. Org. Chem. 66, 6800 (2001);  
(e) Shafiee A., Behnam E.: J. Heterocycl. Chem. 15, 589 (1978).
6. Buu-Hoi N., Saint-Ruf G., Loc T. B., Xuong N. D.: J. Chem. Soc. 2593 (1957).
7. (a) Benkli K., Gundogdu-Karaburun N., Karaburun A. C., Ucucu U., Demirayak S., Kiraz N.: Arch. Pharm. Res. 26, 202 (2003);  
(b) Gundogdu-Karaburun N., Benkli K., Tunali Y., Ucucu U., Demirayak S.: Eur. J. Med. Chem. 41, 651 (2006).
8. Baraldi P. G., Romagnoli R., Beria I., Cozzi P., Geroni C., Mongelli N., Bianchi N., Mischiati C., Gambari R.: J. Med. Chem. 43, 2675 (2000).
9. (a) Li J., Rush T. S., Li W., De Vincentis D., Du X., Hu Y., Thomason J. R., Xiang J. S., Skotnicki J. S., Tam S., Cunningham K. M., Chockalingam P. S., Morris E. A., Levin J. I.: Bioorg. Med. Chem. Lett. 15, 4961 (2005);  
(b) Pestellini V., Giolitti A., Pasqui F., Abelli L., Cutrufo C., De Salvia G., Evangelista S., Meli A.: Eur. Med. Chem. 23, 203 (1988).
10. Leung A. Y., Foster S.: *Encyclopedia of Common Natural Ingredients Used in Food, Drugs, and Cosmetics*, Wiley, New York 1996.
11. Elvers B., Hawkins S., Schulz G.: *Ullmann's Encyclopedia of Industrial Chemistry*, Optical Brighteners, 5th ed., Vol A18, VCH, Weinheim 1999, p153.
12. (a) Thielges S., Meddah E., Bisseret P., Eustache J.: Tetrahedron Lett. 45, 907 (2004);  
(b) Gil M. V., Roman E., Serrano J. A.: Tetrahedron Lett. 41, 10201 (2000);  
(c) Herndon J. W., Zhang Y., Wang H., Wang K.: Tetrahedron Lett. 41, 8687 (2000);  
(d) Arrault A., Touzeau F., Guillaument G., Merour J. Y.: Synthesis 1241 (1999).
13. (a) Hennings D. D., Iwasa S., Rawal V. H.: Tetrahedron Lett. 36, 6379 (1997);  
(b) Xie X., Chen B., Lu J., Han J., She X., Pan X.: Tetrahedron Lett. 45, 6235 (2004);  
(c) Youn S. W., Eom J. I.: Org. Lett. 7, 3355 (2005).
14. (a) Bogdal D., Warzala M.: Tetrahedron 56, 8769 (2000);  
(b) Park K. K., Jeong J.: Tetrahedron 61, 545 (2005);  
(c) Bellur E., Freifeld I., Langer P.: Tetrahedron Lett. 46, 2185 (2005);  
(d) Bogdal D., Bednarz S., Lukasiewicz M.: Tetrahedron 62, 9440 (2006);  
(e) Kraus G. A., Zhang N., Verkade J. G., Nagarajan M., Kisanga P. B.: Org. Lett. 2, 2409 (2000);  
(f) Cruz M. C., Tamariz J.: Tetrahedron Lett. 45, 2377 (2004).
15. (a) Dai W. M., Lai K. W.: Tetrahedron Lett. 43, 9377 (2002);  
(b) Bates C. G., Saejueng P., Murphy J. M., Venkataraman D.: Org. Lett. 4, 4727 (2002).
16. (a) Rap E.: Gazz. Chim. Ital. 285, 2511 (1895);  
(b) Stoermer R.: Liebigs. Ann. Chem. 312, 331 (1900).
17. Rao M. L. N., Awasthi D. K., Banerjee D.: Tetrahedron Lett. 48, 431 (2007).
18. Yoshizawa K., Toyota S., Toda F., Csoregh I.: Green Chem. 5, 353 (2003).
19. Habermann J., Ley S. V., Smits R.: J. Chem. Soc., Perkin Trans. 1 2421 (1999).
20. Varma R. S., Kumar D., Liesen P. J.: J. Chem. Soc., Perkin Trans. 1 4093 (1998).
21. (a) Sharifi A., Mirzaei M., Naimi-Jamal M.R.: J. Chem. Res. 628 (2002);  
(b) Sharifi A., Mirzaei M., Saidi M. R.: Tetrahedron Lett. 40, 1179 (1999);  
(c) Sharifi A., Mirzaei M., Naimi-Jamal M. R.: Monatsh. Chem. 137, 213 (2006);  
(d) Sharifi A., Mirzaei M., Naimi-Jamal M. R., Synth. Commun. 35, 1039 (2005);  
(e) Sharifi A., Salimi R., Mirzaei M., Abaee M. S.: Synth. Commun. 37, 1825 (2007).

## P12 CRYSTAL ENGINEERING OF GLYCOLURIL DIMERS

VLADIMÍR ŠINDELÁŘ and MAREK ŠTANCL

Department of Chemistry, Masaryk University, Kotlářská 2,  
611 37 Brno, Czech Republic,  
sindelar@chemi.muni.cz

### Introduction

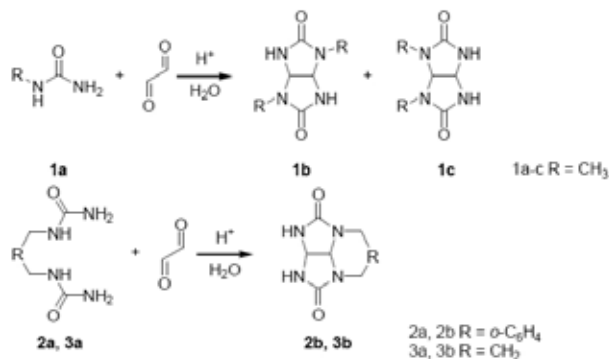
Glycolurils are heterobicyclic compounds that have been used as building blocks of various supramolecular objects. Among others, glycoluril motif has been used in molecular clips<sup>1</sup> and macrocyclic cucurbiturils<sup>2</sup>. Fundamental building block of the latter compounds is methylene-bridged glycoluril dimer. In recent years Isaacs and coworkers prepared such dimers<sup>3</sup> to investigate mechanism of cucurbituril formation and synthesis of new cucurbituril analogues. Depending on the reaction conditions mixture of two diastereomers, S-shaped and C-shaped, was prepared. These dimers were synthesized from *N*-protected glycolurils and formaldehyde to avoid the formation of glycoluril oligomers. Substituted xylylene sidewall was used as a protecting group and was introduced to the molecule of glycoluril using alkylation. Unsubstituted glycoluril is little soluble in common solvents, therefore various groups are introduced to glycoluril in the positions 7 and 8 to increase its solubility.

We decided to expand chemistry of glycoluril by the preparation of glycoluril dimers bearing hydrogen atoms in positions 7, 8 of the glycoluril unit with different terminal units. The reason is to get more information about cucurbituril synthesis and tune the organization of the dimer molecules in the solid state by the modification of its structure.

### Experimental

#### Synthesis of Protected Glycolurils

For the synthesis of the dimers precursors the condensation reaction between glyoxal and substituted urea was chosen at first<sup>4</sup>. Unfortunately, this method gives poor yields of required 1,6-substituted glycoluril and also the isolation of the product is not easy. This method was used for the synthesis of 1,6-dimethylglycoluril **1c** following published procedure<sup>5</sup>.



Scheme 1

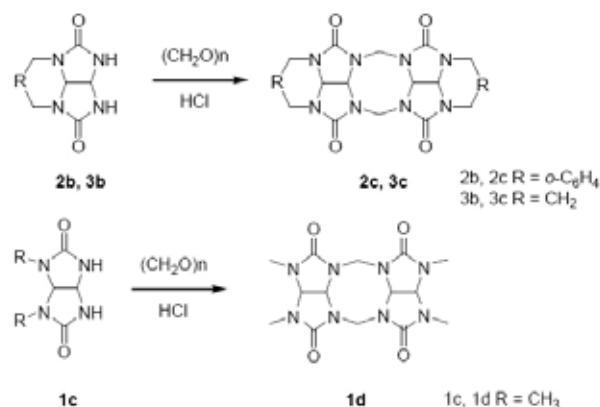
Synthesis of 1,6-substituted glycolurils

Separation from 1,4-dimethylglycoluril required extensive fraction crystallization. We found, that pure product could be obtained after crystallization from 8% H<sub>3</sub>PO<sub>4</sub>. Despite of this improvement, the yield is 9 %.

We envisioned that the preparation of required dimer precursors could be achieved by acid catalyzed cyclocondensation reaction between bisurea and glyoxal. We selected aromatic and aliphatic bisureas **2a**, **3a** and found, that acid catalyzed reaction with glyoxal in water gives 1,6-substituted glycoluril. The product could be easily separated from the reaction mixture by filtration. Yields are modest for aliphatic derivative **3b** (47 %) and good for aromatic **2b** (75 %).

#### Synthesis of Glycoluril Dimers

Protected glycolurils **1c**, **2b** and **3b** were used in acid catalyzed reaction with one equivalent of formaldehyde. Reactions were carried out in concentrated HCl at 80 °C to obtain thermodynamic more stable C-shaped dimer.



Scheme 2

Synthesis of glycoluril dimers

Glycoluril dimers **1d**, **2c**, **3c** were obtained in good yields 90, 94, 81 % respectively. We were able to obtain X-ray crystal structures of these dimers.

### Results

Glycoluril dimer **2c** bearing two xylylene sidewalls is organized into dimeric aggregates; the driving force of the dimerization is the van der Waals interactions together with face-to-face  $\pi$ - $\pi$  stacking interaction of the xylylene rings. Dimer self-assembly was also observed in the crystal structure of **3c**. In this case, the dimerization can be assigned to the van der Waals interactions only. In the crystal structure of **1d** no dimerization was observed. Instead, there is a unique three-dimensional network of molecules. Each molecule is surrounded by two molecules with the same orientation and four molecules which are rotated by 90 ° relative to the central molecule. The stacking of these motifs along the crystallographic *c*-axis results in columns in which the bowl-shaped molecules are packed on top of each other (Fig. 1).

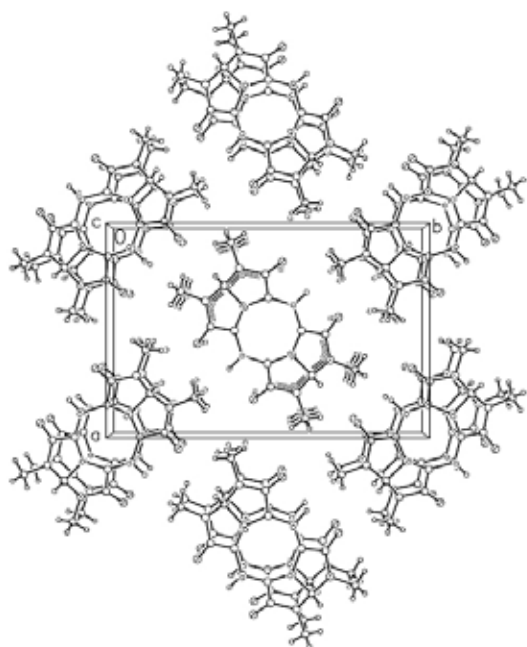


Fig. 1. Crystal structure of methylene-bridged glycoluril dimer **1d**

### Conclusion

We have prepared methylene-bridged glycoluril dimers bearing two hydrogen atoms on the convex face of the glycoluril unit. A new method for the synthesis of 1,6-substituted glycolurils was developed. In the solid state, **3c** and **2c** form dimeric aggregates whereas **1d** is organized into three-dimensional structure.

*This work has been supported by the Grant Agency of the Czech Republic 203/07/P382.*

### REFERENCES

1. Rowan A. E., Elemans J. A. A. W., Nolte R. J. M.: *Acc. Chem. Res.* 1999, 995.
2. Lagona J., Mukhopadhyay P., Chakrabarti S., Isaacs L.: *Angew. Chem. Int. Ed.* 44, 4844 (2005).
3. Wu A., Chakraborty A., Witt D., Lagona J., Damkaci F., Ofori M., Chiles K., Fettinger J. C., Isaacs L.: *J. Org. Chem.* 67, 5817 (2002).
4. Krafchenko A. N., Sigachev A. S., Maksareva E. Yu., Gazieva G. A., Trunova N. S., Lozhkin B. V., Pivina T. S., Il'in M. M., Lyssenko K. A., Nelyubina Yu. V., Davankov V. A., Lebedev O. V., Makhova N. N., Tartakovskiy V. A.: *Russ. Chem. Bull., Int. Ed.* 54, 691 (2005).
5. Nematollahi J., Ketcham R.: *J. Org. Chem.* 28, 2378 (1963).